5-19-2017

Identification Of Novel Nuclear Proteins Required For Meiotic Silencing By Unpaired Dna In Neurospora Crassa

Dilini Ralalage
Illinois State University, disewwandi@yahoo.com

IDENTIFICATION OF NOVEL NUCLEAR PROTEINS REQUIRED FOR MEIOTIC SILENCING BY UNPAIRED DNA IN *NEUROSPORA CRASSA*

Diyagama Arachchi Ralalage Dilini Sewwandi Samarajeewa

140 Pages

A fundamental step that occurs during sexual reproduction is meiosis, which is a specialized type of cell division. During meiosis, pairs of chromosomes exchange genetic information via recombination. At this point, the genome is particularly susceptible to viruses and other foreign genetic invasions. Therefore, it is important to protect the genome to prevent the transmission of foreign genetic materials to the offspring. Several mechanisms work together to protect host genome from foreign genetic materials. These are known as “genome defense mechanisms”.

The fungus *Neurospora crassa* is one of the best organisms for genome defense studies due to the presence of at least three genome defense mechanisms; including Repeat Induced Point mutation (RIP), Quelling, and Meiotic Silencing by Unpaired DNA (MSUD).The main focus of my dissertation is the MSUD pathway.

MSUD is a process that detects and silences unpaired DNA between homologous chromosomes. During MSUD, homologous chromosomes are scanned for unpaired regions by unknown protein complexes. These protein complexes may also contribute to homology search required by some DNA repair pathways. Therefore, identification of these proteins could have a significant impact on cancer research. Hence, one part of my dissertation is to identify and characterize novel proteins that detect unpaired DNA during MSUD. In my findings, I have

found a putative SNF2-family protein (SAD-6) required for efficient MSUD in *Neurospora crassa* and it is closely related to a protein called Rad54, which is involved in the repair of DNA double-strand breaks by homologous recombination.

Moreover, I was able to identify and characterize *Neurospora crassa sad-7*, a gene encoding a protein with RNA recognition motif (RRM). My experiments have confirmed that SAD-7 in *N. crassa*, is required for fully-efficient MSUD in the presence of unpaired DNA.

In addition to my MSUD studies, I have examined meiotic drive elements. These elements are found in eukaryotic genomes. In general, genetic loci are transmitted to the offspring during sexual reproduction according to Mendelian inheritance patterns. However, there are some selfish loci that are capable of biasing their own transmission rates through meiosis or gametogenesis in the presence of a competing locus. These are known as meiotic drive elements. *Neurospora crassa* has a meiotic drive element known as *Spore killer-2 (Sk-2)* and it achieves biased transmission by spore killing.

When *Sk-2* is crossed with a *Spore killer* sensitive opposite mating type (Sk^S), hypothetically there should be a mixed offspring population of killer resistant and killer sensitive ascospores. Surprisingly, when analyzing the ascospores, nearly all the survived ascospores express the *Sk-2* genotype and all the ascospores with the *Spore killer* sensitive genotype are non-viable. However, there is little known about the exact location of the *Sk-2* meiotic drive element and its mechanism of transmission. In my experiments, I was able identify a genetic element located on *N. crassa* chromosome III that is required and sufficient for spore killing.

Overall, my results provide new insights on the search for unpaired DNA during meiosis and the identification of a genetic element required for meiotic drive-based spore killing.

KEYWORDS**:** Meiosis, Meiotic Silencing by Unpaired DNA (MSUD), Spore Killing, Meiotic Drive Element

IDENTIFICATION OF NOVEL NUCLEAR PROTEINS REQUIRED FOR MEIOTIC SILENCING BY UNPAIRED DNA IN *NEUROSPORA CRASSA*

DIYAGAMA ARACHCHI RALALAGE DILINI SEWWANDI SAMARAJEEWA

A Dissertation Submitted in Partial
Fulfillment of the Requirements
for the Degree of

DOCTOR OF PHILOSOPHY

School of Biological Sciences

ILLINOIS STATE UNIVERSITY

2017

IDENTIFICATION OF NOVEL NUCLEAR PROTEINS REQUIRED FOR MEIOTIC SILENCING BY UNPAIRED DNA IN *NEUROSPORA CRASSA*

DIYAGAMA ARACHCHI RALALAGE DILINI SEWWANDI SAMARAJEEWA

COMMITTEE MEMBERS:

Thomas Hammond, Chair

Kevin Edwards

Erik Larson

Wade Nichols

Viktor Kirik

ACKNOWLEDGMENTS

I would like to express my deepest gratitude to my PI, Dr. Thomas Hammond for allowing me the opportunity to work in his lab. His endless guidance and unfailing support gave me throughout these four years have made this dissertation possible. Dr. Hammond not only supported me in my research work, but also took the place of my father walking me down the aisle on my wedding day. I will be forever grateful for his endless encouragement which made me become a stronger person during my four years of knowing him.

I would also like to extend my gratitude to my committee member Dr. Kevin Edwards for teaching me, advising me and, giving me his valuable time to utilize the confocal microscope. I would also like to offer my sincere thanks to my committee members Dr. Erik Larson, Dr. Wade Nichols and, Dr. Viktor Kirik for giving me valuable advice and directing me towards the successful completion of my dissertation. I would also like to thank all the past and current Hammond Lab members and especially the undergraduates who worked with me for the last couple of years. I extend my appreciation to the Illinois State University graduate School and school of Biological Sciences, for providing me a productive learning environment.

Finally, I would like to express gratitude to my family members. My late father, who would have loved to see who I have become today, was the greatest inspiration of my life. My mother and my brother stood up for me and gave me the strength when I needed the most. My husband Dinesh gave me his endless love, great support, and took care of me in dark moments of my life and had faith in me when I lost. My ever loving cat Bo was my greatest emotional support and became the never leaving shadow in dark and light moments of my life. It's adorable face and selfless love gives me the peace of my mind to see the bright side of every matter.

D. A. R. D. S. S.

CONTENTS

		Page
ACKNOWLEDGMENTS		i
CONTENTS		ii
CHAPTER II TABLES		v
CHAPTER III TABLES		vi
CHAPTER IV TABLES		vii
CHAPTER II FIGURES		viii
CHAPTER III FIGURES		ix
CHAPTER IV FIGURES		x
CHAPTER		
I.	INTRODUCTION: *NEUROSPORA CRASSA*	1
	Literature Cited	4
II.	EFFICIENT DETECTION OF UNPAIRED DNA REQUIRES A MEMBER OF THE RAD54-LIKE FAMILY OF HOMOLOGOUS RECOMBINATION PROTEINS	5
	Abstract	6
	Introduction	7
	Materials and Methods	10
	Strain information and culture conditions	10
	Transformations and transformation vectors	10
	MSUD suppression assays	11
	RNA sequencing and analysis	11
	Phylogenetic analysis of SAD-6	12
	Results	13
	Deletion of *ncu06190* suppresses MSUD	13
	SAD-6 is a member of the SNF2 family of chromatin remodeling proteins	13
	sad-6 transcript analysis suggests that it has functions outside of meiosis	15
	Characterization of basic developmental processes in *sad-6*$^{\Delta}$ strains	16

MSUD detects unpaired DNA with a spatially constrained search for DNA homology 16
MSUD is partially functional in homozygous *sad-6*$^{\Delta}$ crosses 17

Discussion 17
Acknowledgments 20
Literature Cited 37

III. AN RNA-RECOGNITION MOTIF-CONTAINING PROTEIN FUNCTIONS IN MEIOTIC SILENCING BY UNPAIRED DNA 44

Abstract 45
Introduction 46
Materials and Methods 52

Strains, media, culture conditions, crosses, and general techniques 52
Genetic modification of *N. crassa* 52
Gene expression analysis 53
Confocal microscopy 54

Results 55

N. crassa gene *ncu01917* is *sad-7* 55
SAD-7 is required for sexual development 56
SAD-7 mutant cultures are indistinguishable from wild type cultures under standard growth conditions 57
Sad-7 expression patterns are most similar to *sad-4* 57
SAD-7 homologs are present in a wide range of ascomycete fungi 59
GFP-SAD7 fusion proteins are found in the nucleus, perinuclear region, and cytoplasmic foci of meiotic cells 61

Discussion 64
Acknowledgments 68
Literature Cited 91

IV. IDENTIFICATION OF A GENETIC ELEMENT REQUIRED AND SUFFICIENT FOR SPORE KILLING IN NEUROSPORA 98

Abstract 99
Introduction 100
Materials and Methods 105

Strains, media, and crossing conditions 105
Transformation, genotype confirmation, and DNA sequencing 105
Statement on data and reagent availability 106

Results 107

Deletion of a DNA interval spanning most of *Sk-2*^{INS1} eliminates spore killing 107
A DNA interval between pseudogene *7378** and gene *6238* is required for spore killing 108
An ascus aborting element exists between pseudogene *7838** and gene *6238* 109
The AH36 interval from an *rfk-1*^{3211} strain does not cause ascus abortion 111
AH36 intervals from an *rfk-1*$^{+}$ strain and an *rfk-1*^{3211} strain have different DNA sequences 111

Discussion 112
Acknowledgments 116
Literature Cited 132

V. SUMMARY 137

Literature Cited 140

CHAPTER II TABLES

Table		Page
1.	Strains used in this study	21
2.	RNA transcript levels for quelling, MSUD, and other genes in *N. crassa* cultures	23
3.	Locations of r^{ef} insertions	24
4.	Oligonucleotide primers used in this study	25
5.	A complete list of crosses performed for probing the limits of unpaired DNA detection	28

CHAPTER III TABLES

Table		Page
1.	Strains used in this study	69
2.	MSUD is suppressed by *sad-7*$^{\Delta}$	70
3.	Homozygous *sad-7*$^{\Delta}$ crosses fail to produce ascospores	71
4.	Oligonucleotides used in this study	72

CHAPTER IV TABLES

Table		Page
1.	Strains used in this study	117
2.	Interval positions	119
3.	PCR primers used in this study	121

CHAPTER II FIGURES

Figure Page

1. Deletion of *ncu06190* suppresses MSUD 30

2. SAD-6 localizes within the nucleus during meiosis 32

3. Rad54-like proteins from four model fungi and humans 33

4. *sad-6*$^{\Delta}$ is similar to wild type in vegetative growth and production of asexual spores under standard growth conditions 34

5. Unpaired DNA detection in *N. crassa* is spatially constrained 35

6. *sad-6*$^{\Delta}$ is homozygous-fertile 36

CHAPTER III FIGURES

Figure		Page
1.	MSUD is suppressed in *sad-7*$^{\Delta}$ heterozygous crosses	73
2.	SAD-7 is required for ascus and ascospore development	74
3.	*sad-7*$^{+}$ is not required for conidiogenesis or linear growth	75
4.	Expression patterns of *sad-7* are most similar to *sad-4*	76
5.	SAD-7 is a widely conserved RRM protein in ascomycete fungi	78
6.	GFP-SAD7 is detected at three different locations in the ascus	80
7.	The meiotic localization pattern of GFP-SAD7 is independent on the first 206 amino acids of the protein	82
8.	SAD-7 homologs are present in a wide range of ascomycete fungi	83
9.	Alignment of RRM domains in a clade of Sordariales fungi	88
10.	The meiotic localization pattern of GFP-SAD-7 does not depend on the first 206 amino acids of the protein	89

CHAPTER IV FIGURES

Figure Page

1. The *Sk-2*^{INS1} locus harbors a genetic element required for spore killing 125

2. *Sk-2*^{INS1} interval positions 126

3. Deletion of a genetic element between pseudogene *7378** and the right border of *Sk-2*^{INS1} eliminates spore killing 127

4. Unpaired *Sk-2*^{INS1}-intervals do not kill ascospores in MSUD-proficient crosses 128

5. A genetic element found between pseudogene *7378** and the right border of *Sk-2*^{INS1} induces an ascus abortion phenotype 129

6. The *AH36* interval from an *rfk-1* mutant does not cause ascus abortion 130

7. Six point mutations exist in *AH36*^{3211} 131

CHAPTER I

INTRODUCTION: *NEUROSPORA CRASSA*

Neurospora crassa is a filamentous heterothallic ascomycete fungus. It was first identified as bread mold from French bakeries nearly two centuries ago. As research evidence, Shear and Dodge (1927) reported the sexual reproductive structures and the presence of two mating types of *Neurospora*. They also described three *Neurospora* species; *N. crassa*, *N. sitophila* and *N. tetrasperma* (Shear and Dodge, 1927). Later on, Beadle and Tatum (1941) conducted studies exposing *Neurospora crassa* to x-rays. It caused gene mutations resulting errors in specific enzymes leading to the failures in metabolic pathways. Following this observation, they proposed the "one gene-one enzyme" hypothesis. Since then *N. crassa* began to use as a model system in biochemical genetics (Beadle and Tatum 1941).

N. crassa spends majority of its life cycle in a haploid vegetative phase, while the diploid phase is limited to the sexual cycle. The vegetative phase composed of thread like hyphae and orange color powdery macroconidia. These macroconidia are dispersed by the wind to establish new colonies. The sexual cycle is induced by nitrogen limitation leading the formation of female sexual organ called protoperithecia (Ricci 1991). The protoperithecia produces a trichogyne which is a specialized form of hyphae (Elliott 1994). During mating, the trichogyne grows towards a male cell (conidium) of the opposite mating type chemotrophically and fuses (Borkovich *et al*. 2004). After completing the cytoplasmic fusion, both nucleus are fused together and undergoes two meiosis divisions and a post-meiotic mitosis division. This produces an ascus containing eight haploid ascospores. After fertilization and meiosis, the female structure turns into a dark color beaked fruiting body called perithecium. A mature perithecium may contain hundreds of asci. The ascospores reached into the maturity in about 14 days post fertilization, and forcibly shot from the perithecium. The disseminated ascospores spend a dormant period until the germination.

The complete genome sequence of *N. crassa* was reported by Galagan *et al*. (2003) enhancing the feasibility of using *N. crassa* as a tool in diverse eukaryotic research studies. *N. crassa* composed of seven chromosomes and the genome is about 43 megabases long. It encodes nearly 10,000 protein coding genes while *S. pombe* encodes nearly 4,800 genes and *S. cerevisiae* encodes about 6,300 genes (Galagan *et al*. 2003). However, a large number of genes in *N. crassa* are non-homologous to the *S. cerevisiae* protein coding genes.

N. crassa genome is protected by three main defense mechanisms throughout its life cycle. These mechanisms activate and silence by duplicated or unpaired genes in the vegetative or sexual phases. Among the defensive mechanisms, quelling is used to suppress transgenes introduced during the vegetative phase and the gene silencing is acquired via RNAi pathway (Romano and Macino 1992). Repeat Induced Point mutation (RIP) detects and silences the gene duplications before the nuclear fusion during sexual phase. The duplicated sequences are marked by converting G-C base pairs to A-T and methylated for degradation (Selker and Garrett 1988; Cambareri *et al*. 1989). Meiotic Silencing by Unpaired DNA (MSUD) is another gene silencing mechanism. It targets unpaired DNA during meiosis and the gene expression is silenced via RNAi pathway (Shiu *et al*. 2001; Aramayo and Metzenberg 1996).

Literature Cited

Beadle, G. W., and E. L. Tatum, 1941 Genetic control of biochemical reactions in Neurospora. Proceedings of the National Academy of Sciences, USA 27: 499–506.

Borkovich, K.A., *et al*, 2004 Lessons from the genome sequence of *Neurospora crassa*: tracing the path from genomic blueprint to multicellular organism. Microbiol. Mol. Biol. Rev. 68: 1–108.

Cambareri, E.B., B.C. Jensen, E. Schabtach, and E.U. Selker, 1989 Repeat-induced G-C to A-T mutations in Neurospora. Science 244 (4912), 1571-1575.

Elliott, C., 1994 Reproduction in Fungi. Chapman and Hall, London.

Galagan, J. E., S. E. Calvo, K. A. Borkovich, E. U. Selker, N. D. Read *et al.*, 2003 The genome sequence of the filamentous fungus *Neurospora crassa*. Nature 422: 859–868.

Ricci, M., D. Krappmann, and V.E.A. Russo, 1991 Nitrogen and carbon starvation regulate conidia and protoperithecia formation in *Neurospora crassa* grown on solid media. Fungal Genetics Newsletter 38: 87-88.

Romano, N., and G. Macino, 1992 Quelling: transient inactivation of gene expression in *Neurospora crassa* by transformation with homologous sequences. Mol Microbiol 6: 3343-3353.

Selker, E. U., and P. W. Garrett, 1988 DNA sequence duplications trigger gene inactivation in *Neurospora crassa*. Proc Natl Acad Sci USA 85: 6870-6874.

Shear, C. L. and B. O. Dodge, 1927 Life histories and heterothallism of the red bread-mold fungi of the *Monilia sitophila* group. Journal of Agricultural Research 34: 1019–1042.

Shiu, P.K., N.B. Raju, D. Zickler, and R.L. Metzenberg 2001 Meiotic silencing by unpaired DNA. Cell 107 (7), 905-916.

CHAPTER II

EFFICIENT DETECTION OF UNPAIRED DNA REQUIRES A MEMBER OF THE RAD54-LIKE FAMILY OF HOMOLOGOUS RECOMBINATION PROTEINS

This work has been published as:

Samarajeewa, D. A., P. A. Sauls, K. J. Sharp, Z. J. Smith, H. Xiao *et al*., 2014 Efficient detection of unpaired DNA requires a member of the rad54-like family of homologous recombination proteins. Genetics 198: 895–904.
(https://www.ncbi.nlm.nih.gov/pubmed/25146971)

Abstract

Meiotic silencing by unpaired DNA (MSUD) is a process that detects unpaired regions between homologous chromosomes and silences them for the duration of sexual development. While the phenomenon of MSUD is well recognized, the process that detects unpaired DNA is poorly understood. In this report, we provide two lines of evidence linking unpaired DNA detection to a physical search for DNA homology. First, we have found that a putative SNF2-family protein (SAD-6) is required for efficient MSUD in *Neurospora crassa*. SAD-6 is closely related to Rad54, a protein known to facilitate key steps in the repair of double-strand breaks by homologous recombination. Second, we have successfully masked unpaired DNA by placing identical transgenes at slightly different locations on homologous chromosomes. This masking falls apart when the distance between the transgenes is increased. We propose a model where unpaired DNA detection during MSUD is achieved through a spatially constrained search for DNA homology. The identity of SAD-6 as a Rad54 paralog suggests that this process may be similar to the searching mechanism used during homologous recombination.

Keywords: Meiosis, Homologous Recombination, Chromosome Pairing, RNA Silencing, Rad54

Introduction

MEIOSIS is fundamental to sexual reproduction. During meiosis, chromosomes are replicated, aligned, recombined, and segregated to nuclei that will develop into gametes. Two of these key processes, alignment and recombination, likely require a search for DNA homology between chromosomes (Barzel and Kupiec 2008; Moore and Shaw 2009). Such homology searching is necessary because sexual organisms inherit a copy of each chromosome from each of its parents. These chromosomes, referred to as homologs, must somehow find each other so that alignment, recombination, and segregation can occur.

Although recent research has improved our understanding of homology search mechanisms (Forget and Kowalczykowski 2012; Renkawitz *et al*. 2013), there are many questions that remain unanswered. The filamentous fungus *Neurospora crassa* may be useful for investigating the unknowns of homology searching because it possesses a genetically tractable phenomenon called meiotic silencing by unpaired DNA (MSUD) (Aramayo and Selker 2013; Billmyre *et al*. 2013). MSUD scans pairs of homologs for segments of DNA that are not accurately paired between them. If improper pairing (i.e., unpairing) is identified, the offending sequences are silenced for the duration of sexual development. For example, if a hypothetical gene called “gene A” is on the left arm of one chromosome but on the right arm of its homolog, it will be silenced. The same holds true if gene A has been lost from one of the homologs.

A functional MSUD response can be easily detected with alleles that affect ascospore (sexual spore) color or shape. Indeed, MSUD was discovered during studies of *ascospore maturation-1* (*asm-1*), a gene required for the production of pigmented (black) ascospores (Aramayo *et al.* 1996). A cross between an *asm-1*$^{+}$ strain and an *asm-1*$^{\Delta}$ strain produces mostly unpigmented (white) ascospores. This is because MSUD silences the unpaired *asm-1*$^{+}$ allele (Aramayo and Metzenberg 1996; Shiu *et al.* 2001). The efficiency of MSUD can be inferred

from such heterozygous *asm-1*$^{+}$/*asm-1*$^{\Delta}$ crosses by determining the ratio of black-to-white ascospores observed within asci (spore sacs) after their extraction from a perithecium (fruiting body). Alternately, because ascospores are forcibly shot to the lid of a crossing plate at the final stage of perithecial development, phenotypic ratios can be determined from ascospore suspensions made by collecting ascospores from a crossing lid.

Any gene that produces an aberrant ascospore phenotype when it is unpaired during meiosis can be used to determine the efficiency of MSUD. In addition to *asm-1*$^{+}$, one of the most common genes used is r^{+} [also referred to as *Round spore* (Mitchell 1966)]. r^{+} expression is required for ascospores to develop their normal shape, which is similar to that of an American football. When MSUD is functional during a heterozygous r^{+}/ r^{Δ} cross, round ascospores are produced instead of football-shaped ascospores because r^{+} is silenced (Shiu *et al.* 2001).

Genes that are required for MSUD can be identified through genetic screens for mutants that suppress MSUD efficiency. For example, the first MSUD gene was discovered by screening UV-induced mutants for the ability to produce black ascospores in crosses that were unpaired for *asm-1*$^{+}$ (Shiu *et al.* 2001). This approach has since been adapted for use with the *N. crassa* knockout collection (Colot *et al.* 2006). Essentially, strains from the collection are put through crosses where *asm-1*$^{+}$ or r^{+} is unpaired during meiosis (Hammond *et al.* 2011a). The production of phenotypically normal ascospores in such crosses suggests that the knockout (*i.e.*, deleted gene) suppresses MSUD, typically because the deleted gene encodes a necessary component of the MSUD machinery.

There are currently eight characterized MSUD genes, seven of which produce proteins that localize in a ring-like pattern around the nucleus. These seven include common RNA interference (RNAi) proteins such as an RNA-directed RNA polymerase called SAD-1 (Shiu *et al.* 2001), an Argonaute protein called SMS-2 (Lee *et al.* 2003), and a Dicer protein called DCL-

1 (Alexander *et al.* 2008). The four others are SAD-2, a presumptive scaffold protein (Shiu *et al.* 2006); SAD-3, a putative helicase (Hammond *et al.* 2011a); SAD-4, a protein required for MSUD-specific small RNA generation (Hammond *et al.* 2013a,b); and QIP, an exonuclease (Lee *et al.* 2010; Xiao *et al.* 2010). The eighth characterized MSUD gene encodes a nuclear protein called SAD-5 (Hammond *et al.* 2013b).

A simple working model of MSUD starts with the detection of unpaired DNA by an undetermined nuclear factor (Hammond *et al.* 2011a; Aramayo and Selker 2013). Unpaired DNA detection may then trigger the production of an "aberrant RNA" (aRNA), which could be delivered to a silencing complex stationed outside the nucleus. There, it could be made double-stranded (dsRNA) and processed into small RNAs by SAD-1 and DCL-1. While the hypothetical aRNA and dsRNA of MSUD have yet to be identified, the small RNAs have recently been discovered by deep sequencing (Hammond *et al.* 2013a,b). These small RNAs, referred to as MSUD-associated small interfering RNAs (masiRNAs), are thought to direct silencing of messenger RNAs by complementary base pairing.

MSUD is a remarkable process. It has the ability to identify and silence an unpaired segment of DNA as small as 700 bp between homologous chromosomes that are millions of base pairs long (Lee *et al.* 2004). Unfortunately, the identities of the proteins that mediate unpaired DNA detection have remained elusive. Although SAD-5 localizes within the nucleus, the role it plays in unpaired DNA detection is difficult to predict because it does not possess a characterized domain.

Here, we report the identification of SAD-6, a protein required for full MSUD functionality. Like SAD-5, SAD-6 is a nuclear MSUD protein, which raises the possibility that it is directly involved in unpaired DNA detection. More importantly, SAD-6 possesses a well-characterized domain that places it within a protein family that includes *Saccharomyces*

cerevisiae Rad54. Enzymes from this family participate in the search for DNA homology during double-strand break repair by homologous recombination. We thus designed a new technique called "unpaired DNA masking" to investigate the (possibly related) search process that occurs during MSUD.

Materials and Methods

Strain information and culture conditions

All strains used in this study are listed in Table 1. Vogel's minimal medium (VMM) (Vogel 1956) was used for vegetative cultures and synthetic crossing medium (SCM) (Westergaard and Mitchell 1947) was used for sexual crosses. While crosses and experiments were performed at room temperature, strain propagation was occasionally performed at 28°. Standard Neurospora techniques were used for all experiments unless otherwise indicated (Davis and De Serres 1970). Genetic markers and knockouts were obtained from the Fungal Genetics Stock Center (FGSC) (McCluskey *et al*. 2010) and the Neurospora Functional Genomics group (Colot *et al*. 2006), and their descriptions can be found in the e-Compendium (http://www.bioinformatics.leeds.ac.uk/~gen6ar/newgenelist/genes/gene_list.htm). Linear growth assays were performed in race tubes as previously described (Perkins and Pollard 1986).

Transformations and transformation vectors

Transformations were performed by electroporation of washed conidia (asexual spores) as described by Margolin *et al.* (1997), except that conidia were separated from the majority of mycelial (vegetative) fragments by filtering through a 100-μm nylon filter (Steriflip; Millipore, Billerica, MA). The transformation vectors for the targeted insertion of ectopic fragments of r^{+} (r^{ef}) were created by double-joint PCR (DJ-PCR) (Yu *et al.* 2004). DJ-PCR was also used to construct the vectors for tagging the native *sad-6* gene at its 5′ end with green fluorescent protein (*gfp*) (Hammond *et al.* 2011b) and the native *spo76* gene at its 5′ end with mCherryNC

(Castro-Longoria *et al.* 2010). A hygromycin resistance marker was used in all transformation vectors (Carroll *et al.* 1994). The *gfp-sad-5* and *gfp-sms-2* tags were described previously (Hammond *et al.* 2011b, 2013b). The sequences of the oligonucleotide primers used to construct all transformation vectors are listed and described in Supporting Information, Table 4.

MSUD suppression assays

MSUD efficiency was quantified with unidirectional or bidirectional crosses. The general method used for unidirectional crosses, where conidia from a "male" strain are used to fertilize protoperithecia (mating structures) of a "female" strain, is depicted in Figure 1, A–D. Detailed methods have been previously described (Hammond *et al.* 2011a). The general method used for bidirectional crosses, where both parents act as males and females, is depicted in Figure 1, E–H. For the bidirectional crosses, ascospores were collected from the lids of the crossing plates 27 days post-inoculation for analysis by low-magnification (100×) light microscopy. At least three replicates were performed for each cross.

RNA sequencing and analysis

We produced two independent RNA-seq datasets for this study. One was produced from strains with a *rid*$^{+}$ background (F2-01 × P9-42), while the other was produced from strains with a *rid* background (F2-26 × P6-07), where *rid* stands for *repeat-induced point mutation (RIP) defective* (Freitag *et al*. 2002).

Total RNA for RNA-seq was extracted from perithecia and associated vegetative tissue from 6-day-old directional crosses with TRIzol (Life Technologies, Grand Island, NY). The extracts were purified from residual genomic DNA and other potential contaminants with the PureLink RNA Mini Kit (Life Technologies). The RNA samples were then sent to the University of Illinois (Roy J. Carver Biotechnology Center, Urbana–Champaign, IL) where they were treated with the RiboZero Human/Mouse/Rat Kit (Illumina, San Diego) and used to make RNA

libraries with a TruSeq Stranded RNA-seq Sample Prep Kit (Illumina). The pooled libraries were then quantified by quantitative PCR (qPCR) and sequenced on one lane for 101 cycles from one end of the cDNA fragments on a HiSequation 2000, using the TruSeq SBS sequencing kit (version 3; Illumina). FASTQ files were generated with CASAVA (version 1.8.2; Illumina). The two data files have been deposited in the National Center for Biotechnology Information's (NCBI) Sequence Read Archive (SRA) (Leinonen *et al.* 2011). The accession numbers are SRR957218 for the *rid*$^{+}$cross and SRR957223 for the *rid* mutant cross.

For comparison of vegetative and sexual transcripts, *N. crassa* vegetative phase RNA-seq datasets SRR90363, SRR90364, and SRR90366 (Ellison *et al.* 2011) were downloaded from the SRA. RNA sequences from the vegetative and sexual datasets were aligned to all predicted *N. crassa* transcripts with Bowtie [version 2-2.1.0 (Langmead and Salzberg 2012)]. Reads per kilobase of exon model per million mapped reads (RPKM) (Mortazavi *et al.* 2008) were calculated with the aid of custom Perl scripts and Microsoft Excel.

Phylogenetic analysis of SAD-6

Amino acid sequences were aligned with Muscle, Version 3.8.31 (Edgar 2004) and a neighbor-joining tree was constructed using the p-distance method and a bootstrap test of 1000 replicates in MEGA5 (Tamura *et al.* 2011).

Results

Deletion of ncu06190 suppresses MSUD

We recently developed a high-throughput genetic screen for suppressors of MSUD (Hammond *et al.* 2011a). Preliminary data from this screen suggested that strains deleted of gene *ncu06190* are MSUD-deficient. To follow up on these data, we examined *ncu06190*$^{\Delta}$ in a quantitative assay of MSUD suppression.

Crosses between *N. crassa* wild-type strains typically produce black and football-shaped ascospores. However, when MSUD is active, crosses produce nearly 100% white ascospores when *asm-1*$^{+}$ is unpaired and nearly 100% round ascospores when *r*$^{+}$ is unpaired (Shiu *et al.* 2001). These aberrant phenotypes can be rescued by suppressing MSUD. Figure 1 details the results of MSUD-suppression assays with strains deleted for *ncu06190*. The results indicate that *ncu06190*$^{\Delta}$ is a suppressor of MSUD (Figure 1, I and J) and that the level of suppression is similar to that of two recently identified *sad*$^{\Delta}$ alleles [*sad-3*$^{\Delta}$ and *sad-4*$^{\Delta}$ (Hammond *et al.* 2011a, 2013b)]. Traditionally, the name "*sad*" is given to an MSUD suppressor because the first one was discovered during studies of strains that **s**uppress **a**scus **d**ominance (Aramayo and Metzenberg 1996; Shiu *et al.* 2001). Since deletion of *ncu06190* suppresses MSUD, we have renamed it *sad-6* for *suppressor of ascus dominance-6*.

SAD-6 is a member of the SNF2 family of chromatin remodeling proteins

The *N. crassa* genome database predicts that *sad-6* encodes an 1870-amino acid polypeptide. A search of NCBI's conserved domain database with this sequence predicts that SAD-6 has a helicase-like domain (data not shown). This is consistent with a recent survey that has placed SAD-6 in a Rad54-like subgroup of SNF2 helicase-related proteins (Flaus *et al.* 2006).

Rad54 and its homologs have been implicated in nuclear processes, including homologous recombination (Mazin *et al.* 2010; Ceballos and Heyer 2011). Therefore, if SAD-6

has Rad54-like functionality, we would expect to observe it in the nucleus. We tested this hypothesis by tagging SAD-6 with green fluorescent protein (GFP) and examining its localization during meiosis. As predicted, SAD-6 was observed to localize in a diffuse pattern within meiotic nuclei (Figure 2A), similar to that reported for SAD-5 (Figure 2C) (Hammond *et al.* 2013b). To determine that the diffuse localization pattern was not due to a technical artifact, we tagged *N. crassa* SPO76 with mCherryNC and visualized its localization pattern during meiosis. In *Sordaria macrospora*, SPO76 localizes to chromosomal axes during meiosis (Storlazzi *et al.* 2008). Our analysis indicates that SPO76 also localizes to chromosomal axes in *N. crassa* (Figure 2B). More importantly, the contrasting localization patterns for SPO76 and SAD-5/SAD-6 suggest that the diffuse patterns observed for SAD-5 and SAD-6 are biologically meaningful. We also reexamined a perinuclear protein, SMS-2. As expected, the perinuclear localization pattern of SMS-2 (Figure 2D) (Hammond *et al.* 2011b) contrasted with the nuclear localization patterns of SAD-5 and SAD-6.

The *N. crassa* ortholog of *S. cerevisiae* Rad54 is MUS-25 (Handa *et al.* 2000; Zhang *et al.* 2013). MUS-25 is the only other SNF2-family protein in *N. crassa* predicted to be a member of the Rad54-like group (Flaus *et al.* 2006), and it has been shown to be important for quelling, a vegetative RNA silencing process (Chang *et al.* 2012; Zhang *et al.* 2013). Accordingly, our own search of the *N. crassa* genome with the sequence of SAD-6 identified MUS-25 as the most similar protein of 24 matches (blastp, all *E* values were better than 1*e*-08).

To further investigate the relationship between SAD-6 and MUS-25, we created a phylogenetic tree with the sequences of Rad54-like proteins from humans and three non-*Neurospora* model fungi. We also included the sequences for SAD-6 and the five *N. crassa* proteins most similar to it. In this tree, SAD-6 clusters with Rad54-like homologs from other organisms, rather than with other SNF2-family proteins from *N. crassa*. This suggests that

SAD-6 and MUS-25 are more closely related to Rad54-like proteins from other organisms than they are to other SNF2 proteins from *N. crassa* (Figure 3).

sad-6 transcript analysis suggests that it has functions outside of meiosis

In a previous study, we used publically available *N. crassa* datasets to examine the transcript levels of MSUD genes under a vegetative culture condition (Hammond *et al.* 2013b). We found that transcripts from MSUD-specific genes are essentially undetectable at this time point in the *N. crassa* life cycle (after 24 hr of vegetative growth). In contrast, transcripts for genes that are shared between MSUD and quelling are easily detected under the same conditions (Hammond *et al.* 2013b).

To determine the expression pattern of *sad-6,* we included it in a similar analysis on three publically available *N. crassa* vegetative RNA datasets that were different from those analyzed in the previous study. In addition, we produced two new RNA datasets for analysis of transcripts from sexual cultures, *i.e.,* fertilized cultures undergoing meiosis and ascospore development. RPKM values (Mortazavi *et al.* 2008) were then calculated for *sad-6, mus-25,* quelling genes, MSUD genes, and two housekeeping genes (Table 2). Transcripts for quelling genes were present at similar levels in vegetative cultures (4.32–155.31 RPKM) and sexual cultures (6.24–247.54 RPKM). In contrast, transcripts for MSUD-specific genes were essentially undetectable in the vegetative RNA datasets (0.00–0.35 RPKM) but were found at relatively high levels in the sexual datasets (9.79–567.76 RPKM). *sad-6* transcripts were at relatively high levels in both vegetative and sexual RNAs (10.93 and 22.61 RPKM), demonstrating that *sad-6*'s expression pattern is more like those of quelling genes than of MSUD-specific genes. Its pattern is also similar to that of *mus-25* (6.56 and 13.51 RPKM), which is known to have roles in vegetative and sexual phases of the *N. crassa* life cycle (Handa *et al.* 2000; Zhang *et al.* 2013).

Overall, *sad-6*'s expression pattern suggests that it has roles in both vegetative and sexual processes.

Characterization of basic developmental processes in sad-6$^{\Delta}$ strains

Deletion or mutation of MSUD genes has not been observed to affect vegetative growth processes, such as growth rate, conidia production, or overall appearance under standard growth conditions (*e.g.*, Hammond *et al.* 2011a, 2013b). We therefore performed assays to determine whether *sad-6$^{\Delta}$* would be the first *sad* mutant associated with such defects. Like previously characterized *sad$^{\Delta}$* strains, *sad-6$^{\Delta}$* appears to have no effect on growth rate or morphological features of *N. crassa* cultures under standard growth conditions (Figure 4, A and B).

With respect to sexual development, many MSUD genes are essential. *sad-1^{+}*, for example, is absolutely required for meiosis and crosses homozygous for *sad-1$^{\Delta}$* are infertile (Shiu *et al.* 2001). However, we have recently found that not all MSUD genes are required for meiosis. An example is *sad-5^{+}*, whose deletion from both parents of a cross has no detectable effect on sexual development and ascospore production (Hammond *et al.* 2013b). We thus sought to examine whether *sad-6^{+}* is essential for sexual development. We found that homozygous *sad-6$^{\Delta}$* crosses complete meiosis and produce abundant levels of ascospores, demonstrating that *sad-6^{+}* is not critical for this part of the *N. crassa* life cycle (Figure 6).

MSUD detects unpaired DNA with a spatially constrained search for DNA homology

To gain new insight into the mechanism of unpaired DNA detection during MSUD, we tested its limits by placing an ectopic fragment of *r^{+}* (*r^{ef}*) at slightly different locations on chromosome VII in different strains (Table 3; Figure 5, A and B). We then performed a series of crosses between the strains and examined the efficiency of MSUD in each cross. Our findings demonstrate that when two *r^{ef}* are separated by a short distance (4.1 kb) on different homologs, they barely trigger MSUD even though they are at different positions (Figure 5C). However, as

the distance between two r^{ef} increases, the strength of MSUD also increases (Figure 5C). This suggests that the closer the fragments are to one another, the more likely they are to escape detection by MSUD. Surprisingly, even when fragments are separated by a distance of 37.6 kb, they often escape detection. Various interpretations of these data and how they could result from a SAD-6-mediated homology search are discussed below.

MSUD is partially functional in homozygous sad-6$^{\Delta}$ crosses

The fact that *sad-6*$^{\Delta}$ strains can be crossed to one another allowed us to test whether MSUD is completely deficient in crosses where both parents lack *sad-6*$^{+}$. Surprisingly, MSUD was partially functional in such crosses (Figure 1K), suggesting that another protein is functionally redundant with SAD-6 in MSUD.

Discussion

MSUD can be divided into at least two distinct processes: detection of unpaired DNA and its silencing. Since the initial discovery of MSUD in the laboratory of R. L. Metzenberg, much has been learned about the latter process. Essentially, it appears to be mediated by an elaborate silencing complex that stations itself around the perimeter of the nucleus, attempting to prevent mRNAs generated by the unpaired DNA from entering the cytoplasm. In contrast, little is known about how MSUD detects unpaired DNA and initiates the silencing process. Here, we have identified a new suppressor of MSUD: *sad-6*$^{\Delta}$. Since it is a nuclear protein, SAD-6 could directly participate in unpaired DNA detection.

The simplest explanation for the MSUD suppression phenotype in *sad-6*$^{\Delta}$ heterozygous crosses is that *sad-6*$^{+}$ encodes an MSUD protein and its absence in one parent results in haploinsufficiency. Additionally, by taking away its pairing partner, the *sad-6*$^{\Delta}$ allele may cause the *sad-6*$^{+}$ allele to undergo self-silencing (Shiu *et al.* 2006; Kasbekar 2012). For either scenario,

haploinsufficiency and/or self-silencing, MSUD suppression most likely results from insufficient levels of SAD-6.

One unexplained result in this study is the finding that MSUD is partially functional in homozygous *sad-6*$^{\Delta}$ crosses. One possibility is that an unidentified protein is functionally redundant with SAD-6. An obvious candidate is MUS-25. Unfortunately, MSUD-suppression assays of *mus-25*$^{\Delta}$ with unpaired *asm-1*$^{+}$ and *r*$^{+}$ have produced conflicting results; while some experiments suggested no difference in MSUD efficiency, others suggested a slight suppression (our unpublished results). This variability may be related to the aberrant meiosis and low fertility of heterozygous *mus-25*$^{+}$/*mus-25*$^{\Delta}$ crosses. While we have not investigated a *mus-25*$^{\Delta}$ *sad-6*$^{\Delta}$ mutant, it seems likely that such a strain would not be more fertile than the *mus-25*$^{\Delta}$ single mutant.

SNF2-family proteins are required for efficient homologous recombination in eukaryotes (Flaus *et al.* 2006; Ceballos and Heyer 2011; Hopfner *et al.* 2012). In *N. crassa*, MUS-25 and at least three other SNF2-family proteins have been implicated in homologous recombination (Handa *et al.* 2000; Zhang *et al.* 2013). These are *swr1* (NCU09993), *chd1* (NCU03060), and *isw1* (NCU03875), two of which are included in Figure 3 because of their similarity to SAD-6. Given the connection between SNF2-family proteins and homologous recombination, it is conceivable that SAD-6 may help detect unpaired DNA during MSUD through a homology search process similar to that used during homologous recombination.

Homologous recombination is one of the methods used to repair double-strand breaks in DNA (San Filippo *et al.* 2008; Jasin and Rothstein 2013). During this process, a Rad51-coated single-stranded (ss) molecule of DNA invades a dsDNA template and searches for homology (Forget and Kowalczykowski 2012; Renkawitz *et al.* 2013). A recently proposed model suggests that Rad54 aids this homology search in at least two ways (Wright and Heyer 2014): first, by

driving together heteroduplex DNA, which consists of the invading strand and its complement within the original dsDNA template; and second, by dissociating the invading strand if it does not encounter a fully homologous complement. The close relationship between SAD-6 and Rad54 suggests that SAD-6 could promote homology identification in a similar manner.

It is also possible that the strand-invasion-based homology search used for homologous recombination is not related to the unpaired DNA detection process of MSUD. Recent evidence suggests that the homology search for *N. crassa* RIP (discussed below) does not require dsDNA strand breaks (Gladyshev and Kleckner 2014). If a similar (break-independent) process is used to identify homology during MSUD, then perhaps SAD-6's role in MSUD is to remodel chromatin. Accordingly, some SNF2-family members are chromatin remodelers and even Rad54 has been shown to possess the ability to translocate on DNA and slide nucleosomes (Alexeev *et al.* 2003; Amitani *et al.* 2006; Ryan and Owen-Hughes 2011). SAD-6's role in MSUD could thus be to clear DNA of associated proteins, making the search for unpaired DNA possible by homologous recombination-related or unrelated mechanisms.

In addition to MSUD, *N. crassa* possesses another genome-scanning process called RIP, which occurs just before meiosis and involves a search for repeated sequences (Galagan and Selker 2004). The scanning process of MSUD may not need to be as broad as it is in RIP and other genome-wide scanning processes; that is, it should be necessary only to compare allelic positions between the paired homologs. However, it may not be as straightforward as lining up the homologs and testing the bases "one by one." In fact, the experimental results reported here have shown that DNA does not have to be perfectly allelic to be considered paired. Unpaired DNA detection thus seems to involve a certain level of chance and the probability of marking homologous DNA fragments as paired decreases as the distance between them increases. This inexact method of homology searching could be a common characteristic of processes that

involve identifying homologous sequences within a genome, which would help explain how such searches are achieved in an energy-efficient and timely manner.

Acknowledgments

We are grateful to the members of our laboratories and colleagues from our community for their help and to the Broad Institute of Harvard and Massachusetts Institute of Technology for access to version 12 of the Neurospora genome and annotation. We acknowledge use of materials generated by the National Institute of General Medical Sciences-funded project "Functional Analysis of a Model Filamentous Fungus" (P01 GM068087). E.C.B. was supported by a Graduate Assistance in Areas of National Need Fellowship from the U.S. Department of Education. This work was supported by the National Science Foundation (MCB1157942, to P.K.T.S.) and the National Institutes of Health (1R15HD076309-01, to T.M.H.).

Table 1. Strains used in this study.

Strain name	Genotype
F2-01	*fl A*
F2-24	*rid his-3*$^{+}$::*asm-1*; *fl*; *asm-1*$^{\Delta}$::*hph a*
F2-26	*rid*; *fl a*
F2-27	*rid r*$^{\Delta}$::*hph*; *fl a*
FGSC 19985	*sad-6*$^{\Delta}$::*hph a*
ISU 3036	*rid*; *fl*; *sad-2*$^{\Delta}$::*hph A*
ISU 3037	*rid*; *fl*; *sad-2*$^{\Delta}$::*hph a*
ISU 3111	*sad-6*$^{\Delta}$::*hph A*
ISU 3112	*sad-6*$^{\Delta}$::*hph a*
ISU 3113	*fl*; *sad-6*$^{\Delta}$::*hph A*
ISU 3114	*rid his-3*; *mus-52*$^{\Delta}$::*bar*; *VIIL*::*r*^{ef4}*-hph A*
ISU 3115	*rid*; *fl*; *VIIL*::*r*^{ef4}*-hph a*
ISU 3116	*rid*; *fl*; *mus-52*$^{\Delta}$::*bar*;*VIIL*::*r*^{ef2}*-hph a*
ISU 3117	*rid his-3*; *VIIL*::*r*^{ef2}*-hph A*
ISU 3118	*rid his-3*; *mus-52*$^{\Delta}$::*bar*; *VIIL*::*r*^{ef1}*-hph A*
ISU 3119	*rid his-3*; *mus-52*$^{\Delta}$::*bar*; *VIIL*::*r*^{ef3}*-hph A*
ISU 3121	*rid his-3*; *gfp-sad-6-hph a*
ISU 3122	*rid his-3*; *gfp-sad-5-hph A*
ISU 3123	*rid*; *mus-52*$^{\Delta}$::*bar mCherryNC-spo76*::*hph a*

(Table continues)

Table 1 continues. Strains used in this study.

Strain name	Genotype
ISU 3127	*rid*; *fl*; *VIIL*::r^{ef5}-*hph a*
P3-07	Oak Ridge wild type (WT) *A*
P6-07	*rid A*
P8-01	*sad-2*$^{\Delta}$::*hph A*
P8-43	*rid his-3*; *mus-52*$^{\Delta}$::*bar A*
P9-42	Oak Ridge wild type (WT) *a*
P10-15	*rid his-3 A*
P15-22	*rid his-3*; *mus-52*$^{\Delta}$::*bar*; *gfp-sms-2*::*hph A*

All strains used in this study are descendants of lines 74-OR23-1VA (FGSC 2489) and 74-ORS-6a (FGSC 4200) (Perkins 2004).
[a]The allele for *mus-52* was not determined (*mus-52*$^{+}$ or *mus-52*$^{\Delta}$::*bar*).
[b]The allele for rid was not determined (*rid*$^{+}$ or *rid*).

Table 2. RNA transcript levels for quelling, MSUD, and other genes in *N. crassa* cultures.

Gene name	Gene no.	Vegetative transcript levels (RPKM)	Sexual transcript levels (RPKM)
Quelling			
dcl-1[a]	*ncu08270*	4.32 ± 0.73	31.96 ± 2.33
dcl-2	*ncu06766*	17.92 ± 18.61	43.13 ± 2.02
qde-1	*ncu07534*	16.31 ± 2.07	19.90 ± 4.55
qde-2	*ncu04730*	155.31 ± 155.10	247.54 ± 2.28
qde-3	*ncu08598*	11.37 ± 1.97	6.24 ± 0.23
qip[a]	*ncu00076*	25.01 ± 10.95	99.55 ± 3.46
MSUD			
sad-1	*ncu02178*	0.35 ± 0.20	16.84 ± 2.82
sad-2	*ncu04294*	0.02 ± 0.03	35.22 ± 2.13
sad-3	*ncu09211*	0.02 ± 0.03	23.50 ± 3.82
sad-4	*ncu01591*	0.15 ± 0.05	9.79 ± 2.65
sad-5	*ncu06147*	0.00 ± 0.00	13.08 ± 1.85
sms-2	*ncu09434*	0.04 ± 0.07	567.76 ± 63.63

(Table continues)

Table 2 continues. RNA transcript levels for quelling, MSUD, and other genes in *N. crassa* cultures.

Gene name	Gene no.	Vegetative transcript levels (RPKM)	Sexual transcript levels (RPKM)
Rad54-like			
mus-25	*ncu02348*	6.56 ± 0.43	13.51 ± 3.54
sad-6	*ncu06190*	10.93 ± 0.71	22.61 ± 1.34
Housekeeping			
β-tubulin	*ncu04054*	1160.22 ± 70.15	131.34 ± 17.73
actin	*ncu04173*	2274.02 ± 256.81	583.44 ± 56.30

RPKM, reads per kilobase of exon model per million mapped reads.
[a]*dcl-1* and *qip* have roles in both MSUD and quelling (Catalanotto *et al*. 2004; Maiti *et al*. 2007; Alexander *et al*. 2008; Lee *et al*. 2010; Xiao *et al*. 2010).

Table 3. Locations of r^{ef} insertions.

r^{ef} vector no.	Location
r1	VII: 214,752–214,773
r2	VII: 218,848 –219,011
r3	VII: 232,895 –232,984
r4	VII: 241,034 –241,159
r5	VII: 256,797 –256,822
r6	VII: 1,918,140 –1,918,315

A 4.1-kb r^{ef}-*hph* fusion construct was placed between the indicated positions on chromosome VII. The sequences between the indicated positions were deleted in the process.

Table 4. Oligonucleotide primers used in this study.

Name	Sequence
r^{ef} fragment amplification	
Eco-RSP-F	CAGAATTCAGTCGAGGACAGAACGCAGCA
Eco-RSP-R	TTGAATTCTTGGACCTCTTCCGCAGTTTCC
hph marker amplification	
APAI-HPH-F	AAGGGCCCAACTGATATTGAAGGAGCAT
APAI-HPH-R	AAGGGCCCAACTGGTTCCCGGTCGGCAT
r^{ef}*-hph* amplification (center fragment for DJ-PCR)	
Rsp-center-A	AGGACAGAACGCAGCAGCAGAGC
Rsp-center-B	ACAGCGAACGAAACCCCTGAAAC
r^{ef}*-hph* insertion between *ncu09443* and *ncu09444*	
Rsp-040613C	TAGTGGAGGGGCTTGGGATGGT
Rsp-040613D	AGAGAAGCTCTGCTGCTGCGTTCTGTCCTCTGCTGAACGAACACC CCTGCT
Rsp-040613E	TAACGGGTTTCAGGGGTTTCGTTCGCTGTCGTCCACTGATCTTCGC TAGAATTT
Rsp-040613F	TCACCGCCCGTCCCTACTATCA
Rsp-040613G	GCCTTGGACTGGTGATGGTGCT
Rsp-040613H	GGAGGAGTCGGTTTGCTTTGGTG
r^{ef}*-hph* insertion between *ncu09444* and *ncu09445*	
Rsp-040613I	ATGAGGGAGGTGCCGTGTCC
Rsp-040613J	AGAGAAGCTCTGCTGCTGCGTTCTGTCCTCCATTCTGCCATTTCCC ATGC
Rsp-040613K	TAACGGGTTTCAGGGGTTTCGTTCGCTGTCCGCACACTTTCTCCAC CCATC
Rsp-040613L	GCAATCCACCTCTGGCATCGAC
Rsp-040613M	AGCCAATCCTTTACCGACTCCAACA
Rsp-040613N	GTGGTTCTCGCCCGCTTTCAAC

(Table continues)

Table 4 continues. Oligonucleotide primers used in this study.

Name	Sequence
r^{ef}*-hph* insertion between *ncu09449* and *ncu09450*	
RSP-042613-A	CGAGGGCCGAGTCTGGTGGTTA
RSP-042613-B	AGAGAAGCTCTGCTGCTGCGTTCTGTCCTGTACTAGCGTTTGCGC GGGACA
RSP-042613-C	TAACGGGTTTCAGGGGTTTCGTTCGCTGTAGGTGGGAAAGTGTTA GTGGTGGA
RSP-042613-D	GTTGAGGGTCTTGAGGGCGAAG
RSP-042613-E	TCTCACACGTTGCTTCGGCTGT
RSP-042613-F	GAGGTTCTGGTTGGCTGGTTGG
r^{ef}*-hph* insertion between *ncu09451* and *ncu17161*	
RSP-042613-A	AAGTGGGCGTTGAAGGAGGATG
RSP-042613-B	AGAGAAGCTCTGCTGCTGCGTTCTGTCCTCGGAGGTCGGAGACGA GATG
RSP-042613-C	TAACGGGTTTCAGGGGTTTCGTTCGCTGTCCAAGTCCTCCATCCG TCCATC
RSP-042613-D	TTCATCCAGCAATCCACCACCA
RSP-042613-E	CCTCTTCACCCTCTACCCAAACGA
RSP-042613-F	AGCGACCATCCCAAACCAACAA
r-hph insertion between *ncu09455* and *ncu09456*	
RSP-050213-A	CAGACAGTGGTGGGAAGGTGGTC
RSP-050213-B	AGAGAAGCTCTGCTGCTGCGTTCTGTCCTCAGTGCGGAAATGGAA GGGAGAG
RSP-050213-C	TAACGGGTTTCAGGGGTTTCGTTCGCTGTCGGCCATCACGGTCAA AGAAAC
RSP-050213-D	ATGGTGCCGACGCTAAAGGAGA
RSP-050213-E	CGTTCCGTCATTCGGGTATTGC
RSP-050213-F	ACGCAGGGAGGGAGATTGCCTA
rad-54$^{\Delta}$::*hph* vector construction (note that gene number has changed since the primers were designed)	
NCU11255-L1	CAGTTTGGGCATCTCATCGCCTAC
NCU11255-L2	ATGCTCCTTCAATATCAGTTCGCTGTAAGGAACGGGCTTTGTT
NCU11255-R1	ATGCCGACCGGGAACCAGTTAGTTTTGGGTGTCGTCGGATGGT
NCU11255-R2	AGCAGTTTCTCTCCCCCTCATTCA
NCU11255-N1	GCGATGACCAACTGGGAGAAGAA
NCU11255-N2	ATTTTCGTGGACGCGGACCAG

(Table continues)

Table 4 continues. Oligonucleotide primers used in this study.

Name	Sequence
Construction *sad-6 gfp* tagging vector	
NCU06190-E	TTGAAAATGCGAGGATAAGACGAAGA
NCU06190-NGFP1	GCAGCCTGAATGGCGAATGGACGCGCCAAGTGTGAAAGCAATCTGTGTTGGA
NCU06190-NGFP2	CAGGAGCGGGTGCGGGTGCTGGAGCGATGGCCGAACTCAACGAAAATGAACC
NCU06190-F	CCTCTCCAAAGTCCAAGACGACCT
NCU06190-G	TGCCCAACAGATAACGTGACTTCG
NCU06190-H	TTGGCATCGGAAAGAAAGGTGCT
onstruction of *spo76 mCherryNC* tagging vector	
NCU00424-E	ACTCGCAAGCAAGGCACTGAA
NCU00424-X1	GCAGCCTGAATGGCGAATGGACGCGCCCTGCGTATGATCTTGAGGACGAG
NCU00424-X2	CAGGAGCGGGTGCGGGTGCTGGAGCGATGGCGCCACGTCGAAGCGCTC
NCU00424-F	TCACTTGGGGTTCCGCTCTTTCT
NCU00424-G	CAAAGGCCCCCATCCAGTACGA
NCU00424-H	TCTTTTCCAACCTGCTCTCCCTTG

Table 5. A complete list of crosses performed for probing the limits of unpaired DNA detection.

Cross #	Strain names	*r*[ef] locations	Round spores (%)	STDEV
1	1005.2 x P10-15	wt x wt	0.00	0.00
2	1005.2 x 7.2.1	wt x r1	0.99	0.00
3	1005.2 x 6.1.3	wt x r2	0.96	0.03
4	6.1.2B x P10-15	r2 x wt	0.98	0.01
5	6.1.2B x 6.1.3	r2 x r2	0.00	0.00
6	6.1.2B x 7.2.1	r1 x r2	0.05	0.01
7	1005.2 x P10-15	wt x wt	0.01	0.00
8	6.1.2B x P10-15	r2 x wt	0.92	0.06
9	1005.2 x 6.1.3	wt x r2	0.94	0.05
10	1005.2 x 13.2.2	wt x r3	0.87	0.15
11	6.1.2B x 6.1.3	r2 x r2	0.00	0.00
12	6.1.2B x 13.2.2	r2 x r3	0.34	0.06
13	RTPS6.1.2B x P10-15	r2 x wt	1.00	0.00
14	RZS1.20 x P10-15	r5 x wt	0.99	0.01
15	1005.2 x RZS1.2	wt x r5	0.97	0.01
16	1005.2 x 6.1.3	wt x r2	0.90**	0.05
17	1005.2 x 13.2.2	wt x r3	0.89	0.05
18	RTPS6.1.2B x RZS1.2	r2 x r5	0.68	0.02
19	RZS1.20 x 6.1.3	r5 x r2	0.54	0.04
20	RZS1.20 x 13.2.2	r5 x r3	0.42	0.06
21	RTPS6.1.2B x 13.2.2	r2 x r3	0.19	0.03
22	RZS1.2 x RZS1.20	r5 x r5	0.00	0.00
23	1005.2 x P10-15	wt x wt	0.00	0.00
24	RTPS6.1.2B x 6.1.3	r2 x r2	0.00	0.00
25	RKS10.1.9 x P10-15	r4 x wt	1.00	0.00
26	RTPS6.1.2B x P10-15	r2 x wt	0.97	0.02
27	1005.2 x RTPS 7.2.1	wt x r1	0.98	0.02
28	1005.2 x RZS1.2	wt x r5	0.97	0.04
29	1005.2 x RKS10.1.8	wt x r4	0.95	0.01
30	1005.2 x RTPS 6.1.3	wt x r2	0.80*	0.15
31	RTPS6.1.2B x RZS1.2	r2 x r5	0.67	0.04
32	RKS10.1.9 x 7.2.1	r4 x r1	0.34	0.07

(Table continues)

Table 5 continues. A complete list of crosses performed for probing the limits of unpaired DNA detection.

Cross #	Strain names	*r*^{ef} locations	Round spores (%)	STDEV
33	RTPS6.1.2B x RKS10.1.8	r2 x r4	0.29	0.06
34	RKS10.1.9 x 6.1.3	r4 x r2	0.21	0.06
35	RKS10.1.9 x RZS1.2	r4 x r5	0.21	0.08
36	RTPS6.1.2B x RTPS7.2.1	r2 x r1	0.05	0.02
37	RTPS6.1.2B x 6.1.3	r2 x r2	0.00	0.01
38	RKS10.1.9 x RKS10.1.8	r4 x r4	0.00	0.00
39	1005.2 x P10-15	wt x wt	0.00	0.00

This table is a complete list of crosses performed during the unpaired DNA masking experiments. The average percentage of round spores produced by each cross (in triplicate) and its standard deviation value are indicated. *An outlier believed to be the result of an experimental artifact.

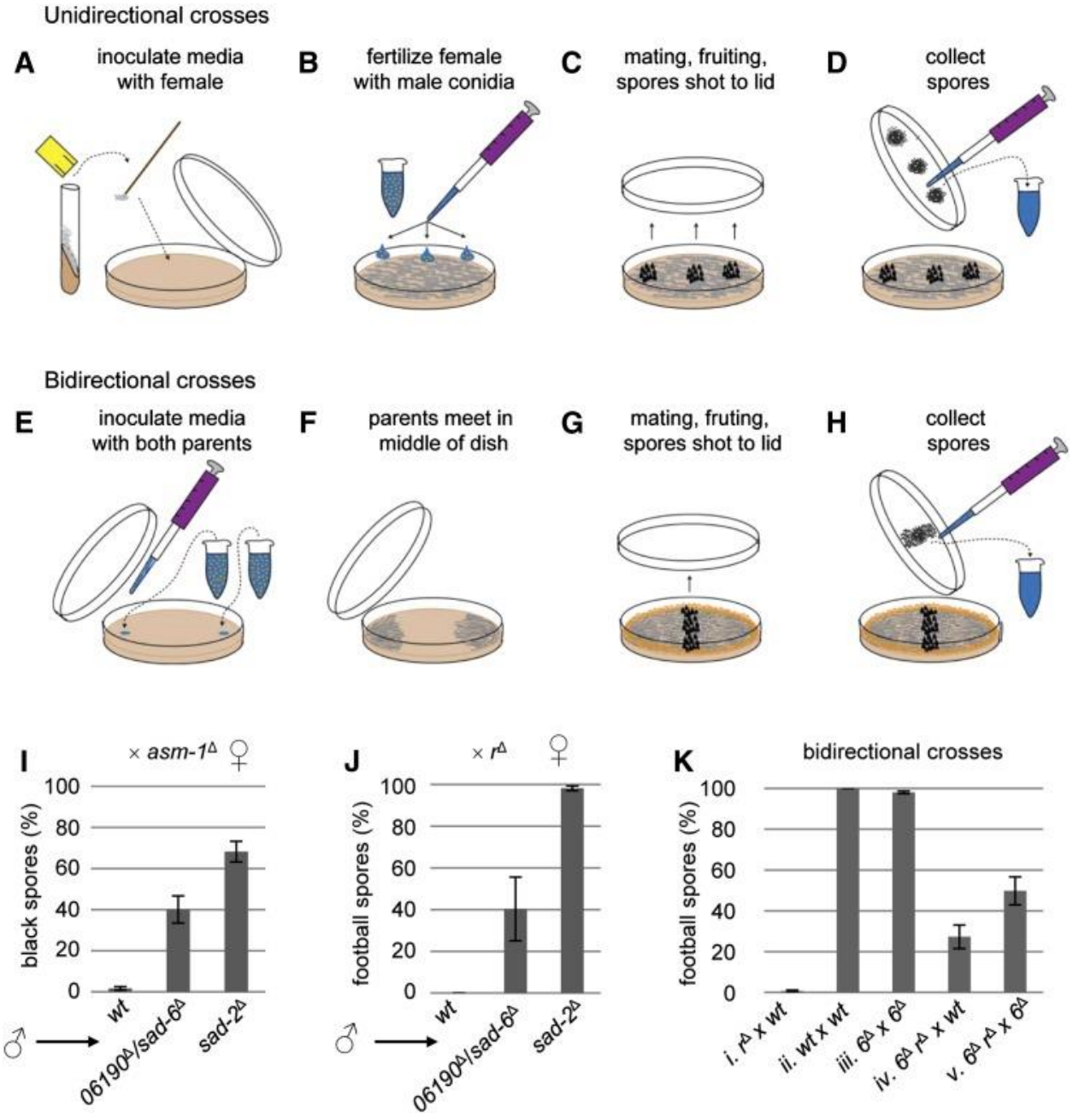

Figure 1. Deletion of *ncu06190* suppresses MSUD. Unidirectional and bidirectional crosses were performed to test whether deletion of *ncu06190* suppresses MSUD. (A–D) The methods used to quantify MSUD efficiency with unidirectional crosses. (A) The female parent was transferred to a 60-mm petri dish containing SCM and cultured for 6 days. (B) The female strain was fertilized at three locations with a suspension of conidia from the male parent. (C) The cultures were incubated at room temperature for 3 weeks, during which perithecia developed and ascospores were shot to the lids of the petri dishes. (D) Ascospores were collected from the lids and suspended in water for analysis by microscopy. (E–H) The methods used to quantify MSUD efficiency with bidirectional crosses. (E) Conidial suspensions of each parent were transferred to the edges of 100-mm petri dishes containing SCM. (F) Parents grew across the petri dishes. (G)

Mating and perithecium development occurred predominantly along the middle of the petri dishes. Conidia developed predominantly along the edges of the petri dishes, but this did not interfere with the experiments. (H) Ascospores were collected from the lids of the petri dishes and suspended in water for phenotypic analysis by microscopy when the crosses were 27 days old. A–H are adapted from Harvey *et al.* (2014). (I) Unidirectional crosses of *wt*, *ncu06190*$^{\Delta}$/*sad-6*$^{\Delta}$, and *sad-2*$^{\Delta}$ (males) to *asm-1*$^{\Delta}$ (female) resulted in 2%, 40%, and 68% black ascospores, respectively, demonstrating that MSUD of unpaired *asm-1*$^{+}$ is suppressed by *ncu06190*$^{\Delta}$/*sad-6*$^{\Delta}$. (J) Unidirectional crosses of *wt*, *ncu06190*$^{\Delta}$/*sad-6*$^{\Delta}$, and *sad-2*$^{\Delta}$ (males) to *r*$^{\Delta}$ (female) resulted in 0%, 40%, and 98% football-shaped ascospores, respectively, demonstrating that MSUD of unpaired *r*$^{+}$ is suppressed by *ncu06190*$^{\Delta}$/*sad-6*$^{\Delta}$. (K) Bidirectional crosses were performed to determine whether MSUD is completely dysfunctional when *ncu06190*$^{+}$/*sad-6*$^{+}$ is missing from both parents. However, the results indicate that MSUD of unpaired *r*$^{+}$ is still partially functional when both parents carry the *ncu06190*$^{\Delta}$/*sad-6*$^{\Delta}$ allele (abbreviated as *6*$^{\Delta}$). (I–K) "*wt*" is used to indicate strains that are wild type for all MSUD genes. The error bars depict standard deviation values. (I and J) Strains: *wt* P3-07, *06190*$^{\Delta}$/*sad-6*$^{\Delta}$ ISU 3111, *sad-2*$^{\Delta}$ P8-01, *asm-1*$^{\Delta}$F3-24, and *r*$^{\Delta}$ F2-27. (K) Strains: i, P12-01 × P9-42; ii, P3-07 × P9-42; iii, ISU 3111 × ISU 3112; iv, ISU 3154 × P9-42; and v, ISU 3154 × ISU 3112.

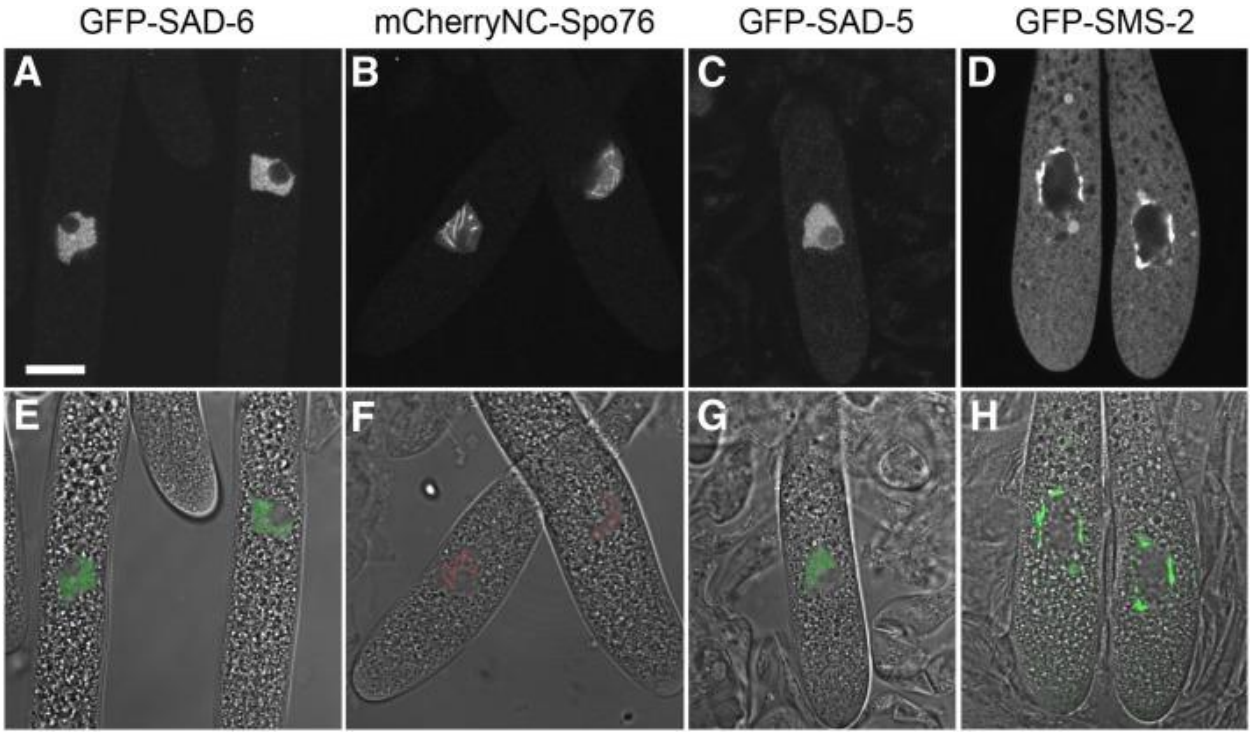

Figure 2. SAD-6 localizes within the nucleus during meiosis. (A and E) SAD-6 displays a diffuse nuclear localization pattern (excluding the nucleolus) within prophase asci (ISU 3036 × ISU 3121). (B and F) SPO76 localizes to chromosomal axes (ISU 3036 × ISU 3123). (C and G) SAD-5 (ISU 3037 × ISU 3122) and (D and H) SMS-2 (ISU 3037 × P15-22) localize within the nuclear and perinuclear regions, respectively, which is consistent with previous findings (Hammond *et al.* 2011b, 2013b). All asci were fixed and prepared for imaging as previously described (Hammond *et al.* 2011b). Images were obtained with a Leica SP2 system. All fluorescent images are shown with original contrast with no σ-curve used. The transmitted light image is shown in grayscale, overlaid with the GFP (green) or mCherryNC (red) image. Bar, 10 μm.

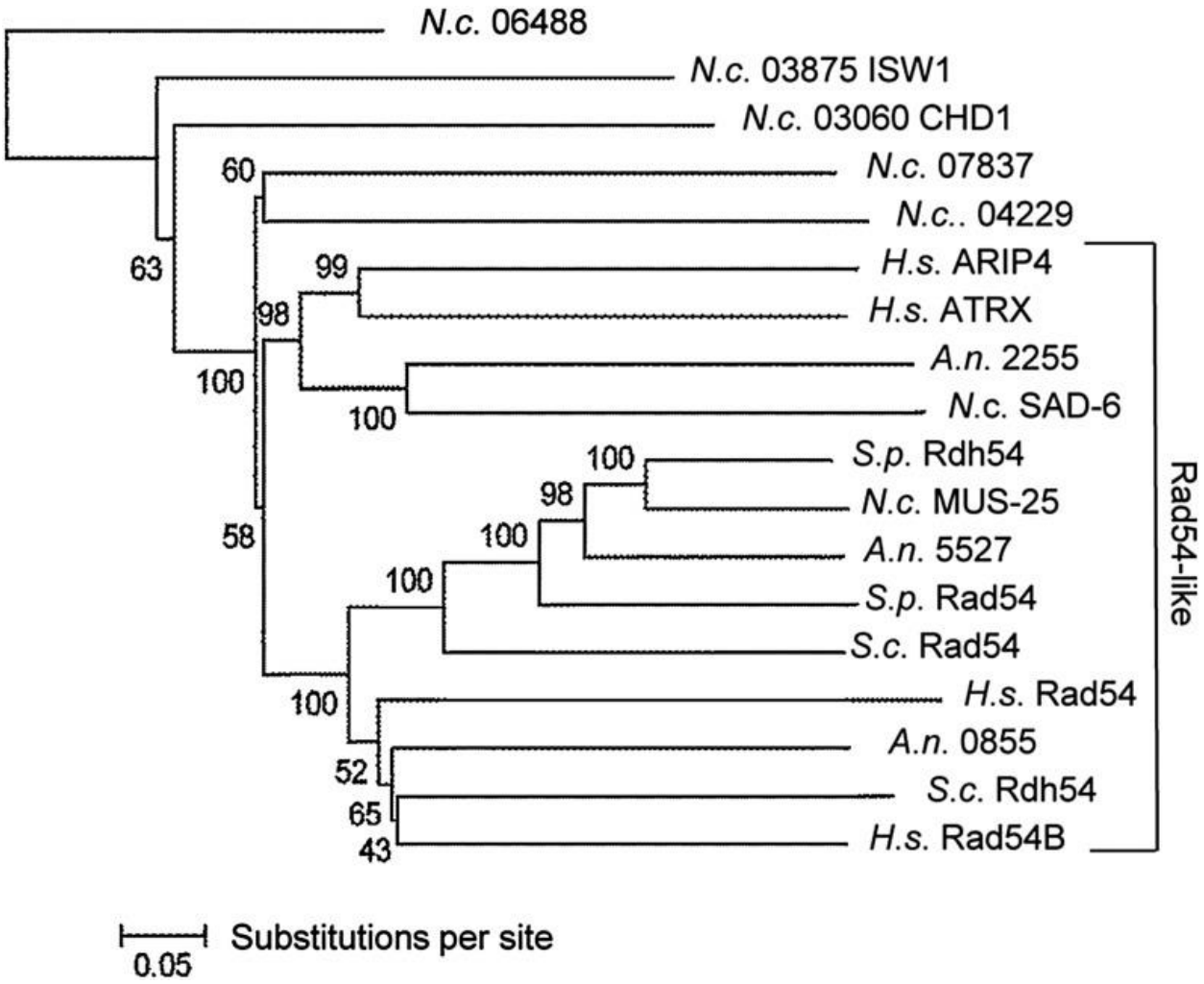

Figure 3. Rad54-like proteins from four model fungi and humans. Sequences of Rad54-like proteins from *Homo sapiens*, *S. cerevisiae*, *Schizosaccharomyces pombe*, and *Aspergillus nidulans* (Flaus *et al.* 2006) were downloaded from the NCBI, while the *N. crassa* sequences were downloaded from the *N. crassa* genome database.

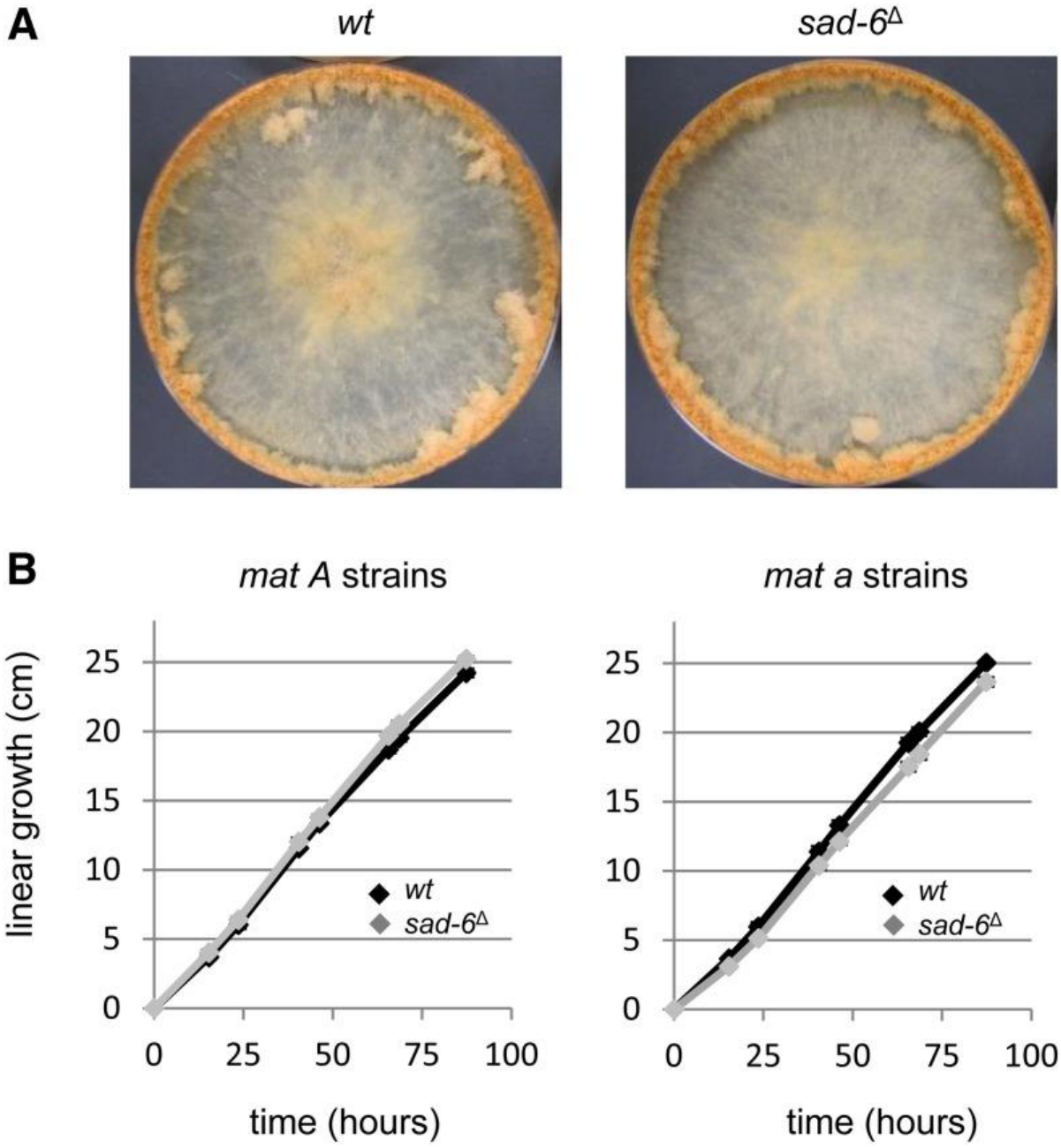

Figure 4. *sad-6*$^{\Delta}$ is similar to wild type in vegetative growth and production of asexual spores under standard growth conditions. (A) For each strain, 3 µl of a conidial suspension (1000 conidia per microliter) was inoculated to the center of a 150-mm culture dish. Three dishes were inoculated for each strain. Photographs were taken after growing the cultures for 8 days at room temperature. Only a single representative photograph is shown for each strain. (B) Linear growth assays were performed in triplicate. Most of the error bars, representing the standard deviation, are too small to be seen in the charts. (A) Left, wt P3-07; right, *sad-6*$^{\Delta}$ ISU 3111. (B) Left, P3- and ISU 3111; right, P9-42 and ISU 3112.

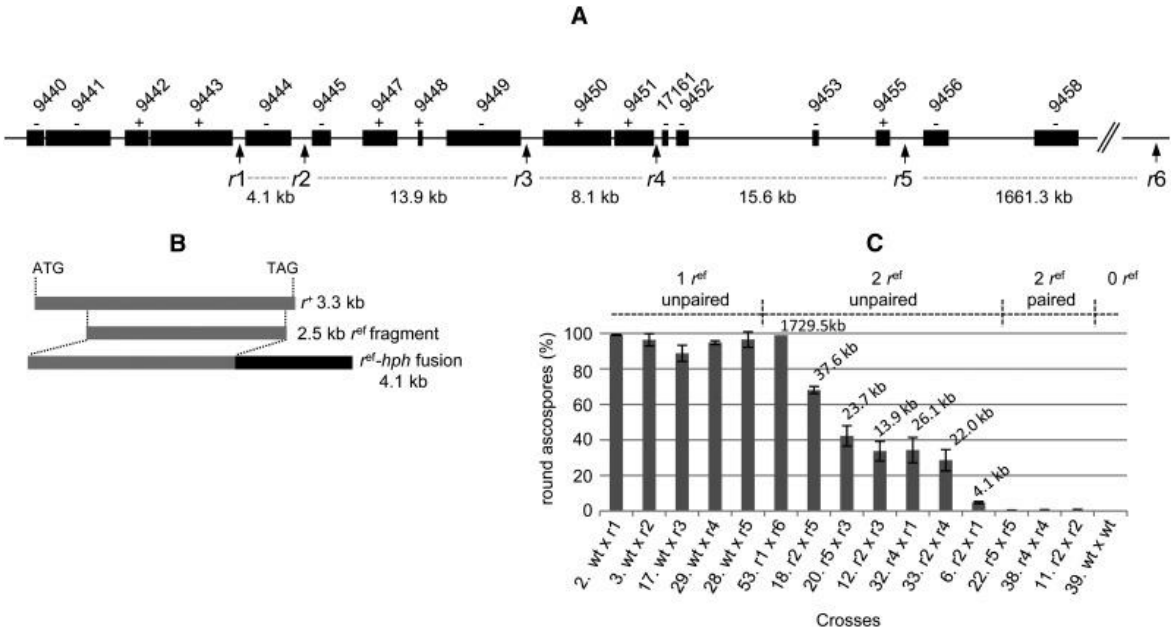

Figure 5. Unpaired DNA detection in *N. crassa* is spatially constrained. (A) Six locations (*r*1–*r*6) on chromosome VII were chosen for the insertion of an ectopic fragment (r^{ef}) of r^{+}. Predicted genes (black boxes) are labeled with their database numbers. Their coding directions are indicated with a "+" (for left to right) and a "–" (for right to left). Distances between the insertion sites are shown below the dashed lines. (B) The components of the r^{ef} construct are shown. The native r^{+} coding region is 3.3 kb long and is found on chromosome I. A 2.3-kb fragment was taken from the 3′ end and joined to a hygromycin resistance cassette (*hph*) to create the 4.1-kb r^{ef}-*hph* fusion construct. Note that each transgenic strain carries, at most, one r^{ef} insertion. "*wt*" is used to indicate a strain that does not carry an r^{ef} insertion. Full genotypes for each strain are listed in Table 1. (C) A series of directional crosses was performed. When a strain carrying an r^{ef} is crossed to a *wt* strain, close to 100% round ascospores are observed (left, 1 r^{ef}, unpaired). This indicates that the r^{ef} is detected as unpaired in such crosses, and as a result the native r^{+} gene on chromosome I is silenced. When a strain carrying an r^{ef} is crossed to a strain carrying an r^{ef} at the exact same position, relatively few round ascospores are produced (right, 2 r^{ef}, paired). This indicates that the r^{ef} are not detected as unpaired in such crosses. Therefore, the native r^{+} on chromosome I is expressed at normal levels. When strains carrying different r^{ef} are crossed, the percentage of round ascospores is proportional to the distance between the markers (middle, 2 r^{ef}, unpaired). For example, when two r^{ef} are separated by a small distance of 4.1 kb, only 5% round ascospores are produced. When two r^{ef} are separated by 37.6 kb, the level of round ascospores increases to 68% (r2 × r5). This suggests that the closer the r^{ef} are to one another on the homologs, the less likely they are to be detected as unpaired. These data represent a fraction of the crosses performed to test the relationship between unpaired DNA detection and distance. Please see Table 5 for a complete list of crosses and results. Crosses: 2, F2-26 × ISU 3118; 3, F2-26 × ISU 3117; 17, F2-26 × ISU 3119; 29, F2-26 × ISU 3114 ; 28, F2-26 × ISU 3124; 53, ISU 3143 × ISU 3141; 18, ISU 3116 × ISU 3124; 20, ISU 3127 × ISU 3119; 12, ISU 3116 × ISU 3119; 32, ISU 3115 × ISU 3118; 33, ISU 3116 × ISU 3114; 6, ISU 3116 × ISU 3118; 22, ISU 3127 × ISU 3124; 38, ISU 3115 × ISU 3114; 11, ISU 3116 × ISU 3117; 39, F2-26 × P10-15.

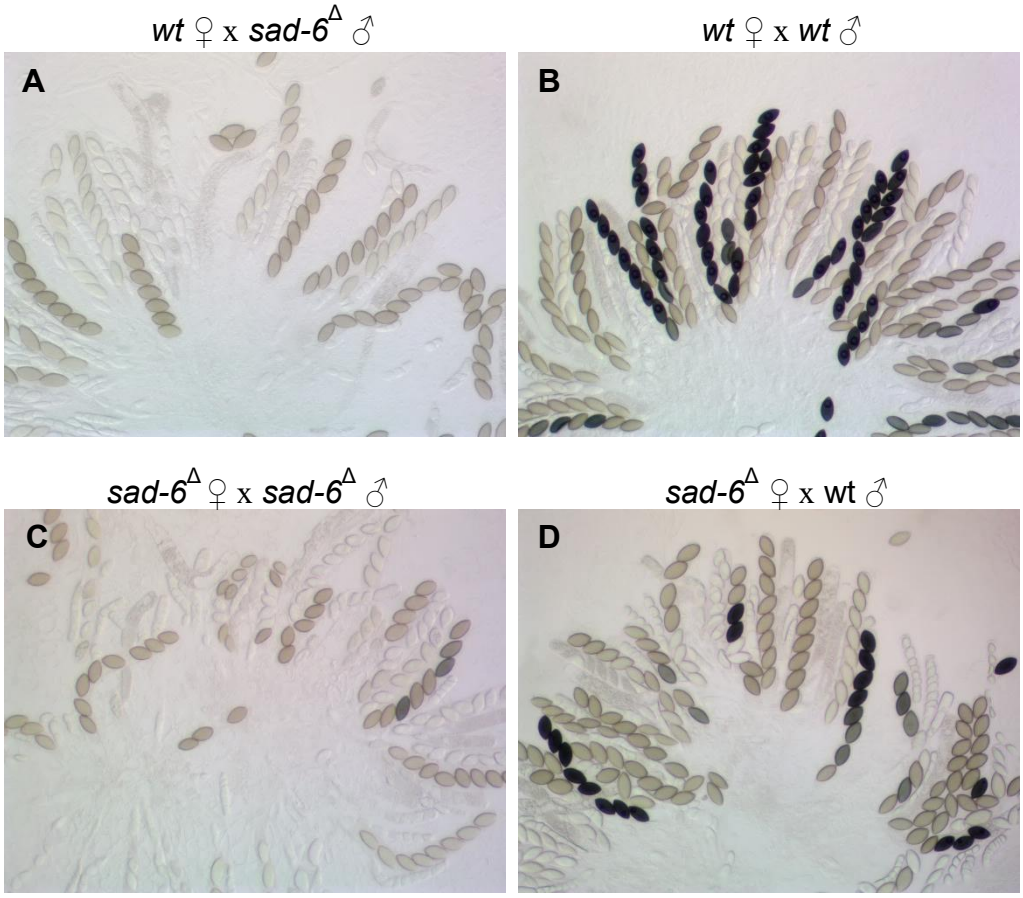

Figure 6. sa*d-6*$^{\Delta}$ is homozygous-fertile. Directional crosses were performed by growing the female strain on synthetic crossing medium for 5 days before qualitative transfer of conidial suspensions made from each male strain to the surface of each female lawn of mycelia. Perithecia were allowed to develop for 14 days before dissection. Rosettes of asci were photographed with a VanGuard 1433PHi Compound Microscope with an attached 10 megapixel digital camera (MP1000, AmScope). Strains: A) F2-01 x 3102, B) F2-01 x P9-42, C) 3113 x 3112, D) 3113 x P9-42. These data show that *sad-6*$^{\Delta}$ strains can successfully mate, undergo meiosis, and produce ascospores.

Literature Cited

Alexander, W. G., N. B. Raju, H. Xiao, T. M. Hammond, T. D. Perdue *et al*., 2008 DCL-1 colocalizes with other components of the MSUD machinery and is required for silencing. Fungal Genet. Biol. 45: 719–727.

Aramayo, R., and R. L. Metzenberg, 1996 Meiotic transvection in fungi. Cell 86: 103–113.

Aramayo, R., and E. U. Selker, 2013 *Neurospora crassa*, a model system for epigenetics research. Cold Spring Harb. Perspect. Biol. 5: a017921.

Bardiya, N., W. G. Alexander, T. D. Perdue, E. G. Barry, R. L. Metzenberg, *et al*., 2008 Characterization of interactions between and among components of the meiotic silencing by unpaired DNA machinery in *Neurospora crassa* using bimolecular fluorescence complementation. Genetics 178: 593–596.

Barzel, A., and M. Kupiec, 2008 Finding a match: how do homologous sequences get together for recombination? Nat. Rev. Genet. 9: 27–37.

Billmyre, R. B., S. Calo, M. Feretzaki, X. Wang, and J. Heitman, 2013 RNAi function, diversity, and loss in the fungal kingdom. Chromosome Res. 21: 561–572.

Carroll, A. M., J. A. Sweigard, and B. Valent, 1994 Improved vectors for selecting resistance to hygromycin. Fungal Genet. Newsl. 41: 22.

Castro-Longoria, E., M. Ferry, S. Bartnicki-Garcia, J. Hasty, and S. Brody, 2010 Circadian rhythms in *Neurospora crassa*: dynamics of the clock component frequency visualized using a fluorescent reporter. Fungal Genet. Biol. 47: 332–341.

Catalanotto, C., M. Pallotta, P. Refalo, M. S. Sachs, L. Vayssie, *et al*., 2004 Redundancy of the two dicer genes in transgene-induced posttranscriptional gene silencing in *Neurospora crassa*. Mol. Cell. Biol. 24: 2536–2545.

Ceballos, S. J., and W. D. Heyer, 2011 Functions of the Snf2/Swi2 family Rad54 motor protein in homologous recombination. Biochim. Biophys. Acta 1809: 509–523.

Chang, S. S., Z. Zhang, and Y. Liu, 2012 RNA interference pathways in fungi: mechanisms and functions. Annu. Rev. Microbiol. 66: 305–323.

Colot, H. V., G. Park, G. E. Turner, C. Ringelberg, C. M. Crew, *et al*., 2006 A high-throughput gene knockout procedure for Neurospora reveals functions for multiple transcription factors. Proc. Natl. Acad. Sci. USA. 103: 10352–10357.

Davis, R.H., and F. J. de Serres, 1970 Genetic and microbiological research techniques for *Neurospora crassa*. Methods Enzymol. 17: 79–143.

Davis, R.H., and D. D. Perkins, 2002 Neurospora: a model of model microbes. Nat. Rev. Genet. 3: 397–403.

Edgar, R. C., 2004 MUSCLE: multiple sequence alignment with high accuracy and high throughput. Nucleic Acids Res. 32: 1792-1797.

Ellison, C. E., C. Hall, D. Kowbel, J. Welch, R. B. Brem *et al*., 2011 Population genomics and local adaptation in wild isolates of a model microbial eukaryote. Proc. Natl. Acad. Sci. USA 108: 2831–2836.

Flaus, A., D. M. Martin, G. J. Barton, T. Owen-Hughes, 2006 Identification of multiple distinct Snf2 subfamilies with conserved structural motifs. Nucleic Acids Res. 34: 2887–2905.

Freitag, M., R. L. Williams, G. O. Kothe, E. U. Selker, 2002 A cytosine methyltransferase homologue is essential for repeat-induced point mutation in *Neurospora crassa*. Proc. Natl. Acad. Sci. 99: 8802–8807.

Galagan, J. E., and E. U. Selker, 2004 RIP: the evolutionary cost of genome defense. Trends Genet. 20: 417–423.

Haber, J. E., 2012 Mating-type genes and MAT switching in *Saccharomyces cerevisiae*. Genetics 191: 33–64.

Hammond, T. M., H. Xiao, E. C. Boone, T. D. Perdue, P. J. Pukkila *et al*., 2011a SAD-3, a putative helicase required for meiotic silencing by unpaired DNA, interacts with other components of the silencing machinery. G3: Genes, Genomes, Genetics 1: 369–376.

Hammond, T. M., H. Xiao, D. G. Rehard, E. C. Boone, T. D. Perdue *et al*., 2011b Fluorescent and bimolecular-fluorescent protein tagging of genes at their native loci in *Neurospora crassa* using specialized double-joint PCR plasmids. Fungal Genet. Biol. 48: 866–873.

Hammond, T. M., W. G. Spollen, L. M. Decker, S. M. Blake, G. K. Springer *et al*., 2013a Identification of small RNAs associated with meiotic silencing by unpaired DNA. Genetics 194: 279-284.

Hammond, T. M., H. Xiao, E. C. Boone, L. M. Decker, S. A. Lee, *et al*., 2013b Novel proteins required for meiotic silencing by unpaired DNA and siRNA generation in *Neurospora crassa*. Genetics 194: 91–100.

Handa, N., Y. Noguchi, Y. Sakuraba, P. Ballario, G. Macino *et al*., 2000 Characterization of the *Neurospora crassa* mus-25 mutant: the gene encodes a protein which is homologous to the *Saccharomyces cerevisiae* Rad54 protein. Mol. Gen. Genet. 264: 154–163.

Jänne, O. A., A. M. Moilanen, H. Poukka, N. Rouleau, U. Karvonen *et al*., 2000 Androgen-receptor-interacting nuclear proteins. Biochem. Soc. Trans. 28: 401–405.

Jasin, M., and R. Rothstein, 2013 Repair of strand breaks by homologous recombination. Cold Spring Harb. Perspect. Biol. 5: a012740.

Kasbekar, D. P., 2012 The Sad paradox: mutation with dominant and recessive phenotypes. J. Biosci. 37: 933-936.

Kelly, W. G., 2006 Standing guard: perinuclear localization of an RNA-dependent RNA polymerase. Proc. Natl. Acad. Sci. USA 103: 2007–2008.

Kelly, W. G., and R. Aramayo, 2007 Meiotic silencing and the epigenetics of sex. Chromosome Res. 15: 633–651.

Langmead, B., and S. L. Salzberg, 2012 Fast gapped-read alignment with Bowtie 2. Nat. Methods 9: 357–359.

Lee, D. W., R. Millimaki, and R. Aramayo, 2010 QIP, a component of the vegetative RNA silencing pathway, is essential for meiosis and suppresses meiotic silencing in *Neurospora crassa*. Genetics 186: 127–133.

Lee, D. W., R. J. Pratt, M. Mclaughlin, and R. Aramayo, 2003 An Argonaute-like protein is required for meiotic silencing. Genetics 164: 821–828.

Lee, D. W., K. Y. Seong, R. J. Pratt, K. Baker, and R. Aramayo, 2004 Properties of unpaired DNA required for efficient silencing in *Neurospora crassa*. Genetics 167: 131–150.

Leinonen, R., H. Sugawara, and M. Shumway, 2011 The sequence read archive. Nucleic Acids Res. 39: D19–21.

Lisby, M., J. H. Barlow, R. C. Burgess, and R. Rothstein, 2004 Choreography of the DNA damage response: spatiotemporal relationships among checkpoint and repair proteins. Cell 118: 699–713.

Maiti, M., H. C. Lee, and Y. Liu, 2007 QIP, a putative exonuclease, interacts with the Neurospora Argonaute protein and facilitates conversion of duplex siRNA into single strands. Genes Dev. 21: 590–600.

Margolin, B. S., M. Freitag, and E. U. Selker, 1997 Improved plasmids for gene targeting at the his-3 locus of *Neurospora crassa* by electroporation. Fungal Genet. Newsl. 44: 34–36.

Mazin, A. V., O. M. Mazina, D. V. Bugreev, and M. J. Rossi, 2010 Rad54, The motor of homologous recombination. DNA Repair 9: 286–302.

McCluskey, K., A. Wiest, and M. Plamann, 2010 The Fungal Genetics Stock Center: a repository for 50 years of fungal genetics research. J. Biosci. 35: 119–126.

Moore, G., and P. Shaw, 2009 Improving the chances of finding the right partner. Curr. Opin. Genet. Dev. 19: 99–104.

Mortazavi, A., B. A. Williams, K. McCue, L. Schaeffer, and B. Wold, 2008 Mapping and quantifying mammalian transcriptomes by RNA-Seq. Nat. Methods 5: 621–628.

Perkins, D. D., 2004 Wild type *Neurospora crassa* strains preferred for use as standards. Fungal Genet. Newsl. 51: 7–8.

Perkins, D., and V. Pollard, 1986 Linear growth rates of strains representing 10 Neurospora species. Fungal Genet. Newsl. 33: 41–43.

Petukhova, G., S. Stratton, and P. Sung, 1998 Catalysis of homologous DNA pairing by yeast Rad51 and Rad54 proteins. Nature 393: 91–94.

San Filippo, J., P. Sung, and H. Klein, 2008 Mechanism of eukaryotic homologous recombination. Annu. Rev. Biochem. 77: 229–257.

Shiu, P. K. T., N. B. Raju, D. Zickler, and R. L. Metzenberg, 2001 Meiotic silencing by unpaired DNA. Cell 107: 905–916.

Shiu, P. K. T., D. Zickler, N. B. Raju, G. Ruprich-Robert, and R. L. Metzenberg, 2006 SAD-2 is required for meiotic silencing by unpaired DNA and perinuclear localization of SAD-1 RNA-directed RNA polymerase. Proc. Natl. Acad. Sci. USA 103: 2243–2248.

Sinha, M., and C. L. Peterson, 2008 A Rad51 presynaptic filament is sufficient to capture nucleosomal homology during recombinational repair of a DNA double-strand break. Mol. Cell 30: 803–810.

Storlazzi, A., S. Tesse, G. Ruprich-Robert, S. Gargano, S. Pöggeler *et al*., 2008 Coupling meiotic chromosome axis integrity to recombination. Genes Dev. 22: 796–809.

Sugawara, N., X. Wang, and J. E. Haber, 2003 In vivo roles of Rad52, Rad54, and Rad55 proteins in Rad51-mediated recombination. Mol. Cell 12: 209–219.

Tamura, K., D. Peterson, N. Peterson, G. Stecher, M. Nei *et al*., 2011 MEGA5: molecular evolutionary genetics analysis using maximum likelihood, evolutionary distance, and maximum parsimony methods. Mol. Biol. Evol. 28: 2731–2739.

Tanaka, K., T. Hiramoto, T. Fukuda, and K. Miyagawa, 2000 A novel human Rad54 homologue, Rad54B, associates with Rad51. J. Biol. Chem. 275: 26316–26321.

Vogel, H. J., 1956 A convenient growth medium for Neurospora (Medium N). Microb. Genet. Bull. 13: 42–43.

Westergaard, M., and H. K. Mitchell, 1947 Neurospora V. A synthetic medium favoring sexual reproduction. Am. J. Bot. 34: 573–577.

Xiao, H., W. G. Alexander, T. M. Hammond, E. C. Boone, T. D. Perdue *et al*., 2010 QIP, a protein that converts duplex siRNA into single strands, is required for meiotic silencing by unpaired DNA. Genetics 186: 119–126.

Yu, J. H., Z. Hamari, K. H. Han, J. A. Seo, Y. Reyes-Domínguez *et al*., 2004 Double-joint PCR: a PCR-based molecular tool for gene manipulations in filamentous fungi. Fungal Genet. Biol. 41: 973–981.

Zhang, Z., S. Chang, Z. Zhang, Z. Xue, H. Zhang *et al*., 2013 Homologous recombination as a mechanism to recognize repetitive DNA sequences in an RNAi pathway. Genes Dev. 27: 145–150.

CHAPTER III

AN RNA-RECOGNITION MOTIF-CONTAINING PROTEIN FUNCTIONS IN MEIOTIC SILENCING BY UNPAIRED DNA

This work has been submitted for publication as:

Samarajeewa D.A., P Manitchotpisit., M. Henderson, H. Xiao, R. Rehard, K.A. Edwards., P.KT Shiu., and T.M. Hammond, 2017 An RNA-recognition motif-containing protein functions in meiotic silencing by unpaired DNA. G3.

Abstract

Meiotic silencing by unpaired DNA (MSUD) is a biological process that searches pairs of homologous chromosomes (homologs) for segments of DNA that are unpaired. Genes found within unpaired segments are silenced for the duration of meiosis. In this report, we describe the identification and characterization of *Neurospora crassa sad-7*, a gene that encodes a protein with an RNA recognition motif (RRM). Orthologs of *sad-7* are found in a wide range of ascomycete fungi. In *N. crassa*, *sad-7* is required for a fully-efficient MSUD response to unpaired genes. Additionally, at least one parent must have a functional *sad-7* allele for a cross to produce ascospores. Although *sad-7*-null crosses are barren, *sad-7*$^{\Delta}$ strains grow at a normal rate and appear normal under standard growth conditions. With respect to expression, *sad-7* is transcribed at base-line levels in early vegetative cultures, at slightly higher levels in mating-competent cultures, and at its highest level during mating. These findings suggest that SAD-7 is specific to mating-competent and sexual cultures. Although the exact role of SAD-7 in MSUD remains elusive, green fluorescent protein (GFP)-based tagging studies place SAD-7 within nuclei, perinuclear regions, and cytoplasmic foci of meiotic cells. This localization pattern is unique among known MSUD proteins and raises the possibility that SAD-7 coordinates nuclear, perinuclear, and cytoplasmic aspects of MSUD.

Keywords: Meiosis, Chromosome Pairing, RNA Silencing, Homology Search, RRM Domain

Introduction

Through the fundamental cell division process of meiosis, homologous chromosomes are grouped into pairs, aligned, shuffled, and segregated to produce genetically variable nuclei to use in reproductive cells. The mechanism by which homologous chromosomes are aligned in most organisms is unknown, but the fact that alignment occurs provides meiotic cells with a unique opportunity to identify genetic abnormalities within pairs of homologous chromosomes. For example, consider the possibility that a transposon exists between two genes on one chromosome but not between the same two genes on the chromosome's homolog. Alignment of these chromosomes during meiosis creates a situation where the genes flanking the transposon are paired while the transposon itself is unpaired. A meiotic cell that could detect this transposon by the fact that it is unpaired could keep it from hopping to a new location, assuming it could activate appropriate defensive measures against it. Although it is difficult to imagine a simple process that could do this, meiotic cells in a few fungi can identify and silence such transposons during meiosis. In these fungi, this process is called meiotic silencing by unpaired DNA (MSUD) (Aramayo and Metzenberg 1996; Shiu *et al.* 2001; Son *et al.* 2011; Nagasowjanya *et al.* 2013; Wang *et al.* 2015).

MSUD was initially discovered in *Neurospora crassa* (Aramayo and Metzenberg 1996; Shiu *et al.* 2001), a filamentous fungus made famous as a research model by Beadle and Tatum (Beadle and Tatum 1941). Although *N. crassa* is haploid for most of its life cycle, it possesses a brief diploid phase that occurs during sexual reproduction. MSUD begins during this diploid phase and continues throughout meiosis; thus, a brief introduction to *N. crassa*'s sexual cycle is necessary for a complete understanding of MSUD [please see the authoritative work by Raju (1980) for a comprehensive review of the *N. crassa* sexual cycle].

In *N. crassa*, the sexual cycle begins with the formation of an immature fruiting body called a protoperithecium. A hair-like cell structure called a trichogyne then extends from the protoperithecium towards an asexual spore (conidium) or hyphal segment of a strain of opposite mating type. Fertilization occurs when the trichogyne fuses with the mating partner and a nucleus travels from the mating partner through the trichogyne to the protoperithecium. The protoperithecium is called a perithecium after fertilization. Within the perithecium, the parental nuclei replicate and, through a series of coordinated events, a nucleus from each parent is sequestered at the top of a cell structure called a crozier hook. The two haploid parental nuclei fuse to form a single diploid nucleus while the tip of the crozier hook elongates to form a tube-like meiotic cell. After nuclear fusion, the seven chromosomes from each parent are paired, aligned, and recombined. Segregation during meiosis I returns the haploid state and meiosis II produces four meiotic products. The four meiotic products then undergo a single round of mitosis to produce a total of eight nuclei in a single meiotic cell. Cell walls and membranes develop around each of the eight nuclei during a process called ascosporogenesis. At this stage, the meiotic cell is generally referred to as an ascus, meaning "spore sac". A perithecium can have hundreds of asci, each of which formed from a unique meiotic event. At maturity, ascospores are shot from perithecia; resulting the accumulation of ascospores on the undersides of crossing lids when crosses are performed in standard petri dishes.

The path to MSUD discovery was paved by scientists who deleted a gene called *ascospore maturation protein-1* (*asm-1*) (Aramayo and Metzenberg 1996). Asm-1 is required for proper ascospore maturation and loss of *asm-1* results in the production of white ascospores (Aramayo *et al.* 1996). Interestingly, even in an $asm\text{-}1^{+} \times asm\text{-}1^{\Delta}$ cross, where four of eight ascospores in each ascus inherit the $asm\text{-}1^{+}$ allele, most asci contain eight white ascospores

(Aramayo and Metzenberg 1996). This phenotype occurs because MSUD detects *asm-1*$^{+}$ as unpaired and silences it throughout meiosis (Shiu *et al.* 2001; Shiu and Metzenberg 2002).

MSUD researchers have found it convenient to use genes like *asm-1* in experiments because they allow for MSUD efficiency to be quantified through analysis of ascospore phenotype. This is useful when characterizing mutations that suppress MSUD. For example, if one adds an MSUD suppressor to an *asm-1*$^{+}$ × *asm-1*$^{\Delta}$ cross, the strength of MSUD suppression can be determined by the percentage of black ascospores produced by the cross (Lee *et al.* 2003, 2010; Xiao *et al.* 2010; Hammond, Xiao, Boone, *et al.* 2011; Hammond, Xiao, *et al.* 2013; Samarajeewa *et al.* 2014). A strong MSUD suppressor will produce a high percentage of black ascospores (because the unpaired *asm-1*$^{+}$ allele will be expressed) while a weak MSUD suppressor will produce a low percentage of black ascospores (because the unpaired *asm-1*$^{+}$ allele will be silenced). In addition to *asm-1*, MSUD scientists often use a gene called *Round spore* (*r*) because this gene must be expressed during meiosis for a cross to produce spindle-shaped ascospores; thus, MSUD causes $r^{+} \times r^{\Delta}$ crosses to produce round ascospores (Shiu *et al.* 2001; Pratt *et al.* 2004). The level of MSUD suppression can be quantified in $r^{+} \times r^{\Delta}$ crosses similar to the way MSUD suppression is quantified in *asm-1*$^{+}$ × *asm-1*$^{\Delta}$ crosses (Maiti *et al.* 2007; Xiao *et al.* 2010; Hammond, Xiao, Boone, *et al.* 2011; Hammond, Xiao, *et al.* 2013; Samarajeewa *et al.* 2014). For example, in $r^{+} \times r^{\Delta}$ cross, a strong MSUD suppressor will produce a high percentage of spindle ascospores (because the unpaired r^{+} will be expressed) and a weak MSUD suppressor will produce a low percentage of spindle ascospores (because the unpaired r^{+} will be silenced).

In both $r^{+} \times r^{\Delta}$ and *asm-1*$^{+} \times$ *asm-1*$^{\Delta}$ crosses, the unpaired r^{+} and *asm-1*$^{+}$ alleles are only 3.5 and 2.3 kb long, respectively (Colot *et al.* 2006). The ability of MSUD to detect such small unpaired segments of DNA within a pair of homologous chromosomes is astonishing. Moreover, evidence suggests that MSUD can identify unpaired DNA segments as short as 1.3 kb (Lee *et al.* 2004). Efforts to determine how MSUD achieves this remarkable feat have focused on identifying MSUD proteins through genetic screens for MSUD suppressors. These efforts have so far identified nine MSUD proteins and a model for the MSUD mechanism has been developed based on cytological analysis of fluorescently-tagged MSUD proteins, bi-molecular fluorescent complementation (BiFC) studies on pairs of MSUD proteins, and inferences based observations of homologs of MUSD proteins in other organisms (for review, please see Hammond *in press*; Aramayo and Selker 2013).

The MSUD model begins with identification of unpaired DNA within pairs of homologous chromosomes through an undetermined mechanism involving two nuclear MSUD proteins SAD-5 and SAD-6 (Hammond, Xiao, *et al.* 2013; Samarajeewa *et al.* 2014). While SAD-5 lacks characterized domains and characterized homologs in other organisms (Hammond, Xiao, *et al.* 2013), SAD-6 contains an SNF2 helicase domain and is related to proteins that mediate DNA homology searches (Samarajeewa *et al.* 2014). After unpaired DNA is detected, theoretical molecules called aberrant RNAs (aRNAs) are thought to be transcribed from unpaired DNA and delivered to extranuclear MSUD proteins docked along the nuclear envelope (Bardiya *et al.* 2008; Decker *et al.* 2015). These molecules are currently called aRNAs because they are assumed to be unique or marked in a manner that allows the cell to distinguish them from "normal" RNAs. The perinuclear-localizing MSUD proteins include SAD-1, an RNA-dependent RNA polymerase thought to use aRNAs as templates for producing double-stranded (ds)RNAs

(Shiu *et al.* 2001, 2006); DCL-1, a Dicer homolog that may process dsRNAs into MSUD-associated small interfering RNAs (masiRNAs) (Alexander *et al.* 2008; Hammond, Spollen, *et al.* 2013); QIP, an exonuclease thought to process masiRNA-like small RNAs into single-strands (Maiti *et al.* 2007; Lee *et al.* 2010; Xiao *et al.* 2010); and SMS-2, an Argonaute protein that may use masiRNAs to identify complementary RNA molecules for silencing by degradation or translational suppression (Lee *et al.* 2003). Three other perinuclear-localizing MSUD proteins are SAD-2, which is required for recruiting most if not all of the known extranuclear MSUD proteins to the perinuclear region (Shiu *et al.* 2006; Decker *et al.* 2015); SAD-3, which has a helicase-like domain and is a homolog of a protein involved in RNAi-mediated heterochromatin formation in *Schizosaccharomyces pombe* (Hammond, Xiao, Boone, *et al.* 2011); and SAD-4, a protein without previously characterized domains or previously-characterized homologs in other organisms (Hammond, Xiao, *et al.* 2013).

Although much of the MSUD model is based on genetic and cytological experiments, and the theoretical aRNAs and dsRNAs have not been detected biochemically, masiRNAs have been identified by RNA sequencing (Hammond, Spollen, *et al.* 2013; Wang *et al.* 2015). These molecules are predominantly 25 nucleotides long with a base for uracil at their 5' ends (Hammond, Spollen, *et al.* 2013; Wang *et al.* 2015). It seems likely that masiRNAs are used to silence any complementary RNA molecules, not just those derived from unpaired DNA. This would explain why unpaired copies of genes like *r* and *asm-1* silence paired copies of the same genes at other locations in the genome (Shiu *et al.* 2001; Lee *et al.* 2004; Xiao *et al.* 2010).

While the above model is useful, it leaves many questions unanswered. For example, if unpaired DNA is detected in the nucleus, why do most MSUD proteins appear to be extranuclear? If aRNAs exist, how are they transferred from unpaired DNA to the perinuclear

region and how do perinuclear MSUD proteins distinguish aRNAs from mRNAs? Answering these questions and others will likely require discovering additional MSUD proteins through genetic screens for MSUD suppressors.

In Hammond, Xiao, Boone, *et al.* (2011), a high-throughput reverse-genetic screen was designed to identify suppressors of MSUD. The screen involves crossing strains from the *N. crassa* knockout library (Colot *et al.* 2006) with strains that have been genetically-engineered to unpair *asm-1* or *r* during meiosis. A strain from the knockout library is marked as a candidate MSUD suppressor if it increases the production of black ascospores when *asm-1* is unpaired or spindle ascospores when *r* is unpaired. Candidate MSUD suppressors are then placed through a series of experiments designed to purify the strain away from possible contaminants and confirm that the gene deletion associated with the knockout strain is the cause of MSUD suppression. The gene is then characterized to help understand why its loss suppresses MSUD. Gene characterization typically involves growth assays, crosses, phylogenetic analysis, gene expression studies, gene-tagging experiments, and fluorescent microscopy. Here, we use the above methods to identify and characterize *sad-7*, a gene required for a fully-efficient MSUD response in *N. crassa*. Evidence suggesting that SAD-7 links the nuclear and extranuclear aspects of MSUD is provided and discussed.

Materials and Methods

Strains, media, culture conditions, crosses, and general techniques

The key strains used in this study are listed along with genotype information in Table 1. The *N. crassa* knockout collection (Colot *et al.* 2006) was obtained from the Fungal Genetics Stock Center (McCluskey *et al.* 2010). All strains were cultured on Vogel's minimal medium (Vogel 1956), except when performing a cross. Crosses were performed on synthetic crossing medium (pH 6.5) (Westergaard and Mitchell 1947) with 1.5% sucrose. Experiments and sexual crosses were performed on a laboratory benchtop at room temperature with ambient lighting unless otherwise indicated. Genomic DNA was isolated from lyophilized mycelia using IBI Scientific's (Peosta, IA) Genomic DNA Mini Kit for Plants. When necessary, PCR products were purified with the IBI Scientific Gel/PCR Fragment Extraction Kit. PCR was generally performed with Phusion DNA Polymerase Kit from Thermo Fisher Scientific (Waltham, MA).

Genetic modification of N. crassa

Transgene vectors were constructed with double-joint polymerase chain reactions (DJ-PCR) (Yu *et al.* 2004; Hammond, Xiao, Rehard, *et al.* 2011). The PCR primers used for vector construction are described in a supplementary table (Table 4). Transformations of conidia were performed by electroporation with the method of Margolin *et al*. (Margolin *et al.* 1997). Conidia were filtered through a 100 μm nylon filter (EMD Millipore, SCNY00100) before collection by centrifugation. Strain P8-43 was used as the transformation host to create the *green fluorescent protein* (*gfp*$^{+}$)-*sad7* fusion strains described below. After transformation, the *gfp*$^{+}$-*sad7* coding regions were PCR-amplified from the transgenes and determined to be free of mutations by Sanger sequencing (data not shown).

Gene expression analysis

A total of 23 RNA sequencing datasets were downloaded from the Sequence Read Archive (SRA) of the National Center for Biotechnology Information (NCBI) (Leinonen *et al.* 2011). Ellison *et al.* 2011 generated datasets 1 through 3 from poly-A RNA; Wu *et al.* 2014 generated datasets 4 through 13 from poly-A RNA; Wang *et al.* 2014 generated datasets 14 through 21 from poly-A RNA; and Samarajeewa *et al.* 2014 generated datasets 22 and 23 from rRNA-reduced total RNA. Although MSUD gene expression levels for some of the 23 datasets were previously examined in Samarajeewa *et al.* 2014 and Wang *et al.* 2014, *sad-7* expression levels were not examined by either study so the datasets were reanalyzed and presented here. The culture methods used to generate each dataset will be briefly described in the results section. Complete culture methods can be obtained from the original reports (Ellison *et al.* 2011; Wang *et al.* 2014; Wu *et al.* 2014; Samarajeewa *et al.* 2014). Reads from each dataset were aligned to all primary transcripts located in version 12 of the *N. crassa* genome annotation, which was provided by the Broad Institute of Harvard and MIT (Galagan *et al.* 2003). Read alignments were performed with Bowtie2 version 2.5 (Langmead and Salzberg 2012) using the local alignment setting. “Reads per kilobase exon model per million mapped reads” (RPKMs) (Mortazavi *et al.* 2008) were calculated from the alignments with custom Perl scripts. Reads aligning to more than one transcript and/or including more than one mismatch were ignored. Accession numbers for the analyzed datasets are as follows: 1) SRR090363, 2) SRR090364, 3) SRR090366, 4) SRR1055985, 5) SRR1055990, 6) SRR1055986, 7) SRR1055991, 8) SRR1055987, 9) SRR1055992, 10) SRR1055988, 11) SRR1055993, 12) SRR1055989, 13) SRR1055994, 14) SRR585661, 15) SRR585662, 16) SRR585663, 17) SRR585664, 18)

SRR585665, 19) SRR585666, 20) SRR585667, 21) SRR585668, 22) SRR957218, and 23) SRR957223.

Confocal microscopy

Six day old perithecia were cut from crossing plates and fixed in a solution of 4% paraformaldehyde (Electron Microscopy Sciences, PA), 100 mM PIPES pH 6.9, 10 mM EGTA, and 5 mM $MgSO_4$ at room temperature for 20 minutes before washing and storing in sodium phosphate buffer (80 mM Na_2HPO_4, 20 mM NaH_2PO_4). Asci were dissected from perithecia in 25% glycerol before transfer by pipette to a drop of mounting medium (25% glycerol, 10 mg/ml DABCO, 100 mM potassium phosphate buffer pH 8.7) on a clean microscope slide. Cover slips were placed over the samples and sealed with clear nail polish after wicking away excess mounting medium with tissue paper. Slides were stored at -20 C for storage before analysis with a Leica SP2 confocal microscope.

Results

N. crassa gene ncu01917 is sad-7

Strain FGSC 13880 from the *N. crassa* knockout library was marked as a putative MSUD suppressor during a screen of mutants in the *N. crassa* knockout collection (Hammond, Xiao, and Shiu, unpublished results). FGSC 13880 is an *ncu01917*-deletion mutant (*ncu01917*$^{\Delta}$), where *ncu01917* refers to a gene of unknown function. To confirm that loss of *ncu01917* from one parent of a cross suppresses MSUD, we performed quantitative MSUD suppression assays by crossing *sad-2*$^{\Delta}$, *ncu01917*$^{\Delta}$, and a control strain (designated wt) with an *r*$^{\Delta}$ strain. Strains deleted of *sad-2* are among the strongest known suppressors of MSUD (Shiu *et al.* 2006). We found that *sad-2*$^{\Delta}$, *ncu01917*$^{\Delta}$, and wt produced 96.1%, 53.2%, and 1.7% spindle ascospores, respectively (Figure 1 and Table 2), thus silencing of *r*$^{+}$ was inefficient when *sad-2*$^{\Delta}$ was a parent in the cross (most ascospores were spindles), more efficient when *ncu01917*$^{\Delta}$ was a parent in the cross (approximately half of the ascospores were spindles), and most efficient when wt was a parent in the cross (few ascospores were spindles). These results suggest that *ncu01917*$^{\Delta}$ suppresses silencing of unpaired *r*$^{+}$, but not as strongly as *sad-2*$^{\Delta}$. Next, we crossed *sad-2*$^{\Delta}$, *ncu01917*$^{\Delta}$, and wt with *asm-1*$^{\Delta}$. We found that *sad-2*$^{\Delta}$, *ncu01917*$^{\Delta}$, and wt produced 60.2%, 67.3%, and 5.9% black ascospores in these crosses, respectively (Table 2); thus, silencing of unpaired *asm-1*$^{+}$ was inefficient with *sad-2*$^{\Delta}$ (the majority of ascospores were black), similarly inefficient with *ncu01917*$^{\Delta}$ (the majority of ascospores were black), and highly efficient with wt (few ascospores were black). These results suggest that *ncu01917*$^{\Delta}$ suppresses silencing of *asm-1*$^{+}$ as well as *sad-2*$^{\Delta}$ because approximately equal percentages of black ascospores were produced in both *ncu01917*$^{\Delta}$ × *asm-1*$^{\Delta}$ and *sad-2*$^{\Delta}$ × *asm-1*$^{\Delta}$ crosses. A hypothesis to explain why *ncu01917*$^{\Delta}$ and *sad-2*$^{\Delta}$ suppress MSUD equally with respect to unpaired *asm-1*$^{+}$ but not unpaired *r*$^{+}$ is discussed

below. Overall, these results support *ncu01917*$^{\Delta}$ as a genuine suppressor of MSUD and, to be consistent with the historical naming system for suppressors of MSUD, from herein we refer to *ncu01917* as *sad-7* [please note that MSUD suppressors are also *suppressors of ascus dominance* (Shiu *et al.* 2001)].

SAD-7 is required for sexual development

The above findings demonstrate that heterozygous *sad-7*$^{\Delta}$ crosses are suppressed for MSUD despite the presence of a *sad-7*$^{+}$ allele in one parent. These findings are consistent with at least two hypotheses: one, SAD-7 is critical for MSUD and decreased levels of the protein during meiosis interfere with MSUD efficiency, and two, SAD-7 is an auxiliary MSUD protein that improves the efficiency of MSUD but is not critical for the process. If the first hypothesis is true, MSUD should be completely inactive in homozygous *sad-7*$^{\Delta} \times$ *sad-7*$^{\Delta}$ crosses. If MSUD is partially active in *sad-7*$^{\Delta} \times$ *sad-7*$^{\Delta}$ crosses, then the second hypothesis must be true. We attempted to distinguish between these two hypotheses by first examining the ability of *sad-7*$^{\Delta}$ to complete the sexual cycle in *sad-7* null crosses. In this experiment, *sad-7*$^{\Delta} \times$ *sad-7*$^{\Delta}$ crosses were compared side-by-side with *sad-7*$^{+} \times$ *sad-7*$^{+}$ crosses. We examined the perithecia of both sets of crosses at 20 days post fertilization and found that perithecia of *sad-7*$^{+} \times$ *sad-7*$^{+}$ had normal beaks while perithecia of *sad-7*$^{\Delta} \times$ *sad-7*$^{\Delta}$ were beakless (Figure 2, A and B). Upon dissection, we found that *sad-7*$^{+} \times$ *sad-7*$^{+}$ crosses contained 100s of asci, most with mature or maturing ascospores (Figure 2E), while *sad-7*$^{\Delta} \times$ *sad-7*$^{\Delta}$ perithecia were lacking asci and ascospores (data not shown). These results are consistent with our inability to detect ascospores in a quantitative assay of ascospore production by *sad-7*$^{\Delta} \times$ *sad-7*$^{\Delta}$ crosses (Table 3). Unfortunately, because at least one *sad-7*$^{+}$ allele is required for completion of the sexual cycle, we were unable to

determine if SAD-7 plays a critical role in MSUD or if it performs an auxiliary role in the mechanism.

SAD-7 mutant cultures are indistinguishable from wild type cultures under standard growth conditions

The discovery of SAD-7 brings the current number of known MSUD proteins to ten. Of the previous nine, none are known to be required for normal growth rate or conidiogenesis under standard growth conditions. We thus examined if loss of SAD-7 would have an effect on growth or conidia production. First, when *sad-7*$^{+}$ and *sad-7*$^{\Delta}$ strains were point-inoculated to the center of petri dishes containing standard medium and cultured for several days on a laboratory bench top, both *sad-7*$^{+}$ and *sad-7*$^{\Delta}$ grew at similar rates and produced qualitatively similar levels of conidia (Figure 3A). Second, when linear growth rate was examined by inoculating *sad-7*$^{+}$ and *sad-7*$^{\Delta}$ to the ends of 30 cm glass tubes filled with standard medium (race tubes), both strains grew with the same maximum linear growth rate (Figure 3B). These data demonstrate that *sad-7*$^{+}$ deletion does not alter growth rate or conidiogenesis (at least with respect to macroconidia) under standard growth conditions.

Sad-7 expression patterns are most similar to sad-4

N. crassa has at least 28 morphologically-distinct cell types (Bistis *et al.* 2003), some of which are restricted to specific stages of the *N. crassa* life cycle. It may be possible to infer the cell types in which SAD-7 functions based on its expression pattern. We thus obtained *N. crassa* RNA sequencing datasets from four independent studies (Ellison *et al.* 2011; Wang *et al.* 2014; Wu *et al.* 2014; Samarajeewa *et al.* 2014) to compare *sad-7* expression patterns with those of all known MSUD genes. We first analyzed three RNA sequencing datasets produced from a study of wild isolates (Ellison *et al.* 2011). In this study, the wild isolates were transferred in hyphal

plugs of actively growing mycelium to the center of a sheet of cellophane over Bird's medium and cultured under constant light for 24 hours (Ellison *et al.* 2011). The *sad-7*$^{+}$ expression levels were close to 0 RPKM in all three strains under these conditions (Figure 4, columns 1-3). This is similar for all other MSUD genes except *dcl-1*, *qip,* and *sad-6* (Figure 4, columns 1-3), the former two of which have been shown to have roles in vegetative processes (Catalanotto *et al.* 2004; Maiti *et al.* 2007). We next analyzed datasets from a study on the effect of light on *N. crassa* grown in liquid shaking cultures (Wu *et al.* 2014). In this study, a standard laboratory strain was cultured in the dark at 25 ^{o}C and 150 RPM in liquid Bird's medium for 24 hours, then exposed to cool white fluorescent light for durations of up to four hours. Interestingly, expression levels were near baseline for every time point in these datasets for all MSUD genes except *dcl-1*and *sad-6* (Figure 4, columns 4-13). We next examined datasets from a study on gene expression changes during sexual development (Wang *et al.* 2014). For these datasets, a standard laboratory strain was allowed to develop protoperithecia on cellophane over carrot agar medium at 26 ^{o}C under constant light. On day seven, protoperithecia were fertilized with a standard laboratory strain of opposite mating type and perithecia were allowed to develop. RNA was sequenced from protoperithecia at zero hours post fertilization and from perithecia at seven different time points after fertilization. The relative expression levels of *qip*, *sad-4*, *sad-6*, and *sad-7* were elevated in protoperthecia with respect to the other MSUD genes in the analysis (Figure 4, column 14) and expression levels of all MSUD genes increased as sexual development progressed (Figure 4, columns 14-21). The last study included in our analysis examined RNA transcripts from crosses between *rid*$^{+}$ or *rid*$^{-}$ (Freitag *et al.* 2002) laboratory strains 144 hours post-fertilization (Samarajeewa *et al.* 2014). Unlike the Wang *et al.* (2014) study, which also examined the 144 hour time point, Samarajeewa *et al.* (2014) performed crosses on miracloth

over synthetic crossing medium at room temperature and ambient light conditions. Despite these differences, expression levels of MSUD genes were less than 2-fold different across all 144 hour datasets from both studies (Figure 4, columns 21-23).

Overall, the above analysis of MSUD gene expression patterns indicates that *sad-7*'s expression pattern is most similar to that of *sad-4.* For example, both *sad-7* and *sad-4* are expressed poorly under early vegetative conditions (Figure 4, columns 1 through 13), upregulated in protoperithecial cultures (Figure 4 column 14), and reach maximum expression levels after fertilization (Figure 4, columns 15 through 23).

SAD-7 homologs are present in a wide range of ascomycete fungi

A search of NCBI's non-redundant protein database with the predicted sequence of *N. crassa* SAD-7 found homologs of SAD-7 in many classes of ascomycete fungi. A synteny analysis suggests that many of these homologs are orthologous (related by speciation). For example, homologs for one or more *N. crassa* genes flanking *N. crassa sad-7* were found flanking genes for putative SAD-7 homologs in Sordariomycete fungi (14 of 14 species analyzed), Leotiomycete fungi (1 of 1 species analyzed), Dothidiomycete fungi (1 of 1 species analyzed), and Eurotiomycete fungi (1 of 1 species analyzed) (Figure 8). In contrast, evidence for shared synteny was not found when genes flanking *N. crassa sad-7* were compared with genes flanking the putative *sad-7* homolog in *Mucor circinelloides*, a zygomycete fungus (data not shown).

To gain knowledge on relationships between SAD-7 homologs in ascomycete fungi, we performed a phylogenetic analysis. A single clade representing 13 SAD-7 homologs in the Sordariales order of fungi is shown in Figure 5A. The clade contains three subclades that are consistent with current designations of the taxa into three families: the Sordariaceae, the

Chaetomiaceae, and the Lasiosphaeriaceae (Federhen 2003). It should be noted that two of the four SAD-7 homologs in the Chaetomiaceae are unusually short (< 419 amino acids) (Figure 5A and 5B). It is unknown if this is a biologically meaningful finding or a result of errors in the available genome sequences and/or annotation for these two fungi. A search of NCBI's conserved domain database (Marchler-Bauer *et al.* 2010) identified an RRM domain in all 13 SAD-7 homologs (Figure 5B). The RRM motif is found in the C-terminal half of each protein (when ignoring the two unusually short Chaetomiaceae proteins) (Figure 5B). The SAD-7 homologs in the Sordariaceae are longer than the SAD-7 homologs in the other two families. For example, the shortest SAD-7 homolog in the Sordariaceae is 827 amino acids, while the longest SAD-7 homolog in the Chaetomiaceae and the Lasiosphaeriaceae is only 763 amino acids (Figure 5B). Pairwise alignments were made to identify a reason for this family-specific length difference. Alignments between *P. anserina* and *M. mycetomatis* SAD-7 reveal a high level of identity along the C-terminal half of the proteins and a comparatively low level of identity along the N-terminal half, despite both proteins being approximately the same length (Figure 5C, top pair). In contrast, the SAD-7 homologs in *N. discreta* and *N. crassa* have a high level of identity along their entire lengths (Figure 5C, bottom pair). Interestingly, alignments between *N. crassa* and *P. anserina* SAD-7 homologs, as well as between *N. crassa* and *M. mycetomatis* SAD-7 homologs, reveal a series of gaps along their N-terminal halves. These data suggest that the N-terminal half of SAD-7 expanded in the lineage leading to the Sordariacea and/or experienced deletions in the lineage leading to the Chaetomiacea and Lasiosphaeriaceae.

We also examined the sequence of the SAD-7 RRM domain. RRM domains are approximately 100 amino acids long and contain a conserved $\beta_1\alpha_1\beta_2\beta_3\alpha_2\beta_4$ fold (reviewed in Maris *et al.* 2005). A consensus sequence called RNP1 ([RK]-G-[FY]-[GA]-[FY]-[ILV]-X-

[FY]) is typically found within β_3 and another called RNP2 ([ILV]-[FY]-[ILV]-X-N-L) is typically found within β_1. The aromatic residues at the 2nd position in RNP2 and the 3rd and 5th positions in RNP1 play critical roles in RNA binding for many RRM-containing proteins (reviewed in Maris *et al.* 2005). Interestingly, the RRM-domain of SAD-7 lacks an aromatic residue at position 3 in RNP1 and at position 2 in RNP2 (Figure 5D). This is not a general feature of RRM domains in *N. crassa* because other RRM-containing proteins in the fungus have aromatic residues at these positions; including NCU04182, NCU04799, and NCU09193. NCU04182 encodes a homolog of HSH49, a spliceosomal protein (Igel *et al.* 1998); NCU04799 encodes a homolog of PAB1, a protein involved in export of mRNA (Brune *et al.* 2005); and NCU09193 encodes a homolog of NOP12, a protein involved in ribosome assembly (reviewed in Konikkat and Woolford 2017). Like SAD-7, NCU08046 lacks an aromatic residue at position 2 (Figure 5D). NCU0846 encodes an homolog of eIF43g, a protein involved in translation (reviewed in Hinnebusch 2014). The biological relevance of the amino acid differences in SAD-7 relative to canonical RRM domains is unclear, but the residue exchanges at these positions are likely important because they are similar for all of the SAD-7 orthologs depicted in panels A and B (Figure 9).

GFP-SAD7 fusion proteins are found in the nucleus, perinuclear region, and cytoplasmic foci of meiotic cells

The detection of unpaired DNA must occur in the nucleus. However, of the nine previously-characterized MSUD proteins, only two have been detected within this region of the meiotic cell. To examine SAD-7's localization patterns during meiosis, we tagged its N-terminal with GFP, performed crosses, and examined meiotic cells by confocal microscopy. For these crosses, we included a mCherry-tagged version of SPO-76 (mCherry-SPO76), which localizes to meiotic

chromosomes (van Heemst *et al.* 1999; Samarajeewa *et al.* 2014). In our *gfp*$^{+}$-*sad7*$^{+}$ × *mCherry*$^{+}$-*spo76*$^{+}$ crosses, GFP-SAD7 was detected at three locations: 1) within nuclei, 2) in a ring around the edges of nuclei, and 3) within randomly distributed cytoplasmic foci (Figure 6A-C). This localization pattern is surprising. Previous studies have detected MSUD proteins either inside or outside of meiotic nuclei, but not in both locations. To examine the possibility that our detection of GFP-SAD7 within nuclei was due to an experimental artefact, we examined GFP-SAD7 localization patterns alongside those of GFP-SAD3 and GFP-SMS2, two GFP-tagged MSUD proteins that were previously shown to be distributed around meiotic nuclei in a perinuclear pattern but not within them (Hammond, Xiao, Rehard, *et al.* 2011; Hammond, Xiao, Boone, *et al.* 2011). As reported in previous studies, GFP-SAD3 and GFP-SMS2 both formed perinuclear rings and neither were detected within nuclei (Figure 6, D-I). We also noted that GFP-SAD7 and GFP-SAD3 were both associated with randomly distributed cytoplasmic foci throughout the cytoplasm (Figure 6 A-F), while GFP-SMS2 was rarely observed in such foci (Figure 6 G-I). The biological significance of the GFP-SAD7 and GFP-SAD3 cytoplasmic foci is unknown.

Identification of an MSUD protein that travels between the nucleus and the cytoplasm could shed light on how unpaired DNA detection in the nucleus is linked to silencing processes outside of the nucleus. If GFP-SAD7 does shuttle back and forth between the nucleus and the cytoplasm, it may be possible to isolate SAD-7 mutants that are unable to travel between the two locations. To test if N-terminal truncations of SAD-7 could disrupt the normal localization pattern, we fused GFP to positions 68 (GFP-SAD7$^{\Delta 1\text{-}67}$), 119 (GFP-SAD7$^{\Delta 1\text{-}118}$), and 207 (GFP-SAD7$^{\Delta 1\text{-}206}$) of the 875 amino acid SAD-7 protein while deleting amino acids prior to the fusion points in the process. We then examined the ability of the GFP-tagged full-length protein (i.e.

GFP-SAD7^{+}) and each GFP-tagged truncated protein to complete the sexual cycle when neither parent carries a *sad-7*$^{+}$ allele. While *sad-7*$^{\Delta}$ × *gfp*$^{+}$*-sad7*$^{+}$ crosses produced phenotypically normal perithecia and asci with ascospores (Figure 2, C and F), *sad-7*$^{\Delta}$ × *gfp-sad7*$^{\Delta 1\text{-}67}$ crosses produced beakless and barren perithecia (Figure 2D and data not shown). Beakless and barren perithecia were also produced by *sad-7*$^{\Delta}$ × *gfp*$^{+}$*-sad7*$^{\Delta 1\text{-}118}$ and the *sad-7*$^{\Delta}$ × *gfp*$^{+}$*-sad7*$^{\Delta 1\text{-}206}$ crosses (data not shown). These findings suggest that at least some of the amino acids prior to position 68 are necessary for SAD-7's function in sexual reproduction (although we cannot discount the possibility that the GFP tag is inhibitory to the truncated SAD-7 protein but not the full length protein). Surprisingly, despite the inability of the truncated proteins to complement the barren phenotype, all three truncated proteins displayed a meiotic localization pattern that was indistinguishable from that of full length SAD7 (Figures 7A-7D, 10), suggesting that some of the amino acids prior to position 68 are required for SAD-7's function in sexual development but none are required for proper localization.

Discussion

In this report, we present evidence demonstrating that *N. crassa* SAD-7 (NCU01917) is an MSUD protein. The strongest evidence for this hypothesis is seen in heterozygous crosses between *sad-7*$^{+}$ and *sad-7*$^{\Delta}$, which are deficient in MSUD. This deficiency phenotype could be due to haploinsufficiency, where one copy of *sad-7*$^{+}$ does not supply enough SAD-7 protein to the meiotic cell, and/or a process called "silencing the silencer", whereby the unpairing of *sad-7*$^{+}$ turns the MSUD machinery against itself (i.e. *sad-7*$^{+}$) (Shiu *et al.* 2001). In either case, decreased levels of SAD-7 most likely cause MSUD deficiency because SAD-7 is an MSUD protein.

Like many MSUD proteins, SAD-7 is required for sexual reproduction. DCL-1, QIP, SAD-1, SAD-2, SAD-3, and SMS-2 are other examples of MSUD proteins required for sexual reproduction (Shiu *et al.* 2001; Lee *et al.* 2003; Shiu *et al.* 2006; Alexander *et al.* 2008; Lee *et al.* 2010; Xiao *et al.* 2010; Hammond, Xiao, Boone, *et al.* 2011). When an MSUD protein is required for sexual reproduction, it is not possible to determine if the protein is required (critical) for MSUD or if it simply improves (dispensable) the efficiency of MSUD. To understand this distinction, it is useful to consider MSUD proteins that are not required for sexual reproduction, such as SAD-5 and SAD-6. MSUD is partially suppressed in *sad-5*$^{+}$ × *sad-5*$^{\Delta}$ crosses but completely absent in *sad-5*$^{\Delta}$ × *sad-5*$^{\Delta}$ crosses (Hammond, Xiao, *et al.* 2013); therefore, SAD-5 is a critical MSUD protein. In contrast, MSUD is only partially suppressed in both *sad-6*$^{+}$ × *sad-6*$^{\Delta}$ and *sad-6*$^{\Delta}$ × *sad-6*$^{\Delta}$ crosses (Samarajeewa *et al.* 2014); therefore, SAD-6 improves the efficiency of MSUD but is not strictly required for the process. The reason why SAD-6 is dispensable for MSUD is not known, but it could be that its role in MSUD is shared with a paralogous protein (Samarajeewa *et al.* 2014). With respect to SAD-7, it is not possible to

determine if it is more like SAD-5 (critical) or more like SAD-6 (dispensable) because sexual reproduction does not occur when a cross is completely deficient in SAD-7.

The *sad-7*$^{\Delta}$ allele suppresses silencing of unpaired *asm-1*$^{+}$ as strongly as the *sad-2*$^{\Delta}$ allele while it suppresses silencing of unpaired *r*$^{+}$ less well than the *sad-2*$^{\Delta}$ allele (Table 2, compare third and fourth columns). This finding is consistent with previous research on alleles that partially suppress silencing of unpaired *asm-1*$^{+}$ and/or *r*$^{+}$ in heterozygous crosses. For example, *sad-4*$^{\Delta}$, *sad-5*$^{\Delta}$, and *sad-6*$^{\Delta}$ alleles are all stronger suppressors of a*sm-1*$^{+}$ silencing than they are of *r*$^{+}$ silencing (Hammond, Xiao, *et al.* 2013; Samarajeewa *et al.* 2014). The Neurospora *Spore killers Sk-2* and *Sk-3*, which are MSUD suppressors, suppress unpaired a*sm-1*$^{+}$ silencing better than they suppress unpaired *r*$^{+}$ silencing (Raju *et al.* 2007). These differences could be related differences in effort MSUD must exert to silence *asm-1*$^{+}$ and *r*$^{+}$ alleles. For example, perhaps *asm-1*$^{+}$ is transcribed in meiotic cells at a higher level than *r*$^{+}$. If true, when MSUD is suppressed it would be more likely to fail to silence all *asm-1*$^{+}$ transcripts than all *r*$^{+}$ transcripts. A number of other possibilities exist to explain the reason why partial suppressors of MSUD suppress silencing of *asm-1*$^{+}$ better than silencing of *r*$^{+}$; however, at this point it seems that investigating the reason behind this phenomenon will offer us less insight into the MSUD mechanism than will other paths of inquiry.

SAD-7 has at least one role in addition to its role in MSUD. For example, in *sad-7*$^{\Delta}$ × *sad-7*$^{\Delta}$ crosses, sexual reproduction stalls before the appearance of elongated meiotic cells. This additional function of SAD-7 thus occurs at or before the initiation of meiosis. An additional function for SAD-7 is consistent with the finding that its expression levels are elevated in mating-competent cultures before fertilization (Figure 4 column 14). Interestingly, SAD-7 is conserved across a diverse range of ascomycete fungi (Figure 8) but MSUD has only been

described in three species, two Neurospora and one Fusarium (Shiu *et al.* 2001; Ramakrishnan *et al.* 2011b; Son *et al.* 2011). Therefore it seems possible that SAD-7's non-MSUD role in sexual reproduction is more broadly conserved than its role in MSUD. Alternatively, MSUD may be more common in ascomycete fungi than is currently suggested by the available literature. For example, research on wild *N. crassa* isolates has shown that MSUD can be difficult to detect even when it is known to exist within a species (Ramakrishnan *et al.* 2011a). Therefore, it is possible that SAD-7 performs similar functions in MSUD and sexual reproduction in a diverse range of ascomycete fungi.

By comparing SAD-7 orthologs from three families in the Sordariales class of ascomycete fungi, we found that the N-terminal halves of SAD-7 proteins have undergone the most diversification, while the C terminal halves have changed comparatively little. The simplest explanation for this is that the N-terminal halves mediate interactions with lineage-specific proteins while the C-terminal halves perform a similar function among the various lineages. Accordingly, the RRM domain of each SAD-7 is found in the C-terminal half of each protein (ignoring the two unusually short Chaetomiaceae SAD-7s). A sequence level analysis of the RRM domain in 12 SAD-7 orthologs revealed all to be missing two aromatic residues typical of canonical RRM domains (Figure 10). The current reason for this is unclear but other scientists have observed similar variations in RRM sequences. These variations appear due to the diverse abilities evolved by different RRM domains, including RNA binding, protein binding, and/or directing cellular localization (for review, Cléry *et al.* 2008; Cassola *et al.* 2010; Muto and Yokoyama 2012). Future investigation on the binding affinities of SAD-7's RRM could help us understand SAD-7's specific role in MSUD and sexual reproduction.

Perhaps the most intriguing finding concerning SAD-7 thus far is its peculiar localization pattern relative to other MSUD proteins. Typically, MSUD proteins are localized by N-terminal or C-terminal tagging of the protein with GFP (Lee *et al.* 2010; Hammond, Xiao, Rehard, *et al.* 2011; Hammond, Xiao, Boone, *et al.* 2011 p. 3; Hammond, Xiao, *et al.* 2013, 2013; Samarajeewa *et al.* 2014). This has invariably produced localization patterns that are nuclear or extranuclear but not both. We thus propose that GFP-SAD-7's unique nuclear and extranuclear localizations are biologically relevant (not artefacts) and are related to the proteins role in MSUD and/or sexual reproduction. Interestingly, SAD-7 appears to require the 67amino acids at its N-terminal end because fusing GFP to the 68th amino acid while eliminating the previous 67 aborts sexual development after fertilization but before elongation of meiotic cells. This finding was made during an an attempt to alter the localization pattern of GFP-SAD7. For example, if loss of the first 67 amino acids eliminated our ability to detect SAD-7 in either the nucleus or the cytoplasm, it would add evidence to the hypothesis that SAD-7 is a RNA shuttling protein. Surprisingly, all three of the truncations examined in this study displayed a localization pattern similar to the full-length protein despite neither of them being sufficient for sexual reproduction. One possibility is that SAD-7 localization is determined by residues after position 206, the site of the GFP fusion in GFP-SAD7$^{\Delta 1\text{-}206}$. However, because it was necessary to perform our analysis of the GFP-SAD7 truncations in heterozygous crosses with full-length SAD-7 (e.g. *sad-7*$^{+}$ × *gfp*$^{+}$*-sad7*$^{\Delta 1\text{-}67}$), it is possible that SAD-7 forms a homodimer through interactions between residues after position 206. In this scenario, localization signals from the full length SAD-7 would direct SAD-7/GFP-SAD-7$^{\Delta 1\text{-}67}$, SAD-7/GFP-SAD-7$^{\Delta 1\text{-}118}$, and SAD-7/GFP-SAD-7$^{\Delta 1\text{-}206}$ dimers to the proper location in the cell.

The presence of SAD-7 in nuclear and extranuclear regions of meiotic cells provides a clue towards understanding how the nuclear aspects of MSUD are linked to perinuclear and cytoplasmic aspects of the process. The MSUD model suggests that aRNAs are transcribed from unpaired DNA and delivered to MSUD proteins present in a perinuclear ring around the nucleus. As the only known MSUD protein with a nuclear and extranuclear localization pattern, SAD-7 is currently the most likely protein to fulfill this function. Future studies on the binding affinities of SAD-7's RRM domain and the identification of proteins that interact with SAD-7 should help determine if and how SAD-7 links nuclear and extranuclear aspects of MSUD.

Acknowledgments

We thank members of the Hammond and Shiu laboratories for assistance with various technical aspects of this work. We are pleased to acknowledge use of materials generated by P01 GM068087 “Functional Analysis of a Model Filamentous Fungus”. This project was supported by start-up funding from Illinois State University (T.M.H) and a grant from the National Institutes of Health (1R15HD076309-01, to T.M.H.). P.K.T.S was supported by the University of Missouri Research Board/Research Council and the National Science Foundation (MCB1157942).

Table 1. Strains used in this study.

Strain name	Genotype
F2-26 (RTH1005.2)	*rid*; *fl a*
F2-27 (RTH1027.3)	*rid* r^{Δ}::*hph*; *fl a*
F3-24 (RTH1083.17)	*rid his-3*$^{+}$::*asm-1*; *fl*; *asm-1*$^{\Delta}$::*hph a*
FGSC 13880	*sad-7*$^{\Delta}$::*hph a*
ISU-3329 (RDS19.3)	*rid; fl; mus-52*$^{\Delta}$::*bar mCherryNC-spo76::hph; sad-2*$^{\Delta}$::*hph*
ISU-3334 (RDS19.9)	*rid; fl; mus-52*$^{\Delta}$::*bar mCherryNC-spo76::hph; sad-2*$^{\Delta}$::*hph*
ISU-3817 (HDS30.1.1)	*rid gfp-sad-7::hph his-3; mus-52*$^{\Delta}$::*bar A*
ISU-4078 (HDS34.1.2)	*rid gfp-sad-7*$^{\Delta 1\text{-}67}$*::hph his-3; mus-52*$^{\Delta}$::*bar A*
ISU-4079 (HDS35.1.1)	*rid gfp-sad-7*$^{\Delta 1\text{-}118}$*::hph his-3; mus-52*$^{\Delta}$::*bar A*
ISU-4134 (RAB1.8)	*rid A*
ISU-4217 (HDS36.1.1)	*rid gfp-sad-7*$^{\Delta 1\text{-}206}$*::hph his-3; mus-52*$^{\Delta}$::*bar A*
ISU-4261	*rid his-3 gfp-sad3::hph*; *mus-51? mus-52? a*
ISU-4262 (RTH1035.7)	*rid sad-7*$^{\Delta}$*::hph A*
ISU-4263 (P16-17)	*a*
ISU-4264 (F5-23)	*fl A*
ISU-4265 (RTH1080.19)	*sad-7*$^{\Delta}$*::hph*; *fl a*
P6-07	*rid A*
P6-08	*rid a*
P8-01	*sad-2*$^{\Delta}$::*hph A*
P8-42	*rid his-3*; *mus-52*$^{\Delta}$::*bar a*
P8-43	*rid his-3*; *mus-52*$^{\Delta}$::*bar A*
P15-22	*rid his-3*; *mus-52*$^{\Delta}$::*bar*; *gfp-sms2*::*hph A*

All strains in this study are descendants of lines 74-OR23-1VA (FGSC 2489) and 74-ORS-6a (FGSC 4200) (Perkins 2004). The *mCherryNC-spo76::hph* allele was derived from ISU-3123 (Samarajeewa *et al.* 2014). ISU-4261 carries a *gfp-sad3::hph* allele identical to the one described in strain F4-31 (Hammond, Xiao *et al.* 2011a). The *gfp-sms2*::*hph* allele in P15-22 was described in Hammond *et al.* (2011b). The r^{Δ}, *asm-1*$^{\Delta}$, *sad-7*$^{\Delta}$, *mus-51*$^{\Delta}$, and *mus-52*$^{\Delta}$ alleles are as described by Colot *et al.* (2006). Mutant *rid* alleles suppress repeat-induced point mutation (Freitag *et al.* 2002). The *fl* allele eliminates macroconidia production (Perkins *et al.* 2000)

Table 2. MSUD is suppressed by *sad-7*$^{\Delta}$.

	wt ♀ total (×10^6)	*r*$^{\Delta}$ ♀ spindle (%)	*asm-1*$^{\Delta}$ ♀ black (%)
wt ♂	8.3 ± 1.0	1.7 ± 1.1	5.9 ± 0.7
sad-7$^{\Delta}$ ♂	8.9 ± 0.2	53.2 ± 6.5	67.3 ± 4.3
sad-2$^{\Delta}$ ♂	8.7 ± 0.3	96.1 ± 1.1	60.2 ± 21.6

Unidirectional crosses were performed between MSUD-testers (females) and *wt*, *sad-7*$^{\Delta}$, or *sad-2*$^{\Delta}$ (males), as previously described (Samarajeewa *et al.* 2014). In short, crosses were performed in triplicate and ascospores were collected from the lids of the crossing plates at 21 days post-fertilization. Ascospores were suspended in water for analysis under magnification. The following phenotypes were analyzed: total ascospores (column 2), percent spindle ascospores (column 3), and percent black ascospores (column 4). For each strain, only the pertinent genotype is provided. Please note that 'wt' is not a true wild type strain but it carries wild type alleles for all genes related to MSUD, *r* and *asm-1*. Strain names: wt ♀ F2-26, *r*$^{\Delta}$ ♀ F2-27, *asm-1*$^{\Delta}$ ♀ F3-24, wt ♂ P6-07, *sad-7*$^{\Delta}$ ♂ ISU-4262, and *sad-2*$^{\Delta}$ ♂ P8-01.

Table 3. Homozygous *sad-7*$^{\Delta}$ crosses fail to produce ascospores.

cross	ascospore total
sad-7$^{\Delta}$ ♀ × wt ♂	3.6 ± 1.6
sad-7$^{\Delta}$ ♀ × *sad-7*$^{\Delta}$ ♂	0
sad-7$^{\Delta}$ ♀ × *sad-2*$^{\Delta}$ ♂	3.7 ± 0.1

Unidirectional crosses were performed between *sad-7*$^{\Delta}$ (female) and *wt*, *sad-7*$^{\Delta}$, or *sad-1*$^{\Delta}$ strains (males) as described in Table 2 to determine the total number of ascospores produced by each cross. Only the pertinent genotype is provided for each crossing parent. Please see Table 1 for complete genotype information. Crossing parents: *sad-7*$^{\Delta}$ ♂ ISU-4265, wt ♂ P6-07, *sad-7*$^{\Delta}$ ♂ ISU-4262, and *sad-2*$^{\Delta}$ ♂ P8-01.

Table 4. Oligonucleotides used in this study

Name	Sequence (5′ to 3′)
Primers for constructing gfp-sad-7	
SAD-7-E	CATTTGCTCTTGCCCCTCTGCTT
SAD-7-NGFP1	GCAGCCTGAATGGCGAATGGACGCGCAGGATGGTTGGTTAGC
SAD-7-NGFP3	CAGGAGCGGGTGCGGGTGCTGGAGCGATGGCGGACATCAAA
SAD-7-I	TTAGGCACGAAGCCCTGACCATT
SAD-7-J	AGTTGTTCTGACGGTTGGCTGCT
SAD-7-K	TTGTTGAAAAGATTGCGTTGCTTGAGG
Primers for constructing gfp-sad-7$^{\Delta 1\text{-}67}$	
SAD-7-E	CATTTGCTCTTGCCCCTCTGCTT
SAD-7-NGFP1	GCAGCCTGAATGGCGAATGGACGCGCAGGATGGTTGGTTAGC
SAD-7-L	CAGGAGCGGGTGCGGGTGCTGGAGCGCCGAATGCTGTCATGG
SAD-7-M	TCAGCAATACGAGAAGGACGGTTT
SAD-7-J	AGTTGTTCTGACGGTTGGCTGCT
SAD-7-O	TAGGCACGAAGCCCTGACCATT
Primers for constructing gfp-sad-7$^{\Delta 1\text{-}118}$	
SAD-7-E	CATTTGCTCTTGCCCCTCTGCTT
SAD-7-NGFP1	GCAGCCTGAATGGCGAATGGACGCGCAGGATGGTTGGTTAGC
SAD-7-P	CAGGAGCGGGTGCGGGTGCTGGAGCGGGAAACCACGGACGC
SAD-7-M	TCAGCAATACGAGAAGGACGGTTT
SAD-7-J	AGTTGTTCTGACGGTTGGCTGCT
SAD-7-Q	GATTGCGCGAAGGCTAGAGGAC
Primers for constructing gfp-sad-7$^{\Delta 1\text{-}206}$	
SAD-7-E	CATTTGCTCTTGCCCCTCTGCTT
SAD-7-NGFP1	GCAGCCTGAATGGCGAATGGACGCGCAGGATGGTTGGTTAGC
SAD-7-R	CAGGAGCGGGTGCGGGTGCTGGAGCGAATCAGCAGGCAGGC
SAD-7-M	TCAGCAATACGAGAAGGACGGTTT
SAD-7-J	AGTTGTTCTGACGGTTGGCTGCT
SAD-7-S	GGCGGTGGTTGAGAAGGAAGTG

The above oligonucleotides were used as primers for constructing four *gfp-sad-7* tagging vectors with DJ-PCR as described by Hammond *et al.* (2011). For each set of six primers listed above, the first two were used to amplify the left flank, the middle two were used to amplify the right flank, and the last two were used as nested primers to amplify the final vector.

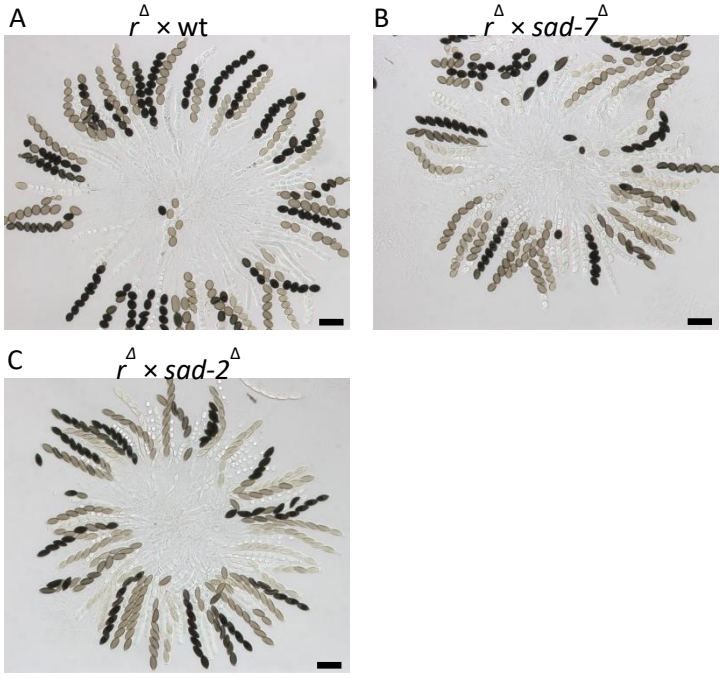

Figure 1. MSUD is suppressed in *sad-7*$^{\Delta}$ heterozygous crosses. (A) Asci from an r^{Δ} × wt perithecium. Most mature (black pigmented) ascospores are round because of MSUD. (B) Asci from an r^{Δ} × *sad-7*$^{\Delta}$ perithecium. Some mature ascospores are spindle-shaped while others are round because MSUD is partially suppressed by *sad-7*$^{\Delta}$. (C) Asci from an r^{Δ} × *sad-2*$^{\Delta}$ perithecium. Mature ascospores are spindle-shaped because *sad-2*$^{\Delta}$ is a strong suppressor of MSUD. The designated female strain in all crosses (r^{Δ} ♀) is F2-27. The designated male strains are wt ♂ P6-07, *sad-7*$^{\Delta}$ ♂ ISU-4262, and *sad-2*$^{\Delta}$ ♂ P8-01. Bars are approximately 50 µm. Quantitative analysis of ascospore phenotypes from each cross is provided in Table 2.

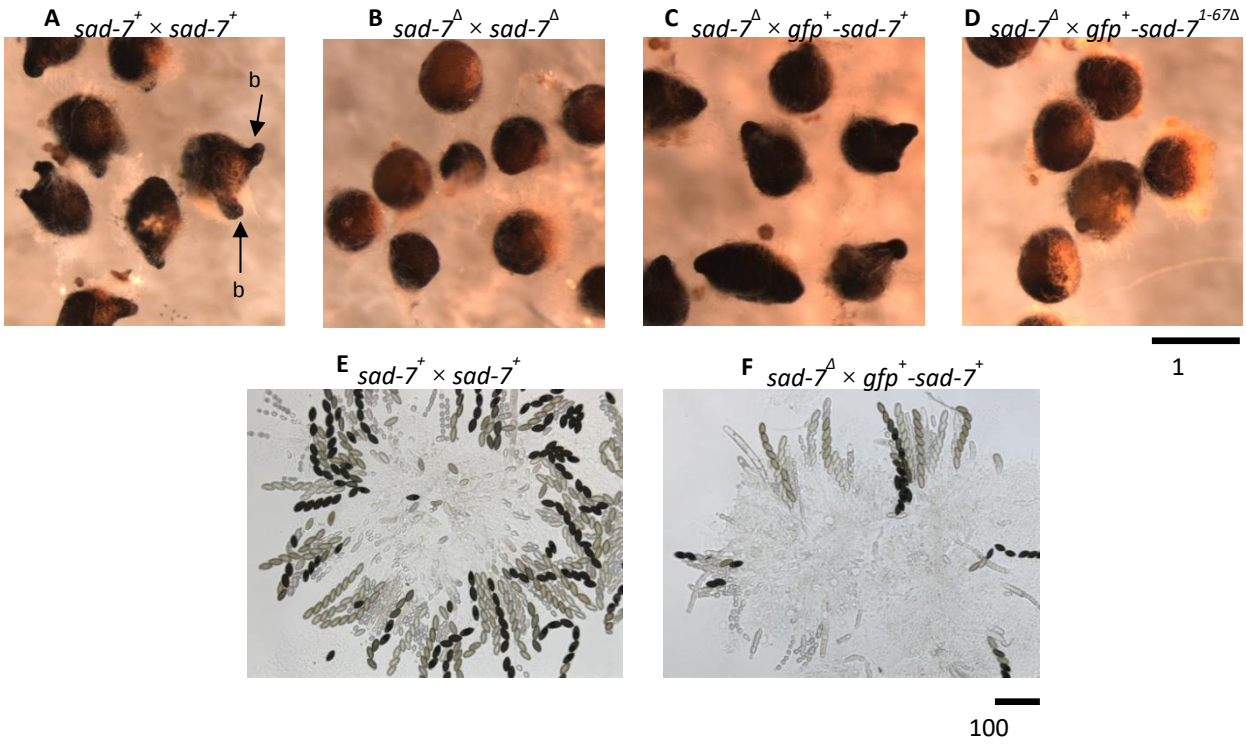

Figure 2. SAD-7 is required for ascus and ascospore development. (A-D) Perithecia were isolated from crosses 20 days post fertilization (dpf) and examined in water under magnification. (A) Perithecia from a *sad-7*$^{+}$ × *sad-7*$^{+}$ cross [ISU-4264 × ISU-4263]. Perithecial beaks (bk) are present and two are highlighted in the image. (B) Perithecia from a *sad-7*$^{\Delta}$ × *sad-7*$^{\Delta}$ cross [ISU-4265 × ISU-4262]. No beaks are observed. (C) Perithecia from a *sad-7*$^{\Delta}$ × *gfp*$^{+}$*-sad7*$^{+}$ cross [ISU-4265 × ISU-3817]. Perithecial beak development appears normal. (D) Perithecia from a *sad-7*$^{+}$ × *gfp-sad7* $^{\Delta 1\text{-}67}$ cross [ISU-4265 × ISU-4078]. No beaks are observed. (E) Asci from a *sad-7*$^{+}$ × *sad-7*$^{+}$ cross [ISU-4264 × ISU-4263]. Phenotypically-normal asci and ascospores are detected. (F) Asci from a *sad-7*$^{\Delta}$ × *gfp-sad7*$^{+}$ cross [ISU-4265 × ISU-3817]. Phenotypically-normal asci and ascospores are detected. In summary, these results demonstrate that at least one parent of a cross must have a functional SAD-7 protein to complete the sexual cycle and, unlike tagging a truncated SAD-7 at its N-terminal end with GFP, tagging the full length SAD-7 with GFP at its N-terminal end does not prevent SAD-7 from performing its function in sexual reproduction.

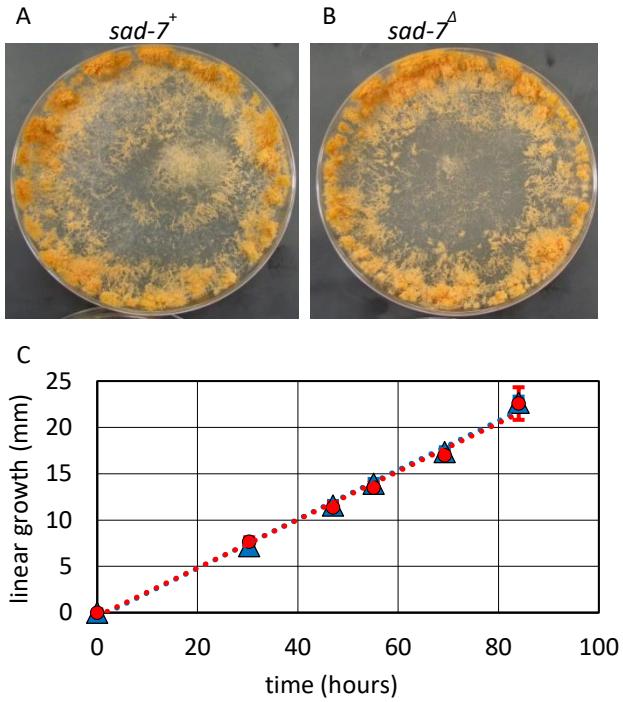

Figure 3. *sad-7*$^{+}$ is not required for conidiogenesis or linear growth. (A and B) Cultures of *sad-7*$^{+}$ [P6-08] and *sad-7*$^{\Delta}$ [ISU-4262] are indistinguishable when incubated on standard growth medium at room temperature on a laboratory benchtop. (C) *sad-7*$^{+}$ [ISU-4134, red circles] and *sad-7*$^{\Delta}$ [ISU-4262, blue triangles] have similar growth rates on standard growth medium at room temperature on a laboratory bench top. Linear growth rate was measured with a race tube assay (Perkins and Pollard 1986). Strains were allowed two days to colonize race tubes before collecting data. Error bars are standard deviation values.

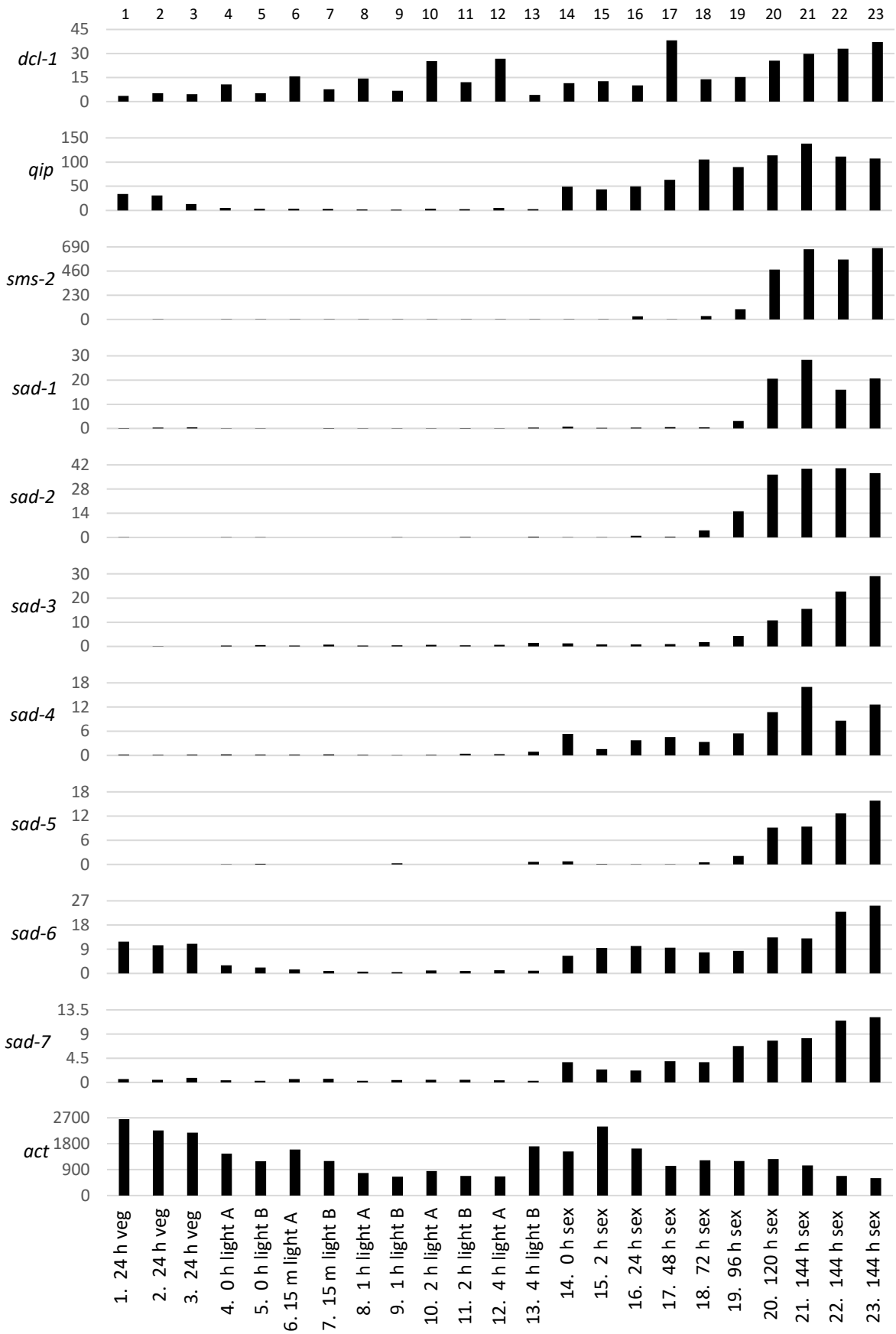
1 2 3 4 5 6 7 8 9 10 11 12 13 14 15 16 17 18 19 20 21 22 23
dcl-1
45
30
15
0
qip
150
100
50
0
sms-2
690
460
230
0
sad-1
30
20
10
0
sad-2
42
28
14
0
sad-3
30
20
10
0
sad-4
18
12
6
0
sad-5
18
12
6
0
sad-6
27
18
9
0
sad-7
13.5
9
4.5
0
act
2700
1800
900
0
1. 24 h veg
2. 24 h veg
3. 24 h veg
4. 0 h light A
5. 0 h light B
6. 15 m light A
7. 15 m light B
8. 1 h light A
9. 1 h light B
10. 2 h light A
11. 2 h light B
12. 4 h light A
13. 4 h light B
14. 0 h sex
15. 2 h sex
16. 24 h sex
17. 48 h sex
18. 72 h sex
19. 96 h sex
20. 120 h sex
21. 144 h sex
22. 144 h sex
23. 144 h sex

Figure 4. Expression patterns of *sad-7* are most similar to *sad-4*. The transcript levels of MSUD genes under different culture conditions according to RNA sequencing analysis are shown. The Y axis marks the expression level of each gene in "reads per kilobase exon model per million mapped reads" (RPKM). The 23 datasets included in the analysis (Ellison *et al.* 2011; Wang *et al.* 2014; Wu *et al.* 2014; Samarajeewa *et al.* 2014) are plotted along the X axis. Please see the methods and results sections for a full description of each dataset. In short, datasets 1-3 are of vegetative cultures on solid medium, datasets 4-13 are of vegetative cultures in liquid medium, and datasets 14-23 are of sexual cultures on solid medium. For datasets 1-3, time refers to the age of the vegetative tissue, datasets 4-13, time refers to hours after exposure to light, and for datasets 14-23, time refers to hours post fertilization. The "A" and "B" designations refer to replicate datasets that were generated with slightly different methods after RNA isolation (Wu *et al.* 2014). Five of the datasets (1-3, 22 and 23) used in this study were examined by Samarajeewa *et al.* (2014) and eight (14-21) were examined by Wang *et al.* (2014) with respect to MSUD gene expression, but *sad-7* expression was not examined in either study. Overall, *sad-7* expression patterns are most similar to *sad-4*, with barely detectable expression during early vegetative culture conditions (datasets 1 through 13), elevated expression in protoperithecial cultures (dataset 14), and maximum expression in sexual cultures (datasets 15-23).

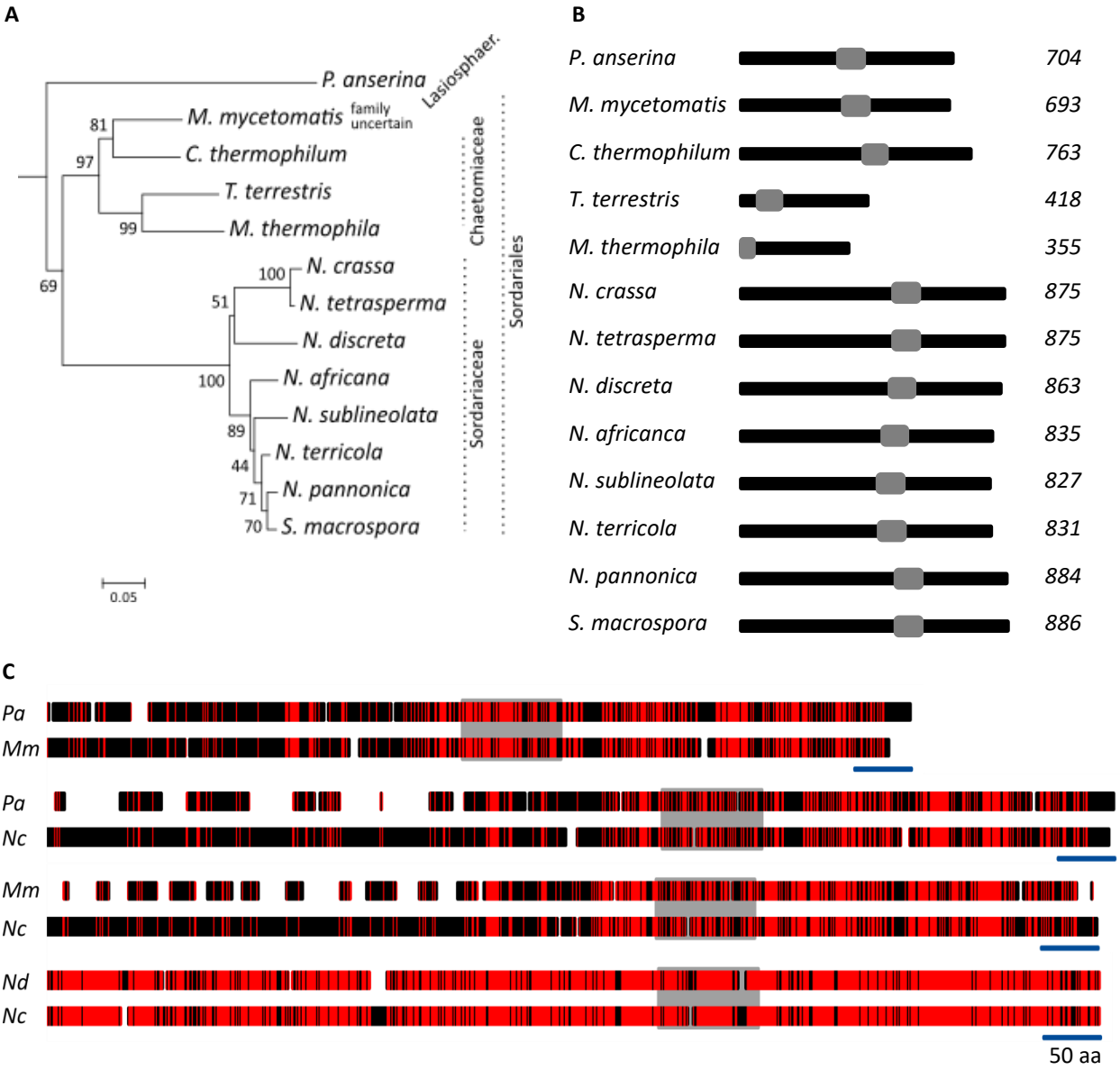
A
P. anserina
M. mycetomatis family uncertain
C. thermophilum
T. terrestris
M. thermophila
N. crassa
N. tetrasperma
N. discreta
N. africana
N. sublineolata
N. terricola
N. pannonica
S. macrospora
Lasiosphaer.
Chaetomiaceae
Sordariales
Sordariaceae
81
97
99
100
51
69
100
89
44
71
70
0.05
B
P. anserina 704
M. mycetomatis 693
C. thermophilum 763
T. terrestris 418
M. thermophila 355
N. crassa 875
N. tetrasperma 875
N. discreta 863
N. africanca 835
N. sublineolata 827
N. terricola 831
N. pannonica 884
S. macrospora 886
C
Pa
Mm
Pa
Nc
Mm
Nc
Nd
Nc
50 aa
D
RNP2
123456
NCU04182 SAP49 93 KTVDIGAELFINNLDPQVDEKI---------- 114
NCU04799 PAB1 142 LRKTGAGNIFIKNLDAAIDNK---------- 162
NCU09193 NOP12 311 APVDHKRCVFVGNLGFVDDETVLQVKVDEDGKEVTEKKKRTKQPMDVEEGL 361
NCU08046 eIF3g 298 GERDDLATLRVTNVSEMAEEQE---------- 319
NCU01917 SAD-7 499 ASASDAGVVKITNLPYTTTHQEIK---------- 522
RNP1
12345678
NCU04182 SAP49 115 LYDTFSQFGQILRQPNIVRDDNNISKGYGFVSFGSFEASD 154
NCU04799 PAB1 163 ALHDTFAAFGNILSCKVAQDEHGNSKGYGFVHYETDEAAS 202
NCU09193 NOP12 362 WRVFGKEGGKVESVRVVRDPVTRVGKGFAYVQFCDENAVE 401
NCU08046 eIF3g 320 LRDMFERFGRVTRVFLAKDRDTGLAKGFAFISFADRSDAV 359
NCU01917 SAD-7 523 ALLGRNAKLLTEESVHVIMERINGKTQDAYIEFCSQDDAI 562

Figure 5. SAD-7 is a widely conserved RRM protein in ascomycete fungi. (A) A diagram depicting relationships between SAD-7 homologs in a clade of Sordariales fungi. The diagram is a subset of homologs from a more complete phylogenetic analysis presented in Figure S2. The families of 12 of the 13 taxa into Sordariaceae, Chatomiaceae, and Lasiosphaeriaceae families are indicated (Federhen 2003). (B) RRM (NCBI CDD: cl17169) locations of SAD-7 homologs. RRM-domains are indicated with gray boxes. The predicted number of amino acids in each protein is listed along the right side of the panel. (C) Graphical depictions of Clustal W (Thompson *et al.* 1994) alignments between pairs of SAD-7 homologs. Identical amino acids are indicated with red shading. Different amino acids are indicated with black shading. Gap positions are indicated by gaps. The locations of the RRM-domains are indicated with a gray box. The blue scale bar is equivalent to 50 amino acids. In summary, these results show that SAD-7 is an RRM-domain containing protein conserved across a wide range of ascomycete fungi. They suggest that the N-terminal halves of the protein have changed more than the C-terminal halves during evolution of the Sordariaceae, Chatomiaceae, and Lasiosphaeriaceae fungi. (D) A manual alignment of RRM domains from five *N. crassa* proteins is shown. The residues are shaded according to the PAM120 similarity matrix. The positions of RNP1 and RNP2 are indicated. Sequences can be obtained from GenBank or FungiDB with the following accession numbers: *Podospora anserina* (*Pa*) CAP60824.1; *Madurella mycetomatis* (*Mm*) KXX77199.1; *Chaetomium thermophilum* EGS22685.1; *Thielavia terrestris* AEO64981.1; *Myceliophthora thermophila* AEO61061.1; *Neurospora crassa* (*Nc*) EAA36312.1; *Neurospora tetrasperma* EGO51840.1; *Neurospora discreta* (*Nd*) NEUDI 136685; *Neurospora africana* GCA 000604205.2; *Neurospora africana* GCA 000604205.2; *Neurospora sublineolata* GCA 000604185.2; *Neurospora terricola* GCA 000604245.2; *Neurospora pannonica* GCA 000604225.2; *Sordaria macrospora* XP 003349025.1.

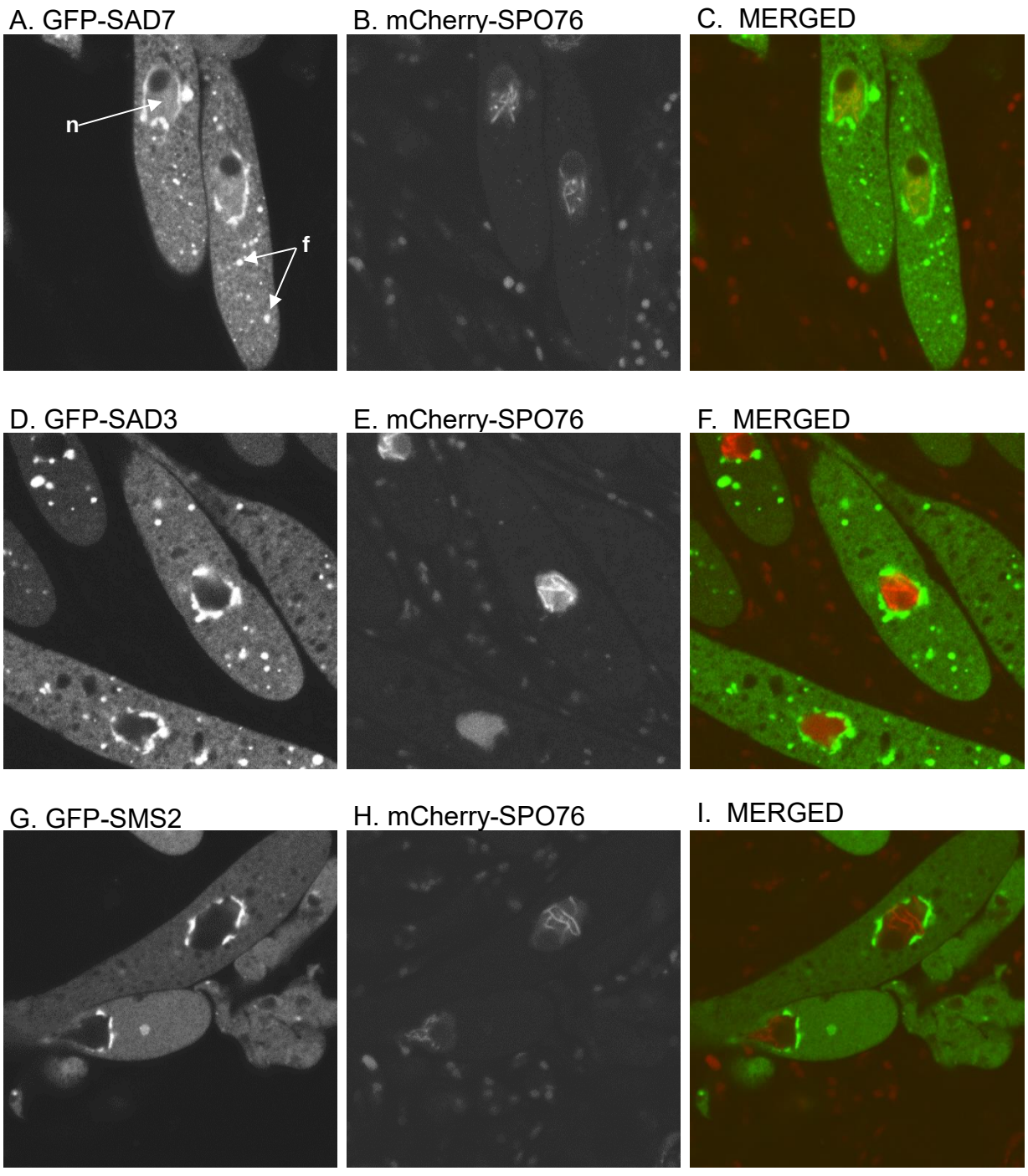
A. GFP-SAD7
B. mCherry-SPO76
C. MERGED
n
f
D. GFP-SAD3
E. mCherry-SPO76
F. MERGED
G. GFP-SMS2
H. mCherry-SPO76
I. MERGED

Figure 6. GFP-SAD7 is detected at three different locations in the ascus. A) Asci from a *gfp-sad7*$^{+}$ × *mCherry-Spo76 sad-2*$^{\Delta}$ cross are shown. When SAD-7 is tagged with GFP (GFP-SAD7), a GFP signal is detected throughout the nucleus (n) except for within a spherical-subnuclear domain representing the nucleolus. The GFP-SAD7 signal is most intense around the nucleus and within cytoplasmic foci (f). mCherry-SPO76 is used to depict the position of the chromosomes (van Heemst *et al.* 1999; Samarajeewa *et al.* 2014), while *sad-2*$^{\Delta}$ is used to allow expression of tagged and unpaired alleles during meiosis. Cross: ISU-3334 × ISU-3817. B) Asci from a *gfp-sad3*$^{+}$ × *mCherry-Spo76 sad-2*$^{\Delta}$ cross are shown. When SAD-3 is tagged with GFP (GFP-SAD3), the GFP signal is similar to GFP-SAD7 except that there is no signal within the nucleus. Cross: ISU-3329 × ISU-4261. (C) Asci from a *gfp-sms2*$^{+}$ × *mCherry-Spo76 sad-2*$^{\Delta}$ cross are shown. When SMS-2 is tagged with GFP, the GFP signal is strong around the nucleus but absent from within the nucleus. Cytoplasmic foci are uncommon for GFP-SMS2. Cross: ISU-3334 × P15-22.

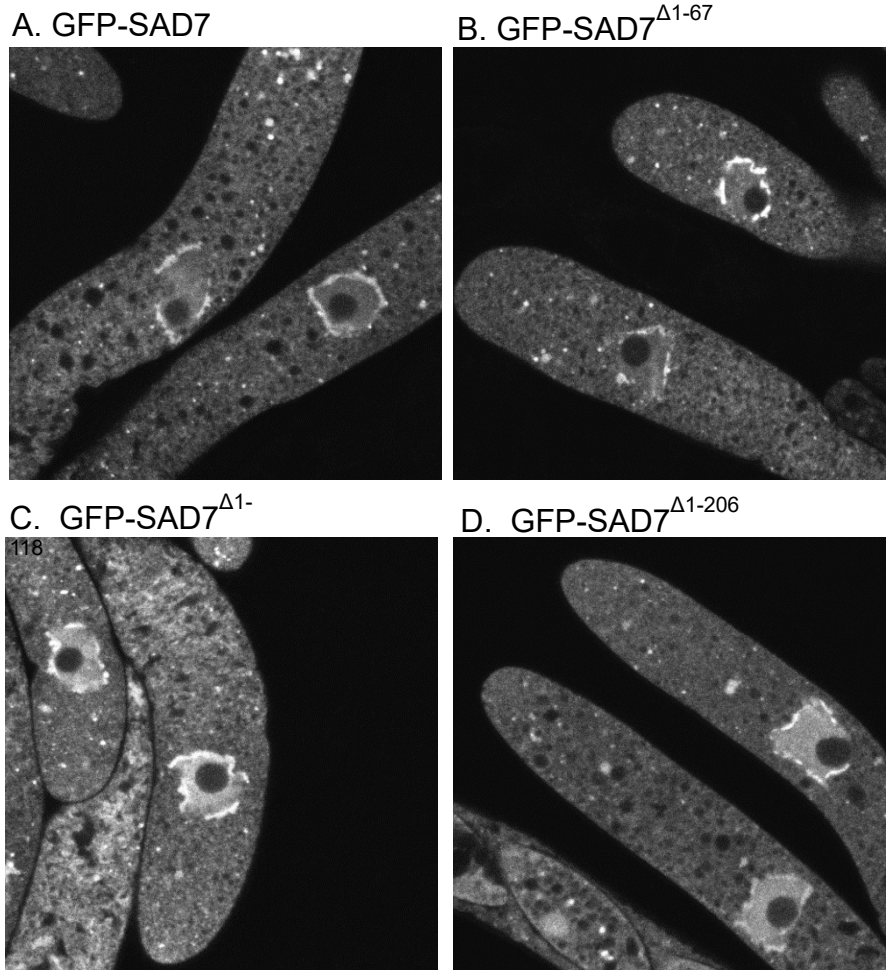

Figure 7. The meiotic localization pattern of GFP-SAD7 is independent on the first 206 amino acids of the protein. A series of truncated SAD-7 proteins was created by fusing GFP to different positions from the N-terminal end of SAD-7. Amino acids prior to the fusion point were deleted in the process. Representative images of GFP signal within asci in meiotic prophase I from crosses between ISU-3334 (a *sad-2*$^{\Delta}$ *mcherry-spo76* strain) and various GFP-SAD7 truncation strains are shown. In all crosses, GFP signal was detected within nuclei, perinuclear regions, and cytoplasmic foci despite loss of up to 206 amino acids from the N-terminal end of SAD-7. (A) ISU-3334 × ISU-3817, (B) ISU-3334 × ISU-4078, (C) ISU-3334 × ISU-4079, and (D) ISU-3334 × ISU-4217.

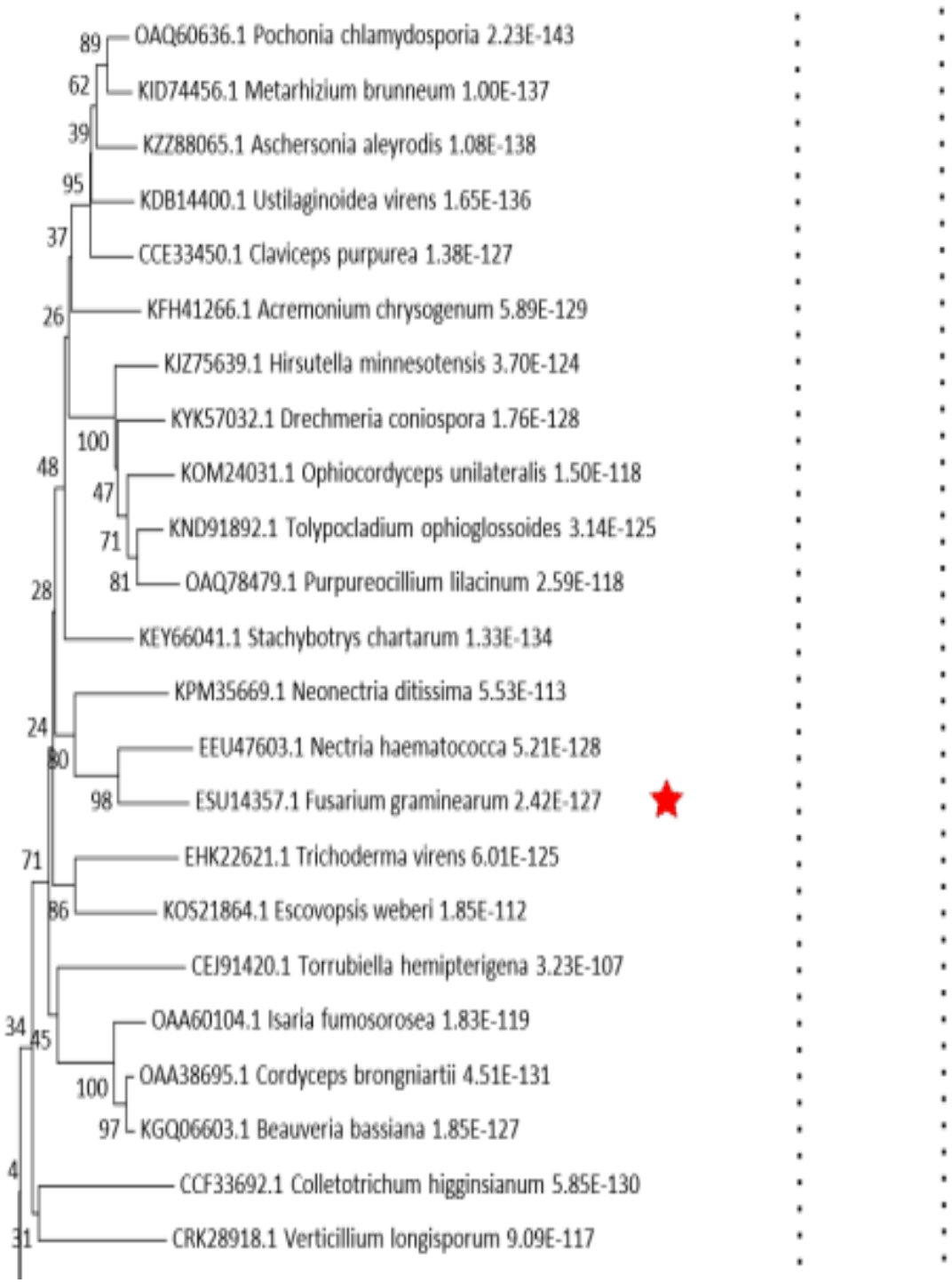

(Figure continues)

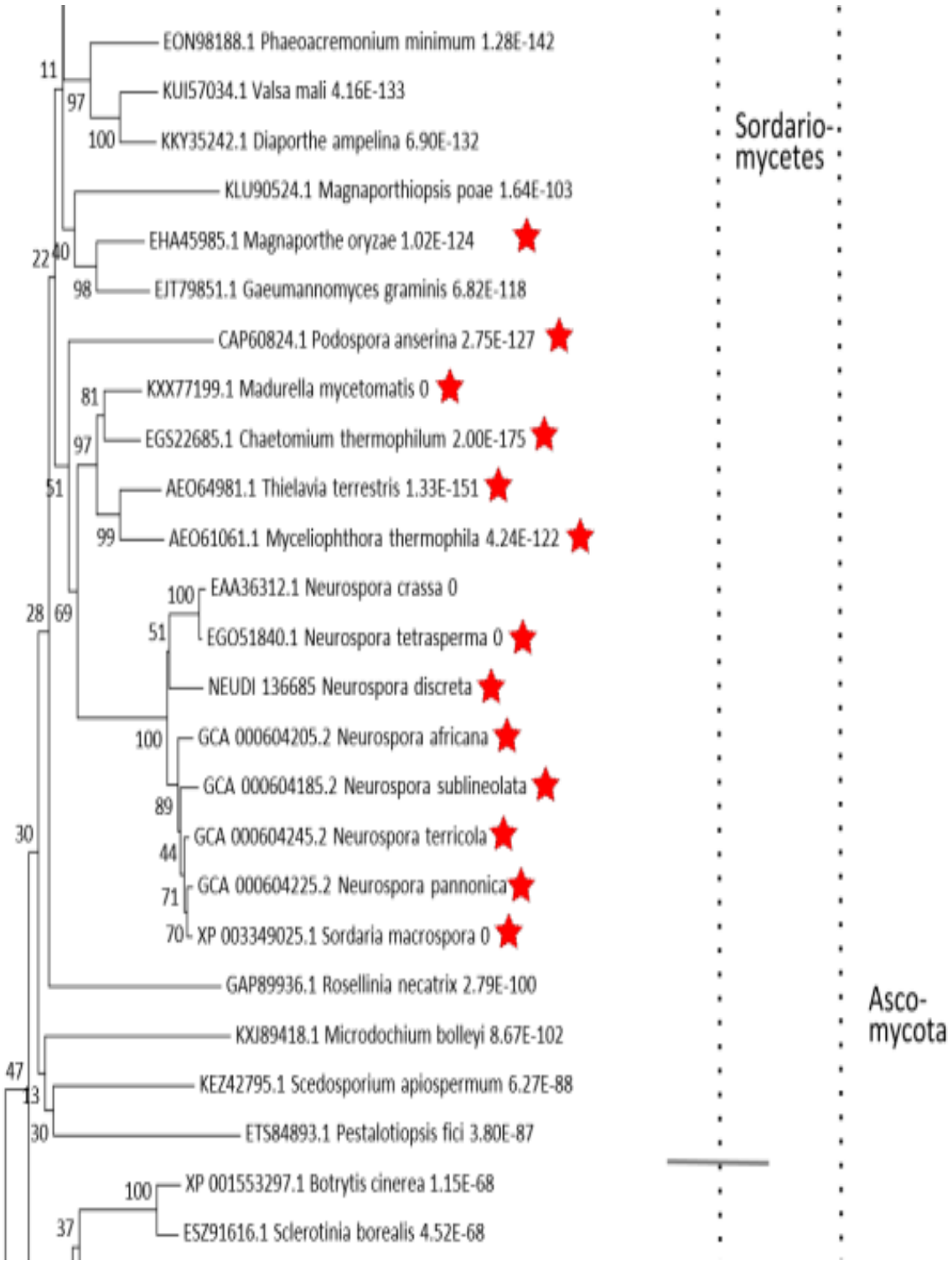

(Figure continues)

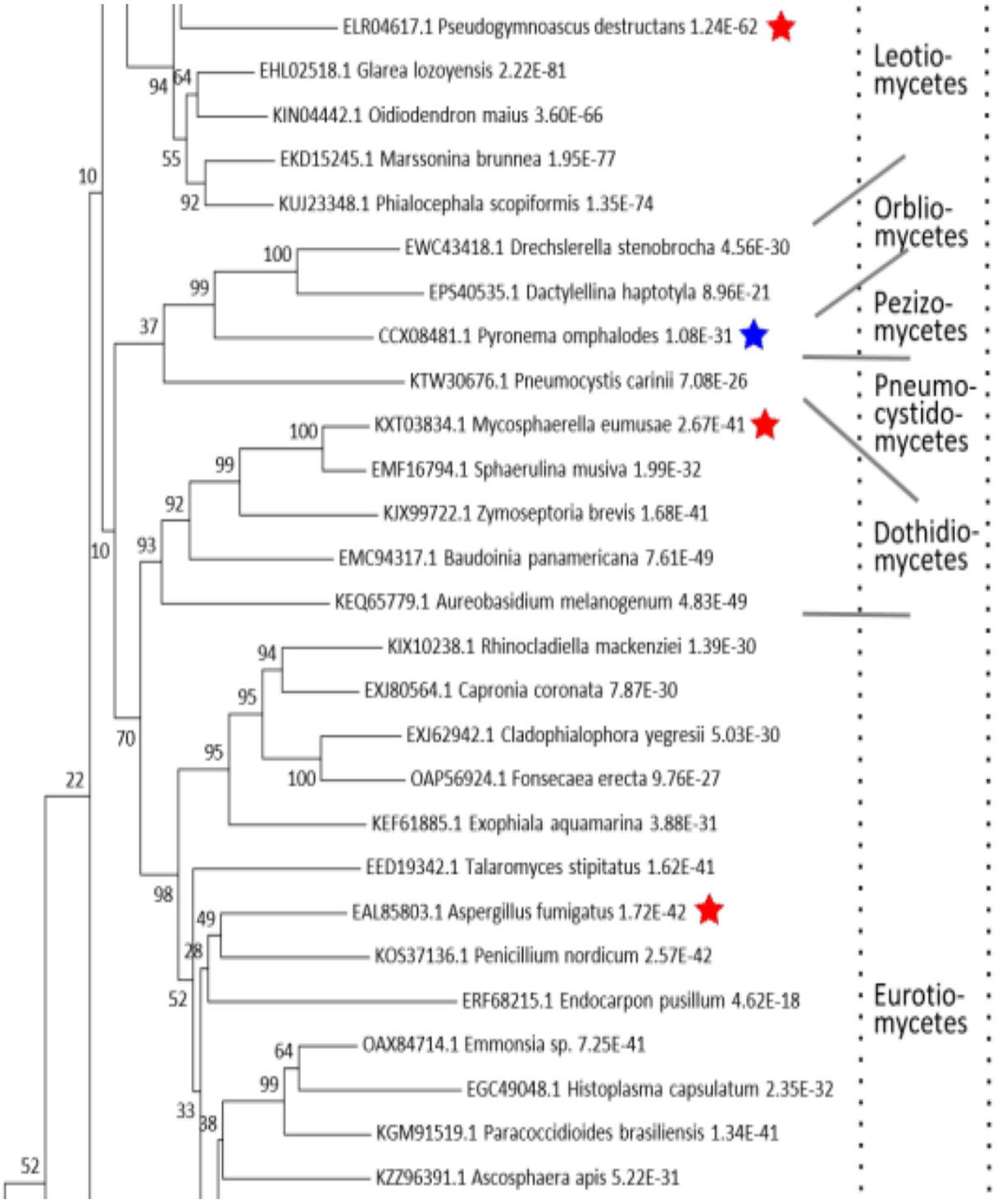

(Figure continues)

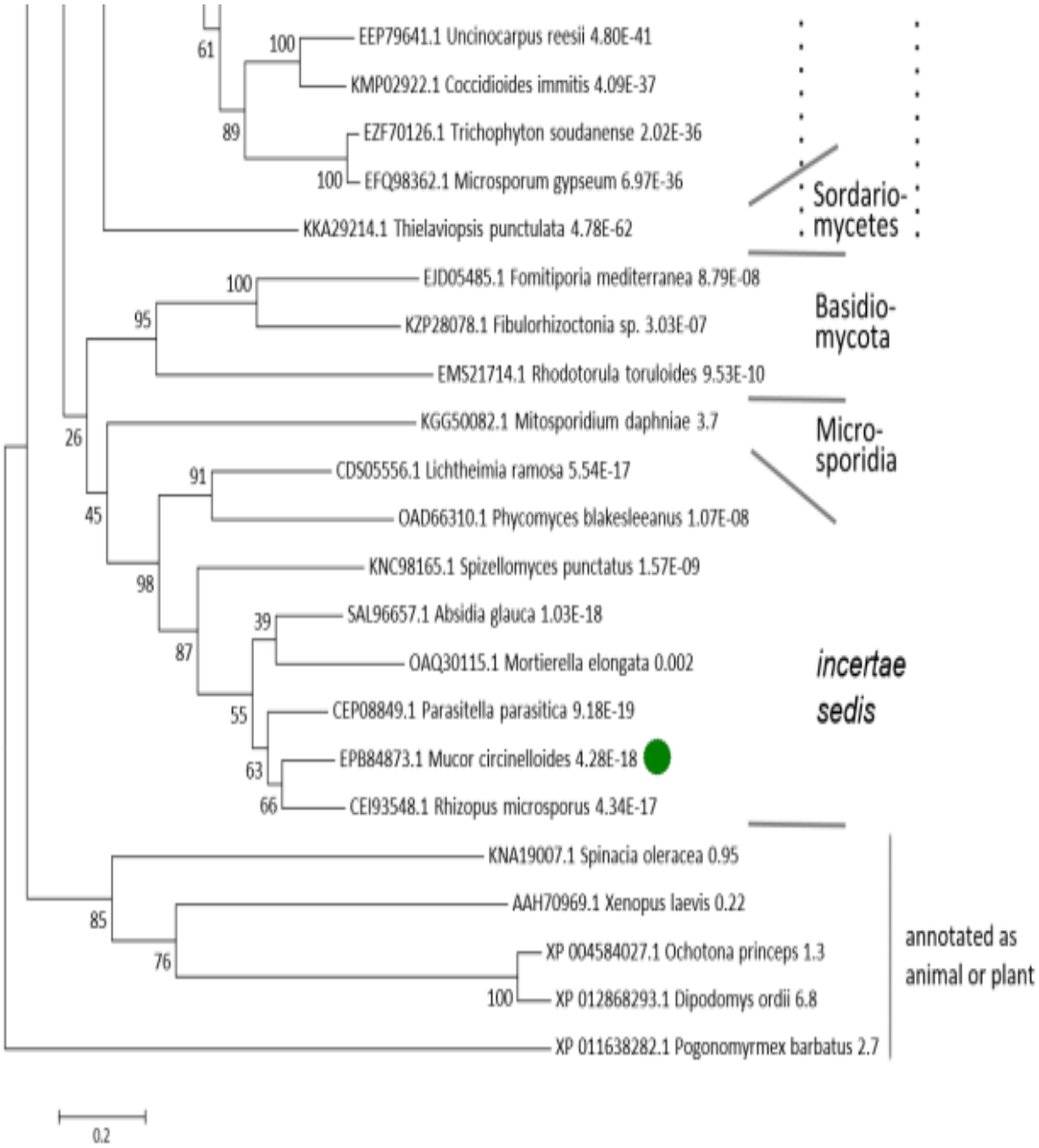
EEP79641.1 Uncinocarpus reesii 4.80E-41
KMP02922.1 Coccidioides immitis 4.09E-37
EZF70126.1 Trichophyton soudanense 2.02E-36
EFQ98362.1 Microsporum gypseum 6.97E-36
KKA29214.1 Thielaviopsis punctulata 4.78E-62
Sordario-mycetes
EJD05485.1 Fomitiporia mediterranea 8.79E-08
KZP28078.1 Fibulorhizoctonia sp. 3.03E-07
EMS21714.1 Rhodotorula toruloides 9.53E-10
Basidio-mycota
KGG50082.1 Mitosporidium daphniae 3.7
CDS05556.1 Lichtheimia ramosa 5.54E-17
OAD66310.1 Phycomyces blakesleeanus 1.07E-08
Micro-sporidia
KNC98165.1 Spizellomyces punctatus 1.57E-09
SAL96657.1 Absidia glauca 1.03E-18
OAQ30115.1 Mortierella elongata 0.002
CEP08849.1 Parasitella parasitica 9.18E-19
EPB84873.1 Mucor circinelloides 4.28E-18
CEI93548.1 Rhizopus microsporus 4.34E-17
incertae sedis
KNA19007.1 Spinacia oleracea 0.95
AAH70969.1 Xenopus laevis 0.22
XP 004584027.1 Ochotona princeps 1.3
XP 012868293.1 Dipodomys ordii 6.8
XP 011638282.1 Pogonomyrmex barbatus 2.7
annotated as animal or plant
0.2

Figure 8. SAD-7 homologs are present in a wide range of ascomycete fungi**.** The sequence of *N. crassa* SAD-7 was used as the query in a blastp search (Altschul *et al.* 1997) of NCBI's non-redundant protein database. The highest scoring subject sequence was selected for each *Neurospora* species present in the results (*N. crassa* and *N. tetrasperma*). The single most significant subject sequence for each other genus represented in the results was also selected. Each selected sequence was then used as the query in a reciprocal blastp search of all predicted *N. crassa* proteins. Those that identified SAD-7 as the most significant match were included in the SAD-7 phylogenetic analysis. SAD-7 sequences for *N. discreta*, *N. africana*, *N. sublineolata*, *N. terricola*, and *N. pannonica* were also included. These sequences were obtained from fungiDB (*N. discreta*) or a draft genome assembly downloaded from NCBI. Sequences were imported into MEGA (7.0.18) (Kumar *et al.* 2016) and aligned with MUSCLE using default settings. Positions having less than 95% coverage were eliminated and a Neighbor-Joining tree was constructed from the 220 remaining positions in MEGA using the Poisson correction method (Zuckerland and Pauling 1965). A bootstrap test (Felsenstein 1985) with 1000 replicates was performed. Each tip of the tree was labeled with the GenBank accession number, FungiDB number, or Genome Assembly number (NCBI) of the corresponding sequence. Species names and the Expect value for each sequence, which was obtained from the original blastp search of NCBI's non-redundant protein database with SAD-7 as query, were also included in the labels. NCBI's taxonomy database (Federhen 2003) was used to organize clades by phylum, as well as by class for sequences from ascomycete fungi. Syntenic relationships between some of the genes of the putative SAD-7 homologs were examined. Fourteen genes, including *N. crassa's* version, were confirmed to be adjacent to a gene predicted to encode an ARP2/3 complex protein (red stars). One *sad-7* homolog (blue star) was four genes away from a ubiquitin C-terminal hydrolase-encoding gene, while *N. crassa sad-7* was two genes away from a similar gene. Putative homologs of the four genes immediately surrounding *sad-7* in the *N. crassa* genome (*ncu01915*, *ncu01916*, *ncu01918*, and *ncu01919*) were not found near the putative *sad-7* homolog from *M. circinelloides* (green circle), suggesting the relationship between these two putative genes may not be biologically significant. Syntenic relationships were not investigated for other sequences in the tree.

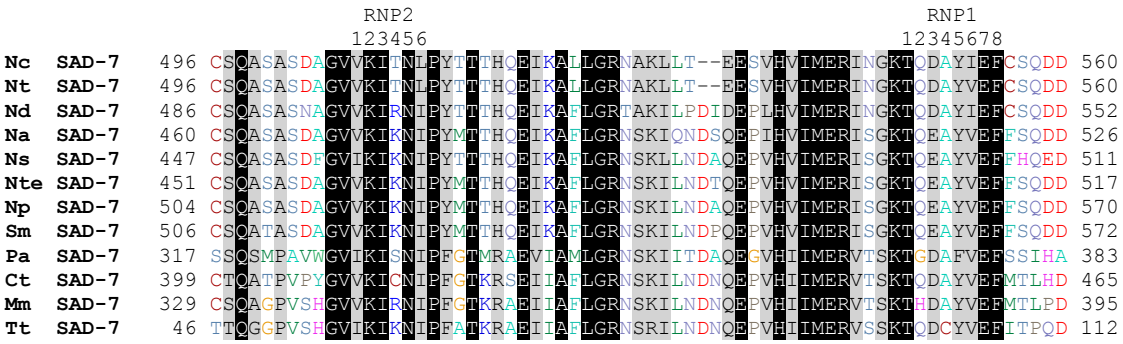

Figure 9. Alignment of RRM domains in a clade of Sordariales fungi. Amino acids are shaded according to the BLOSUM62 similarity matrix. Positions of the RNP1 and RNP2 motifs are indicated. Sequences can be obtained from GenBank or FungiDB with the following accession numbers: *Neurospora crassa* (*Nc*) EAA36312.1; *Neurospora tetrasperma* EGO51840.1; *Neurospora discreta* (*Nd*) NEUDI 136685; *Neurospora africana* (*Na*) GCA 000604205.2; *Neurospora sublineolata* (*Ns*) GCA 000604185.2; *Neurospora terricola* (*Nte*) GCA 000604245.2; *Neurospora pannonica* (*Np*) GCA 000604225.2; *Sordaria macrospora* (*Sm*) XP 003349025.1; *Podospora anserina* (*Pa*) CAP60824.1; *Chaetomium thermophilum* (*Ct*) EGS22685.1; *Madurella mycetomatis* (*Mm*) KXX77199.1; and *Thielavia terrestris* (*Tt*) AEO64981.1.

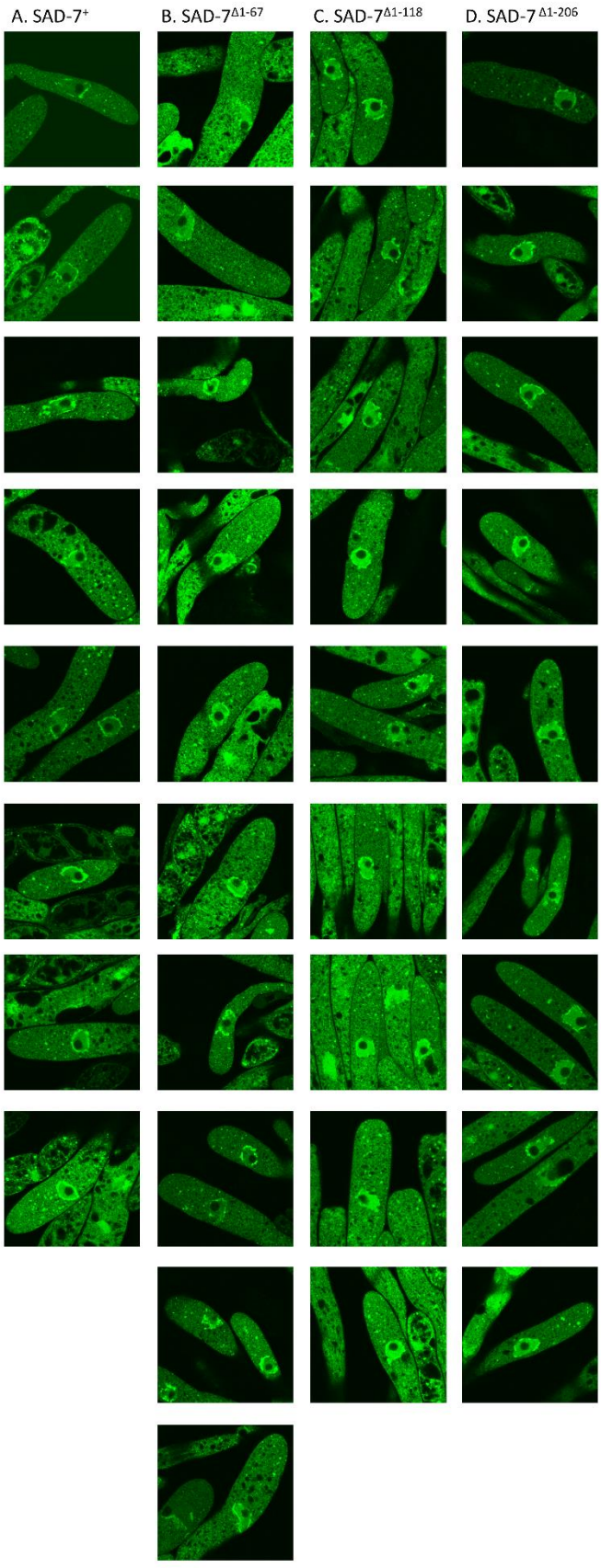
A. SAD-7+
B. SAD-7Δ1-67
C. SAD-7Δ1-118
D. SAD-7 Δ1-206

Figure 10. The meiotic localization pattern of GFP-SAD-7 does not depend on the first 206 amino acids of the protein. A series of truncated SAD-7 proteins was created by fusing GFP to different positions from the N-terminal end of SAD-7. Amino acids prior to the fusion point were deleted during the process. Representative images of GFP signal from asci undergoing meiosis I were shown in Figure 7. Additional images for each GFP-SAD-7 are shown here. (A) GFP was fused to the first amino acid of SAD-7 (ISU-3334 × ISU-3817). (B) GFP was fused to the 68th amino acid of SAD-7 (ISU-3334 × ISU-4078). (C) GFP was fused to the 119th amino acid of SAD-7 (ISU-3334 × ISU-4079). (D) GFP was fused to the 206th amino acid of SAD-7 (ISU-3334 × HDS36.1.1). The female strain in each cross is ISU-3334. This strain carries a *sad-2*$^{\Delta}$ allele, which allows the GFP-SAD-7 transgenes to be expressed despite being unpaired during meiosis.

Literature Cited

Alexander, W. G., N. B. Raju, H. Xiao, T. M. Hammond, T. D. Perdue *et al.*, 2008 DCL-1 colocalizes with other components of the MSUD machinery and is required for silencing. Fungal Genet. Biol. 45: 719–727.

Aramayo, R., and R. L. Metzenberg, 1996 Meiotic transvection in fungi. Cell 86: 103–113.

Aramayo, R., Y. Peleg, R. Addison, and R. Metzenberg, 1996 Asm-1+, a *Neurospora crassa* gene related to transcriptional regulators of fungal development. Genetics 144: 991–1003.

Aramayo, R., and E. U. Selker, 2013 *Neurospora crassa*, a model system for epigenetics research. Cold Spring Harb. Perspect. Biol. 5: a017921.

Bardiya, N., W. G. Alexander, T. D. Perdue, E. G. Barry, R. L. Metzenberg *et al.*, 2008 Characterization of interactions between and among components of the meiotic silencing by unpaired DNA machinery in *Neurospora crassa* using bimolecular fluorescence complementation. Genetics 178: 593–596.

Beadle, G. W., and E. L. Tatum, 1941 Genetic control of biochemical reactions in *Neurospora*. Proc. Natl. Acad. Sci. U. S. A. 27: 499–506.

Bistis, G. N., D. D. Perkins, and N. D. Read, 2003 Different cell types in *Neurospora crassa*. Fungal Genet. Newsl. 50: 17–19.

Brune, C., S. E. Munchel, N. Fischer, A. V. Podtelejnikov, and K. Weis, 2005 Yeast poly(A)-binding protein Pab1 shuttles between the nucleus and the cytoplasm and functions in mRNA export. RNA 11: 517–531.

Cassola, A., G. Noé, and A. C. Frasch, 2010 RNA recognition motifs involved in nuclear import of RNA-binding proteins. RNA Biol. 7: 339–344.

Catalanotto, C., M. Pallotta, P. ReFalo, M. S. Sachs, L. Vayssie *et al.*, 2004 Redundancy of the two dicer genes in transgene-induced posttranscriptional gene silencing in *Neurospora crassa*. Mol. Cell. Biol. 24: 2536–2545.

Cléry, A., M. Blatter, and F. H.-T. Allain, 2008 RNA recognition motifs: boring? Not quite. Curr. Opin. Struct. Biol. 18: 290–298.

Colot, H. V., G. Park, G. E. Turner, C. Ringelberg, C. M. Crew *et al.*, 2006 A high-throughput gene knockout procedure for *Neurospora* reveals functions for multiple transcription factors. Proc. Natl. Acad. Sci. USA. 103: 10352–10357.

Decker, L. M., E. C. Boone, H. Xiao, B. S. Shanker, S. F. Boone *et al.*, 2015 Complex formation of RNA silencing proteins in the perinuclear region of *Neurospora crassa*. Genetics 199: 1017–1021.

Ellison, C. E., C. Hall, D. Kowbel, J. Welch, R. B. Brem *et al.*, 2011 Population genomics and local adaptation in wild isolates of a model microbial eukaryote. Proc. Natl. Acad. Sci. U. S. A. 108: 2831–2836.

Federhen, S., 2003 The taxonomy project, in *The NCBI Handbook [Internet]*, National Center for Biotechnology Information (US).

Freitag, M., R. L. Williams, G. O. Kothe, and E. U. Selker, 2002 A cytosine methyltransferase homologue is essential for repeat-induced point mutation in *Neurospora crassa*. Proc. Natl. Acad. Sci. 99: 8802–8807.

Galagan, J. E., S. E. Calvo, K. A. Borkovich, E. U. Selker, N. D. Read *et al.*, 2003 The genome sequence of the filamentous fungus *Neurospora crassa*. Nature 422: 859–868.

Hammond, T. M., 2016 Sixteen years of meiotic silencing by unpaired DNA, in Advances in Genetics, Academic Press. DOI: 10.1016/bs.adgen.2016.11.001.

Hammond, T. M., W. G. Spollen, L. M. Decker, S. M. Blake, G. K. Springer *et al.*, 2013 Identification of small RNAs associated with meiotic silencing by unpaired DNA. Genetics 194: 279–284.

Hammond, T. M., H. Xiao, E. C. Boone, L. M. Decker, S. A. Lee *et al.*, 2013 Novel proteins required for meiotic silencing by unpaired DNA and siRNA generation in *Neurospora crassa*. Genetics 194: 91–100.

Hammond, T. M., H. Xiao, E. C. Boone, T. D. Perdue, P. J. Pukkila *et al.*, 2011 SAD-3, a putative helicase required for meiotic silencing by unpaired DNA, interacts with other components of the silencing machinery. G3 1: 369–376.

Hammond, T. M., H. Xiao, D. G. Rehard, E. C. Boone, T. D. Perdue *et al.*, 2011 Fluorescent and bimolecular-fluorescent protein tagging of genes at their native loci in *Neurospora crassa* using specialized double-joint PCR plasmids. Fungal Genet. Biol. 48: 866–873.

Hinnebusch, A. G., 2014 The scanning mechanism of eukaryotic translation initiation. Annu. Rev. Biochem. 83: 779–812.

Igel, H., S. Wells, R. Perriman, and M. Ares, 1998 Conservation of structure and subunit interactions in yeast homologues of splicing factor 3b (SF3b) subunits. RNA 4: 1–10.

Konikkat, S., and J. L. Woolford, 2017 Principles of 60S ribosomal subunit assembly emerging from recent studies in yeast. Biochem. J. 474: 195–214.

Langmead, B., and S. L. Salzberg, 2012 Fast gapped-read alignment with Bowtie 2. Nat. Methods 9: 357–359.

Lee, D. W., R. Millimaki, and R. Aramayo, 2010 QIP, a component of the vegetative RNA silencing pathway, is essential for meiosis and suppresses meiotic silencing in *Neurospora crassa*. Genetics 186: 127–133.

Lee, D. W., R. J. Pratt, M. McLaughlin, and R. Aramayo, 2003 An Argonaute-like protein is required for meiotic silencing. Genetics 164: 821–828.

Lee, D. W., K.-Y. Seong, R. J. Pratt, K. Baker, and R. Aramayo, 2004 Properties of unpaired DNA required for efficient silencing in *Neurospora crassa*. Genetics 167: 131–150.

Leinonen, R., H. Sugawara, and M. Shumway, 2011 The sequence read archive. Nucleic Acids Res. 39: D19-21.

Maiti, M., H.-C. Lee, and Y. Liu, 2007 QIP, a putative exonuclease, interacts with the Neurospora Argonaute protein and facilitates conversion of duplex siRNA into single strands. Genes Dev. 21: 590–600.

Marchler-Bauer, A., S. Lu, J. B. Anderson, F. Chitsaz, M. K. Derbyshire *et al.*, 2010 CDD: a Conserved Domain Database for the functional annotation of proteins. Nucleic Acids Res. 39: D225–D229.

Margolin, B. S., M. Freitag, and E. U. Selker, 1997 Improved plasmids for gene targeting at the *his-3* locus of *Neurospora crassa* by electroporation. Fungal Genet. Newsl. 44: 34–36.

Maris, C., C. Dominguez, and F. H.-T. Allain, 2005 The RNA recognition motif, a plastic RNA-binding platform to regulate post-transcriptional gene expression. FEBS J. 272: 2118–2131.

McCluskey, K., A. Wiest, and M. Plamann, 2010 The Fungal Genetics Stock Center: a repository for 50 years of fungal genetics research. J. Biosci. 35: 119–126.

Mortazavi, A., B. A. Williams, K. McCue, L. Schaeffer, and B. Wold, 2008 Mapping and quantifying mammalian transcriptomes by RNA-Seq. Nat. Methods 5: 621–628.

Muto, Y., and S. Yokoyama, 2012 Structural insight into RNA recognition motifs: versatile molecular Lego building blocks for biological systems. Wiley Interdiscip. Rev. RNA 3: 229–246.

Nagasowjanya, T., K. B. Raj, K. Sreethi Reddy, and D. P. Kasbekar, 2013 An apparent increase in meiotic silencing strength in crosses involving inbred *Neurospora crassa* strains. Fungal Genet. Biol. 56: 158–162.

Perkins, D. D., 2004 Wild type *Neurospora crassa* strains preferred for use as standards. Fungal Genet. Newsl. 51: 7–8.

Perkins, D. D., A. Radford, and M. S. Sachs, 2000 *The Neurospora Compendium: Chromosomal Loci*. Academic Press.

Perkins, D., and V. Pollard, 1986 Linear growth rates of strains representing 10 *Neurospora species*. Fungal Genet. Newsl. 33: 41–43.

Pratt, R. J., D. W. Lee, and R. Aramayo, 2004 DNA methylation affects meiotic trans-sensing, not meiotic silencing, in *Neurospora*. Genetics 168: 1925–1935.

Raju, N. B., 1980 Meiosis and ascospore genesis in Neurospora. Eur. J. Cell Biol. 23: 208–223.

Raju, N. B., R. L. Metzenberg, and P. K. T. Shiu, 2007 Neurospora *Spore killers Sk-2* and *Sk-3* suppress meiotic silencing by unpaired DNA. Genetics 176: 43–52.

Ramakrishnan, M., T. N. Sowjanya, K. B. Raj, and D. P. Kasbekar, 2011a A factor in a wild isolated *Neurospora crassa* strain enables a chromosome segment duplication to suppress repeat-induced point mutation. J. Biosci. 36: 817–821.

Ramakrishnan, M., T. N. Sowjanya, K. B. Raj, and D. P. Kasbekar, 2011b Meiotic silencing by unpaired DNA is expressed more strongly in the early than the late perithecia of crosses

involving most wild-isolated *Neurospora crassa* strains and in self-crosses of *N. tetrasperma*. Fungal Genet. Biol. FG B 48: 1146–1152.

Samarajeewa, D. A., P. A. Sauls, K. J. Sharp, Z. J. Smith, H. Xiao *et al.*, 2014 Efficient detection of unpaired DNA requires a member of the rad54-like family of homologous recombination proteins. Genetics 198: 895–904.

Shiu, P. K. T., and R. L. Metzenberg, 2002 Meiotic silencing by unpaired DNA: properties, regulation and suppression. Genetics 161: 1483–1495.

Shiu, P. K., N. B. Raju, D. Zickler, and R. L. Metzenberg, 2001 Meiotic silencing by unpaired DNA. Cell 107: 905–916.

Shiu, P. K. T., D. Zickler, N. B. Raju, G. Ruprich-Robert, and R. L. Metzenberg, 2006 SAD-2 is required for meiotic silencing by unpaired DNA and perinuclear localization of SAD-1 RNA-directed RNA polymerase. Proc. Natl. Acad. Sci. USA. 103: 2243–2248.

Son, H., K. Min, J. Lee, N. B. Raju, and Y.-W. Lee, 2011 Meiotic silencing in the homothallic fungus *Gibberella zeae*. Fungal Biol. 115: 1290–1302.

Thompson, J. D., D. G. Higgins, and T. J. Gibson, 1994 CLUSTAL W: improving the sensitivity of progressive multiple sequence alignment through sequence weighting, position-specific gap penalties and weight matrix choice. Nucleic Acids Res. 22: 4673–4680.

Van Heemst, D., F. James, S. Pöggeler, V. Berteaux-Lecellier, and D. Zickler, 1999 Spo76p is a conserved chromosome morphogenesis protein that links the mitotic and meiotic programs. Cell 98: 261–271.

Vogel, H. J., 1956 A convenient growth medium for *Neurospora* (Medium N). Microb. Genet Bull 13: 42–43.

Wang, Z., F. Lopez-Giraldez, N. Lehr, M. Farré, R. Common *et al.*, 2014 Global gene expression and focused knockout analysis reveals genes associated with fungal fruiting body development in *Neurospora crassa*. Eukaryot. Cell 13: 154–169.

Wang, Y., K. M. Smith, J. W. Taylor, M. Freitag, and J. E. Stajich, 2015 Endogenous small RNA mediates meiotic silencing of a novel DNA transposon. G3 Bethesda Md 5: 1949–1960.

Westergaard, M., and H. K. Mitchell, 1947 Neurospora V. A synthetic medium favoring sexual reproduction. Am. J. Bot. 34: 573–577.

Wu, C., F. Yang, K. M. Smith, M. Peterson, R. Dekhang *et al.*, 2014 Genome-wide characterization of light-regulated genes in *Neurospora crassa*. G3 Bethesda Md 4: 1731–1745.

Xiao, H., W. G. Alexander, T. M. Hammond, E. C. Boone, T. D. Perdue *et al.*, 2010 QIP, a protein that converts duplex siRNA into single strands, is required for meiotic silencing by unpaired DNA. Genetics 186: 119–126.

Yu, J.-H., Z. Hamari, K.-H. Han, J.-A. Seo, Y. Reyes-Domínguez *et al.*, 2004 Double-joint PCR: a PCR-based molecular tool for gene manipulations in filamentous fungi. Fungal Genet. Biol. 41: 973–981.

CHAPTER IV

IDENTIFICATION OF A GENETIC ELEMENT REQUIRED AND SUFFICIENT FOR SPORE KILLING IN NEUROSPORA

This work has been submitted for publication as:

Harvey A[1]., N. Rhoades[1], D.A. Samarajeewa[1], J. Svedberg, P. Manitchotpisit, K.J. Sharp, D.G Rehard, D.W. Brown, H. Johannesson, P.K.T. Shiu, and T.M. Hammond, 2017 Identification of a genetic element required and sufficient for spore killing in Neurospora. G3.

Abstract

Meiotic drive elements possess an ability to be transmitted through meiosis to the next generation in a biased manner. *Spore killer-2* (*Sk-2*) in Neurospora is a classic example of a meiotic drive element. When *Sk-2* is crossed with a *Spore killer* sensitive mating partner (Sk^S), nearly all of the surviving ascospores (offspring) are of the *Sk-2* genotype. Analysis of the ascospore sacs (asci) finds that half of the offspring are dead and the dead progeny are presumed to be of the Sk^S genotype. While the mechanistic details of *Sk-2*-based meiotic drive are unknown, the existence of a resistance protein and a killer molecule has been proposed. Previously, we identified a locus named *rfk-1*, which is required for spore killing and maps to a 45 kb region of chromosome III (within *Sk-2*). Here, we identify a genetic element that is both required and sufficient for spore killing. This element is found within a 1481 bp interval (called $AH36^{Sk\text{-}2}$) of DNA from the 45 kb *rfk-1* region. Deletion of this interval from *Sk-2* results in loss of spore killing, while placement of the interval in Sk^S creates a meiotic abortion phenotype consistent with the presence of a killer. Additionally, the 1481 bp interval of an *rfk-1* mutant (ISU-3211) carries six mutations, one or more of which could be responsible for loss of killing. Future work will seek to determine the nature of the killer within *AH36* as well as its relationship to the previously defined *rfk-1* locus.

Keywords: Meiotic Drive, Transmission Ratio Distortion, Spore Killing, MSUD

Introduction

In eukaryotic organisms, genetic loci are typically transmitted through sexual reproduction to the next generation in a Mendelian manner. However, some loci possess the ability to bias their own transmission rates through meiosis or gametogenesis at the expense of a competing locus. These "selfish" loci are often referred to as meiotic drive elements (Zimmering *et al.* 1970). The genomic conflict caused by such selfish loci may have profound evolutionary impacts on factors ranging from gametogenesis to mating system evolution and speciation (Lindholm *et al*. 2016). Meiotic drive elements are found across the eukaryote tree of life (Burt and Trivers 2008), and classic examples include *SD* in fruit flies (reviewed by Larracuente and Presgraves 2012), the *t*-complex in mice (reviewed by Lyon 2003; Sugimoto 2014), and *Ab10* in *Zea mays* (Rhoades 1952; Kanizay *et al.* 2013). In the fungal kingdom, meiotic drive elements can achieve biased transmission through spore killing (reviewed by Raju 1994). While the prion-based spore killing mechanism of *Podospora anserina het-s* has been characterized (Dalstra *et al.* 2003; Saupe 2011), the mechanisms by which other fungal meiotic drive elements kill spores are mostly obscure.

Two of the first fungal meiotic drive elements to be discovered were identified in *Neurospora intermedia* (Turner and Perkins, 1979). This species is closely related to the genetic model *Neurospora crassa* (Davis 2000) and the mating processes in both fungi are essentially identical. Mating begins with fertilization of an immature fruiting body called a protoperithecium by a mating partner of the opposite mating type. After fertilization, the protoperithecium develops into a mature fruiting body called a perithecium. The nuclei from each parent multiply within the developing perithecium, and a single nucleus from each parent is sequestered into a tube-like meiotic cell. Meiosis begins with fusion of the parental nuclei and ends with production

of four recombinant daughters (Raju 1980). Each recombinant proceeds through a single round of mitosis, resulting in a total of eight nuclei in the meiotic cell. A process known as ascosporogenesis then constructs cell walls and membranes around each nucleus to produce sexual spores called ascospores. Maturing ascospores accumulate a dark pigment and develop the shape of a spindle; thus, at the end of ascosporogenesis, the mature meiotic cells appear to contain eight miniature black American footballs. The meiotic cells also serve as ascospore sacs (asci) (Figure 1A). A single perithecium can produce hundreds of asci, each derived from a unique meiotic event (Raju 1980).

During an effort in the 1970s to collect and characterize Neurospora isolates from around the world, Turner and Perkins discovered pairs of compatible mating partners that did not produce asci with eight viable ascospores. This outcome was more common when crosses were performed between isolates from widely separated populations, and in some cases the abnormal asci were attributed to heterozygosity of chromosome rearrangements between mating partners (Perkins 1974; Turner and Perkins 1979). However, for a few isolates of *N. intermedia*, asci with atypical phenotypes were determined to be due to chromosomal factors called *Spore killer-2* (*Sk-2*) and *Spore killer-3* (*Sk-3*) (Turner and Perkins 1979). *Sk-2* and *Sk-3* are not single genes, rather, they are complexes of genes that span approximately 30 cM of chromosome III (Turner and Perkins 1979; Campbell and Turner 1987). Furthermore, they are transmitted through meiosis as single units due to a recombination suppression mechanism thought to be enforced by inversions throughout the elements (Turner and Perkins 1979; Campbell and Turner 1987; Hammond *et al.* 2012; Harvey *et al.* 2014). Unlike standard genetic elements, which display a Mendelian transmission rate (50%) through meiosis and ascosporogenesis, *Sk-2* and *Sk-3* are transmitted at levels approaching 100% (Turner and Perkins 1979). This biased transmission rate

occurs because *Sk-2* and *Sk-3* kill ascospores that do not inherit resistance to spore killing (Raju 1979; Turner and Perkins 1979). For example, in *Sk-2* × *Spore killer*-sensitive (Sk^S) crosses, asci with four black ascospores and four clear ("white") ascospores are produced (Figure 1A). This phenotype is symbolized as 4B:4W. The four black ascospores are typically viable and nearly always of the *Sk-2* genotype, while the four white ascospores are inviable and presumed to be of the Sk^S genotype (Turner and Perkins 1979). The same phenomenon occurs in *Sk-3* × Sk^S crosses, except the four black ascospores are of the *Sk-3* genotype instead of the *Sk-2* genotype (Turner and Perkins 1979).

Although *Spore killers* have not yet been detected in wild isolates of *N. crassa*, *Sk-2* and *Sk-3* have been introgressed into *N. crassa* for genetic analysis (Turner and Perkins 1979). This introgression has allowed for the discovery of resistance to spore killing in natural *N. crassa* populations (Turner and Perkins 1979; Turner 2001). One of these natural isolates (FGSC 2222) contains a gene whose function is best described by its name: *resistance to spore killer* (*rsk*). Crosses of rsk^{LA} × *Sk-2*, where rsk^{LA} refers to the genotype of FGSC 2222, produce asci with an 8B:0W phenotype because ascospores inherit either rsk^{LA} or *Sk-2*, both of which are sufficient for resistance to *Sk-2*-based spore killing (Hammond *et al.* 2012). Discovery of rsk^{LA} has made identifying other *rsk* alleles possible, some of which do not provide resistance to known *Spore killers*. For example, the Oak Ridge *rsk* allele (rsk^{OR}), typical of most laboratory strains, is resistant to neither *Sk-2* nor *Sk-3* (Hammond *et al.* 2012). Some *rsk* alleles confer resistance to *Sk-3* but not *Sk-2*. An example is rsk^{PF5123}, which exists in an *N. intermedia* isolate from French Polynesia (Turner 2001; Hammond *et al.* 2012). *Sk-2* and *Sk-3* themselves also carry resistant versions of *rsk*, referred to as $rsk^{Sk\text{-}2}$ and $rsk^{Sk\text{-}3}$, respectively (Hammond *et al.* 2012). This helps explain why homozygous *Sk-2* (i.e., *Sk-2* × *Sk-2*) and homozygous *Sk-3* crosses produce asci

with an 8B:0W phenotype (Turner and Perkins 1979); that is, each ascospore inherits a resistant *rsk* allele. It also helps explain why heterozygous crosses between different *Spore killers* (i.e., *Sk-2* × *Sk-3*) produce asci with a 0B:8W phenotype (Turner and Perkins 1979). In *Sk-2* × *Sk-3* heterozygous crosses, each ascospore inherits either $rsk^{Sk\text{-}2}$ or $rsk^{Sk\text{-}3}$ but not both, and $rsk^{Sk\text{-}2}$ ascospores are killed by *Sk-3* and $rsk^{Sk\text{-}3}$ ascospores are killed by *Sk-2*.

The Killer Neutralization (KN) model has been proposed to explain how *Sk-2* and *Sk-3* achieve biased transmission through meiosis and ascosporogenesis (Hammond *et al.* 2012). The KN model holds that *Sk-2* and *Sk-3* each achieve biased transmission with a resistance protein and a spore killing molecule (i.e., a killer), both of which are active throughout meiosis and ascosporogenesis. For example, during the early stages of meiosis in an Sk^{S} × *Sk-2* cross, both the resistance protein and the killer are thought to be free to diffuse throughout the meiotic cell. Unrestricted movement allows the resistance protein to neutralize the killer wherever it may be found. However, once ascospores are separated from the cytoplasm, the resistance protein is thought to be restricted to only those ascospores that produce it (i.e., *Sk-2* ascospores), and ascospores that do not carry a resistant version of *rsk* (i.e., Sk^{S} ascospores) are subsequently killed because either the killer is able to move between ascospores after delimitation, or, the killer has a long half-life and remains functional in all ascospores after delimitation.

Evidence for the KN model is seen in the outcome of Sk^{S} × *Sk-2* $rsk^{\Delta Sk\text{-}2}$ crosses, where the latter strain has been deleted of its *rsk* allele. Such crosses produce asci that abort meiosis before ascospore production; this is, these crosses typically produce asci without ascospores (Hammond *et al.* 2012). Meiotic cells of these crosses may express the killer in the absence of a resistance protein, causing the killing process to begin early in meiosis at the ascus level rather than during ascosporogenesis at the ascospore level. The KN model is also supported by the

existence of different *rsk* alleles. Previous studies have demonstrated the sequence of RSK to be the most important factor towards determining which killer it neutralizes (Hammond *et al.* 2012), suggesting RSK and the killer interact by a "lock and key" mechanism. However, testing this model has been difficult because the molecular nature of the killer remains unknown. The killer could be a protein encoded by a single gene, a heterodimer encoded by two genes, a metabolite produced by an enzyme, a toxic RNA molecule, or perhaps even an epigenetically-modified interval of DNA.

As described above, Sk^{S} × *Sk-2* $rsk^{\Delta Sk\text{-}2}$ crosses produce early abortive asci. We recently used this characteristic of Sk^{S} × *Sk-2* $rsk^{\Delta Sk\text{-}2}$ crosses to screen for mutations that disrupt spore killing (Harvey *et al.* 2014). Specifically, we fertilized an Sk^{S} mating partner with mutagenized *Sk-2* $rsk^{\Delta Sk\text{-}2}$ conidia (asexual spores that also function as fertilizing propagules). We reasoned that only an *Sk-2* $rsk^{\Delta Sk\text{-}2}$ conidium mutated in a gene "required for killing" would produce large numbers of viable ascospores when crossed with Sk^{S}. Our prediction appears to have been accurate because the screen allowed us to isolate six *required for killing* (*rfk*) mutants (Hammond *et al.* 2012). Complementation analysis of the six mutant strains suggested all to be mutated at the same locus, subsequently named *rfk-1*, and we mapped this locus to a 45 kb region within *Sk-2* on chromosome III (Harvey *et al.* 2014). Herein, we present evidence for a genetic element that is both required and sufficient for spore killing. This element exists within a 1481 bp interval (called $AH36^{Sk\text{-}2}$) of the 45-kb *rfk-1* region.

Materials and Methods

Strains, media, and crossing conditions

Most knockouts and markers used in this study were obtained from the Fungal Genetics Stock Center (FGSC; McCluskey *et al*. 2010). The key strains used in this study are listed along with genotype information in Table 1. Strains are available upon request. Vogel's minimum medium (Vogel 1956) was used to grow and maintain all strains. Synthetic crossing medium (pH 6.5) with 1.5% sucrose, as described by Westergaard and Mitchell (1947), was used for all crosses. Crosses were performed on a laboratory benchtop at room temperature under ambient lighting. Crosses were unidirectional, meaning one parent was designated as female and the other as male. The female parent was inoculated to the center of a 60 mm or 100 mm Petri dish and cultured at room temperature for a period of five to seven days. These female cultures were then fertilized with suspensions of conidia from the male parent. Crosses were allowed to mature for 12-16 days before perithecial dissection in 25 or 50% glycerol. Asci were examined with a standard compound light microscope and imaging system.

Transformation, genotype confirmation, and DNA sequencing

A technique called double-joint PCR was used to construct twelve deletion vectors (Yu *et al.* 2004; Hammond *et al.* 2011). Each required eight oligonucleotide PCR primers, descriptions of which are provided in supporting information (Table 3). In brief, a hygromcycin resistance marker (*hph*) from plasmid pCB1004 (Carroll *et al.* 1994) was fused to 0.5-1.0 kb intervals of DNA derived from both sides of the deletion target.

Transgene insertion vectors were created with pTH1256.1 (Smith *et al.* 2016), a plasmid designed to integrate transgenes along with *hph* next to the *his-3* gene on chromosome I. Transgenes were PCR-amplified from strain F2-19, unless otherwise indicated, and cloned into

the *Not*I site of pTH1256.1. Primer sequences are provided in Table 3. Transformations were performed by electroporation of conidia as previously described (Margolin *et al*. 1997). Transformation hosts for gene deletion experiments were either P15-53 or ISU-3223. Transformation hosts for transgene integration experiments were either P8-42 or P8-43. Homokaryons were derived from heterokaryotic transformants with a microconidium isolation technique (Ebbole and Sachs, 1990) or by crossing to obtain homokaryotic ascospores. Genomic DNA was isolated from lyophilized mycelia (vegetative mass) using IBI Scientific's (Peosta, IA) Genomic DNA Mini Kit for Plants, and gene deletions and transgene integrations were confirmed by PCR with the Phusion DNA Polymerase Kit (Thermo Fisher Scientific, Waltham, MA). Although most transgenes were not sequenced to eliminate the possibility of mutation during cloning and transformation, four key transgenes were determined to be free of mutation after transformation. These are $AH30^{Sk\text{-}2}$, $AH32^{Sk\text{-}2}$, $AH36^{Sk\text{-}2}$, and $AH36^{3211}$. Specifically, a transformant was isolated, purified to homogeneity, and used to produce genomic DNA, which was then used as template for amplification of the transgene by PCR. The PCR products were purified with IBI Scientific's Gel/PCR Fragment Extraction Kit and sequenced by Sanger sequencing. Sequences were analyzed with BioEdit (Hall 1999).

Statement on data and reagent availability

All strains generated during this study are available upon request.

Results

Deletion of a DNA interval spanning most of Sk-2^{INS1} eliminates spore killing

The 45 kb *rfk-1* region contains 14 putative protein-coding genes and two putative pseudogenes (Figure 1B) (Harvey *et al.* 2014). It also contains part of an inverted sequence (*Sk-2*^{INV1}), an inversion breakpoint, and an 11 kb insertion (*Sk-2*^{INS1}) (Figure 1B) (Harvey *et al.* 2014). In an attempt to refine the location of *rfk-1* within this 45 kb region, we focused on three intervals. The first interval, *v3*, is found in the intergenic region between genes *6192* and *6191* (Figure 1B and Table 2). The second interval is referred to as *v4*. It is located in the intergenic region between genes *6239* and *6240* (Figure 1B and Table 2). The third interval, *v5*, spans most of the sequence between genes *6191* and *6238* (Figures 1B and 2A, and Table 2). Unlike *v3* and *v4*, which are short intervals of intergenic DNA (originally intended for use in mapping experiments similar to those described by (Harvey *et al.* 2014)), *v5* is a relatively long interval and includes most of *Sk-2*^{INS1}. Intervals *v3*, *v4*, and *v5* were each replaced with a hygromycin resistance gene (*hph*) and the resulting transgenic strains were crossed with an *Sk*^{S} mating partner. Crosses of *Sk*^{S} × *Sk-2 v3*$^{\Delta}$ produced asci with a 4B:4W phenotype (Figure 1C), indicating that spore killing occurs and interval *v3* is not required for spore killing. Similarly, *Sk*^{S} × *Sk-2 v4*$^{\Delta}$ crosses produced 4B:4W asci (Figure 1D), demonstrating interval *v4* is also not required for spore killing. In contrast, crosses of *Sk*^{S} × *Sk-2 v5*$^{\Delta}$ produced asci with an 8B:0W phenotype (Figure 1E), indicating deletion of interval *v5* eliminates *Sk-2*'s ability to kill ascospores. Therefore, interval *v5* overlaps a genetic element required for spore killing.

A DNA interval between pseudogene 7378 and gene 6238 is required for spore killing*

We sought to further refine the position of the killing element within *v5* by defining nine subintervals of *v5* (Figure 2B and Table 2), deleting these subintervals, and crossing the deletion strains with an Sk^S mating partner. Crosses of Sk^S × *Sk-2* $v31^{\Delta}$ produced asci with a 4B:4W phenotype. Because interval *v31* overlaps genes *16627* and *6412* (Figure 2B and Table 2), we can conclude genes *16627* and *6412* are not required for spore killing. Similarly, crosses of Sk^S × *Sk-2* $v32^{\Delta}$, Sk^S × *Sk-2* $v33^{\Delta}$, and Sk^S × *Sk-2* $v34^{\Delta}$ (Figure 3, B–D) all produced asci with a 4B:4W phenotype, demonstrating that gene *6413,* as well as pseudogenes *4949** and *7838**, (Figure 2B and Table 2) are also not required for spore killing. In contrast, crosses of Sk^S × *Sk-2* $v35^{\Delta}$ produced asci with an 8B:0W phenotype (Figure 3E). Interval *v35* contains pseudogenes *4949** and *7838**, as well as much of the intergenic region between pseudogene *7838** and gene *6238* (Figure 2B and Table 2). Because the pseudogenes *4949** and *7838** were already shown to be dispensable for spore killing (Figure 3, C and D), the 8B:0W phenotype resulting from $v35^{\Delta}$ must be due to deletion of the intergenic region between pseudogene *7838** and gene *6238*. This hypothesis is consistent with crosses of Sk^S × *Sk-2* $v37^{\Delta}$, Sk^S × *Sk-2* $v38^{\Delta}$, Sk^S × *Sk-2* $v39^{\Delta}$, and Sk^S × *Sk-2* $v40^{\Delta}$, all of which produced asci with an 8B:0W phenotype (Figure 3, F, G, H, and I) and three of which involve only deletions of the intergenic region between pseudogene *7838** and gene *6238* (Figure 2B and Table 2). In summary, the results of these experiments demonstrate that a genetic element required for spore killing is located within the intergenic region between pseudogene *7838** and gene *6238.*

An ascus aborting element exists between pseudogene 7838 and gene 6238*

To investigate whether the genetic element in the intergenic region between pseudogene *7838** and gene *6238* is sufficient for spore killing, we constructed eight transgenic strains, each carrying a different interval from *Sk-2*^{INS1} at the *his-3* locus in an otherwise *Sk*^{S} genetic background. [The *his-3* locus is a standard location for integration of transgenes in *N. crassa* (Margolin *et al.* 1997)]. The transgenes are *AH4*$^{Sk-2}$, *AH6*$^{Sk-2}$, *AH14*$^{Sk-2}$, *AH30*$^{Sk-2}$, *AH31*$^{Sk-2}$, *AH32*$^{Sk-2}$, *AH36*$^{Sk-2}$, and *AH37*$^{Sk-2}$ (Figure 2C and Table 2), where the non-superscripted characters refer to the interval and the superscripted characters refer to the source of the interval. For example, *AH4*$^{Sk-2}$ is a transgene containing interval *AH4* from an *Sk-2* strain. Crosses of *Sk*^{S} × *AH4*$^{Sk-2}$ produced asci with an 8B:0W phenotype (Figure 4A). This phenotype is expected because *AH4* overlaps genes *16627* and *6412* (Figure 2C and Table 2), neither of which are required for spore killing (based on the deletion experiments described above). However, all of the crosses involving Sk^{S} and a transgene-carrying strain produced asci with an 8B:0W phenotype (Figure 4, B-H), even when the transgene contained DNA from the region between pseudogene *7838** and the gene *6238* (i.e. the region required for spore killing according to deletion analysis). At least two reasons exist to explain the 8B:0W phenotype of these crosses: first, while some of the examined intervals contain a genetic element that is required for spore killing, none of them contain a genetic element that is sufficient for spore killing; and second, some of the examined intervals contain a genetic element that is required and sufficient for spore killing, but the genetic element is silenced when it is unpaired during meiosis.

Meiotic silencing by unpaired DNA (MSUD) is an epigenetic process that allows meiotic cells to identify and silence unpaired DNA during meiosis (for review, Hammond 2016; Aramayo and Selker 2013). When an *Sk*^{S} strain is crossed to a mating partner carrying an ectopic

transgene, MSUD typically identifies the transgene as lacking a pairing partner and attempts to silence it for the duration of meiosis (Shiu *et al.* 2001; Lee *et al.* 2004). Therefore, in order to detect phenotypes that depend on the expression of unpaired transgenes during meiosis, it is often necessary to perform experimental crosses in an MSUD-deficient background. This can be achieved by deleting a gene called *sad-2* from one of the crossing parents (Shiu *et al.* 2006). By crossing our transgenic strains containing different intervals of the *Sk-2*^{INS1} region to a parent containing *sad-2*, we were able to detect a spore killing-like phenomenon with some, but not all, interval-carrying transgenes. Specifically, *AH4*$^{Sk-2}$, *AH6*$^{Sk-2}$, *AH14*$^{Sk-2}$, and *AH32*$^{Sk-2}$ each produced asci with an 8B:0W phenotype when crossed to *Sk*^{S} *sad-2*$^{\Delta}$ (Figure 5, A–C and H), demonstrating that intervals *AH4*, *AH6*, *AH14*, and *AH32* are not sufficient for spore killing. Additionally, because genes and pseudogenes *16627*, *6412*, *6413*, *4949** and *7838** are located in these intervals (Figure 2C and Table 2), we can conclude that none of these genes are sufficient for spore killing. In contrast, *AH30*$^{Sk-2}$, *AH31*$^{Sk-2}$, *AH36*$^{Sk-2}$, and *AH37*$^{Sk-2}$ produced either aborted asci or bubble asci when crossed to *Sk*^{S} *sad-2*$^{\Delta}$ (Figure 5, D–G), demonstrating intervals *AH30*, *AH31*, *AH36*, and *AH37* all induce ascus and/or ascospore abortion [The "bubble" phenotype was originally described by Raju *et al*. (1987). It is thought to arise when ascospores abort shortly after ascospore delimitation]. We currently assume the abortion phenotype and spore killing to be different manifestations of the same biological mechanism (discussed below) and it is important to note that all abortion-inducing intervals overlap positions 27,900–29,380 of the 45 kb *rfk-1* region (Table 2). Although interval *AH32* partially overlaps these positions (i.e., 28,304–29,702) (Figure 2C and Table 2), it did not correlate with an abortion phenotype (Figure 5H). A reason could be that *AH32* lacks positions 27,900–28,303 (Figure 2C; Table 2), and these positions are necessary for the killing and abortion sufficiency.

The AH36 interval from an rfk-1^{3211} strain does not cause ascus abortion

The shortest abortion-inducing interval is *AH36*, which contains positions 27,900–29,380. The research path that led us to this 1481 bp region began with *rfk-1* mapping; thus, it is reasonable to assume *rfk-1* is found within these positions. If true, then the *AH36* interval from the *rfk-1* mutant allele used for *rfk-1* mapping (*rfk-1*^{3211}) (Harvey *et al.* 2014) should not induce ascus/ascospore abortion in an *Sk*^{S} genetic background. To test this hypothesis, we transferred the *AH36* interval of an *rfk-1*^{3211} strain (ISU-3211) to *Sk*^{S}. As a control, we repeated the procedure using the *AH36* interval from a standard *Sk-2* strain. As predicted, *Sk*^{S} × *AH36*^{3211} crosses produced asci with a normal 8B:0W phenotype whether or not MSUD was proficient (Figure 6, A and B). Also as predicted, the *Sk*^{S} × *AH36*$^{Sk\text{-}2}$ control crosses produced 8B:0W asci when MSUD was proficient (Figure 6C) and aborted asci/ascospores when MSUD was deficient (Figure 6D). These findings demonstrate that *AH36*^{3211} carries at least one mutation that disrupts spore killing.

AH36 intervals from an rfk-1^{+} *strain and an rfk-1*^{3211} *strain have different DNA sequences*

The sequence of *AH36*$^{Sk\text{-}2}$ is 1481 bp long (Figure 7A). Previous *in silico* analysis of *Sk-2*^{INS1} did not identify a putative protein-coding sequence within this region, possibly because the *Sk-2*^{INS1} sequence was used to search a database of *N. crassa* proteins (Harvey *et al.* 2014). Interestingly, performing a BLASTX (2.6.1) search (Altschul *et al.* 1997) of the National Center for Biotechnology Information's (NCBI's) non-redundant protein database with *AH36*$^{Sk\text{-}2}$ as the query identified a 35 amino acid (aa) segment of a hypothetical protein (NCBI reference number: XP_009850392) from *Neurospora tetrasperma* as a related sequence (Expect value: 1.8e-2) (Figure 7A, underlined bases). However, a search of NCBI's conserved domain database (Marchler-Bauer *et al.* 2015) with the entire predicted sequence of the putative *N. tetrasperma*

protein as query did not identify a conserved domain to help infer its function (data not shown). *AH36*$^{Sk-2}$ contains another region of interest: a 46–48 bp tandem repeat (7.17 repeats) between positions 28,384 and 28,722 (Figure 7, A and B). The biological significance of this repetitive element is unknown, and a BLASTN 2.6.1+ search (Zhang *et al.* 2000; Morgulis *et al.* 2008) of NCBI's non-redundant nucleotide database with the repetitive element as query failed to identify a related element in another organism (data not shown).

The different phenotypes associated with *AH36*$^{Sk-2}$ and *AH36*^{3211} suggest they differ at the sequence level. Indeed, sequencing the different alleles allowed us to identify six mutations in *AH36*^{3211}, at least one of which must disable the abortion phenotype associated with *AH36*$^{Sk-2}$. Each mutation results from a guanine to adenine transition, with a guanine occurring in *AH36*$^{Sk-2}$ and an adenine in *AH36*^{3211} (Figure 7A). All six mutations are found between positions 27,945 and 28,326; thus, they are located at approximately the same location as the sequences with similarity to the aforementioned hypothetical protein from *N. tetrasperma* (Figure 7A; compare highlighted and underlined bases).

Discussion

The Neurospora *Spore killers* are meiotic drive elements that exhibit biased transmission through meiosis and ascosporogenesis. The biological mechanism used by the Neurospora *Spore killers* to achieve biased transmission is poorly understood. We recently discovered a spore-killing resistance gene called *rsk* (Hammond *et al.* 2012) and a mutant locus called *rfk-1* (Harvey *et al.* 2014). While *rsk* provides resistance to spore killing, a mutation in *rfk-1* disrupts spore killing. The *rfk-1* locus is located within a 45 kb region of *Sk-2* on chromosome III (Hammond *et al.* 2012). Here, we have provided multiple lines of evidence supporting the following primary

hypothesis: a genetic element that is required and sufficient for spore killing is transcribed from a 1481 bp interval (referred to as *AH36)* within the 45 kb *rfk-1* region.

The first line of evidence supporting our primary hypothesis involves our deletion and transgene-integration experiments. We created twelve different deletion strains, each deleted for a specific interval of the 45 kb *rfk-1* region (Figure 1B and 2B). Half of the deletion strains had no effect on spore killing, while the other half eliminated the process (Figure 3). By deductive reasoning, we concluded that the intergenic region between pseudogene *7838** and gene *6238* must contain a genetic element required for spore killing. This hypothesis is supported by findings from our transgene-integration experiments, where eight different intervals of *Sk-2* were placed as transgenes next to a gene called *his-3* in an *Sk*^{S} genetic background (Figure 2C). Four of these transgenes had no qualitative effect on ascus development under MSUD-proficient and MSUD-deficient conditions (Figures 4 and 5). The other four had no qualitative effect on ascus development under MSUD-proficient condition but they produced aborted asci or (presumably) aborted ascospores under MSUD-deficient conditions (Figures 4 and 5). All abortion-inducing intervals have one characteristic in common: they contain positions 27,900–29,380 of the 45 kb *rfk-1* region. This interval has been defined as *AH36* (Figure 2C and Table 2). Accordingly, deletions that eliminate spore killing also remove at least some positions from interval *AH36*.

The results of this study suggest that *AH30*, *AH31*, *AH36*, and *AH37* contain a genetic element required and sufficient for spore killing. If this is true, why do three of these intervals appear to produce aborted asci (*AH30*, *AH31*, *AH37*), while one of them (*AH36*) appears to produce aborted ascospores. The answer may be related to the lack of resistance in such crosses and the expression level of the killer. For example, the KN model holds that the resistance protein (RSK) and the killer are both active during early stages of meiosis (Hammond *et al.*

2012). Lack of a resistant version of RSK, along with high expression of the killer, may cause asci to abort (i.e. be killed) early in meiosis before ascospore delimitation. In contrast, lack of a resistant version of RSK, along with low expression of the killer, may allow asci to progress past ascospore delimitation before abortion. If this explanation is true, the killer should be expressed at higher levels from intervals *AH30*, *AH31*, and *AH37*, than it is from interval *AH36*. *AH36* is the shortest abortion-inducing interval, suggesting it could lack regulatory sequences associated with the other three abortion-inducing intervals.

The second line of evidence supporting our primary hypothesis comes from a comparison of the *AH36* interval between an *Sk-2* strain and an *Sk-2 rfk-1*^{3211} mutant. In brief, the *AH36* interval from *Sk-2* (*AH36*$^{Sk-2}$) correlates with an abortion phenotype, while the *AH36* interval from *Sk-2 rfk-1*^{3211} (*AH36*^{3211}) does not. Sequencing analysis of the two *AH36* alleles revealed the difference to be due to one or more of six point mutations present in *AH36*^{3211}; thus, the abortion phenotype caused by *AH36*$^{Sk-2}$ can be eliminated by mutation. Intriguingly, the mutations we identified in *AH36*^{3211} were found clustered around a region with similarity to a predicted protein in *N. tetrasperma*. At this point, we do not know if the relationship between *AH36* and this putative *N. tetrasperma* protein is coincidental or biologically relevant for spore killing. A second interesting characteristic of *AH36* is a 46–48 bp DNA sequence present in 7.17× tandem repeats. We also do not know if this element is biologically important for spore killing, and we have been unable to identify similar sequences in NCBI's non-redundant nucleotide database.

Finally, although the first and second lines of evidence support the existence of a genetic element required and sufficient for spore killing within interval *AH36*, we also propose that a transcript must be produced from *AH36*$^{Sk-2}$ to cause spore killing. To understand our reasoning, it

is necessary to understand a few mechanistic details of MSUD. MSUD silences transcripts from unpaired DNA during meiosis through the production of MSUD-associated small interfering RNAs (masiRNAs) (Hammond *et al.* 2013a,b; Wang *et al.* 2015). These molecules are approximately 25 bases long and are derived directly or indirectly from unpaired DNA during meiosis. Based on analogy to small RNA-based silencing systems in other organisms, and the involvement of canonical RNA interference proteins in MSUD (Shiu *et al.* 2001; Lee *et al.* 2003; Alexander *et al.* 2008), masiRNAs probably help meiotic cells identify complementary mRNAs for degradation or translational suppression. In an $Sk^{S} \times AH36^{Sk\text{-}2}$ cross, the $AH36^{Sk\text{-}2}$ transgene lacks a pairing partner. Thus, MSUD identifies the transgene as unpaired and attempts to silence it through the production of $AH36^{Sk\text{-}2}$-specific masiRNAs. MSUD must succeed in this silencing attempt because crosses between an Sk^{S} strain and a transgene-carrying mating partner (e.g., $Sk^{S} \times AH36^{Sk\text{-}2}$) produce asci with an 8B:0W phenotype. However, when we add a $sad\text{-}2^{\Delta}$ allele to one of the parents (e.g., Sk^{S} $sad\text{-}2^{\Delta} \times AH36^{Sk\text{-}2}$), abortion is induced. The $sad\text{-}2^{\Delta}$ allele is a well-known suppressor of MSUD (Shiu *et al.* 2006), thus the most likely explanation for ascus abortion is the failure of MSUD to silence an abortion-inducing transcript from $AH36^{Sk\text{-}2}$. Future work will investigate this hypothesis further by attempting to molecularly identify the transcript and determine if it functions as an mRNA or a non-protein coding RNA.

While this report represents a significant step towards understanding the mechanism of spore killing in $Sk^{S} \times Sk\text{-}2$ crosses, it also leaves many questions unanswered. For example, because *rfk-1* mapping was used to identify the $AH36^{Sk\text{-}2}$ interval (Harvey *et al.* 2014), it seems *rfk-1* should be found within $AH36^{Sk\text{-}2}$. In future work, we will seek to determine if the $AH36^{Sk\text{-}2}$ interval can complement *rfk-1* mutants. We will also examine if $AH36^{Sk\text{-}2}$ and $rsk^{Sk\text{-}2}$ can be combined in a single transgenic construct capable of driving through meiosis and

ascosporogenesis. However, at this point, we consider *rfk-1* to represent a genetically-defined mutant locus that disrupts spore killing and maps to a 45 kb region of *Sk-2*, and we consider *AH36* to be a molecularly-defined 1481 bp interval within the same 45 kb region that is required and sufficient for spore killing.

Acknowledgments

We are grateful to members of the Hammond, Shiu, Johannesson, and Brown laboratories for assistance with various technical aspects of this work. We are pleased to acknowledge use of materials generated by P01 GM068087 "Functional Analysis of a Model Filamentous Fungus". This project was supported by start-up funding from Illinois State University (T.M.H), a New Faculty Initiative grant from Illinois State University (T.M.H.), and a grant from the National Science Foundation (MCB# 1615626) (T.M.H.). P.K.T.S was supported by the University of Missouri Research Board/Research Council and the National Science Foundation (MCB# 1157942). H.J. was supported by the European Research Council and the Swedish Research Council. Mention of trade names or commercial products in this article is solely for the purpose of providing specific information and does not imply recommendation or endorsement by the U.S. Department of Agriculture. USDA is an equal opportunity provider and employer.

Table 1. Strains used in this study.

Name (alias)	Genotype
F2-19	*rid; fl; Sk-2; A*
F2-23 (RTH1005.1)	*rid; fl A*
F2-26 (RTH1005.2)	*rid; fl a*
ISU-3017 (RKS2.1.2)	*rid$^{?}$; Sk-2 leu-1 v4$^{\Delta}$::hph; mus-51$^{?}$ a*
ISU-3023 (RKS1.1.6)	*rid$^{?}$; Sk-2 leu-1 v3$^{\Delta}$::hph; mus-51$^{?}$ a*
ISU-3224 (HAH8.1.3)	*rid his-3^{+}::AH4^{Sk-2}::hph; A*
ISU-3228 (HAH10.1.1)	*rid his-3^{+}::AH6^{Sk-2}::hph; A*
ISU-3029 (RKS3.2.5)	*rid; Sk-2 leu-1 v5$^{\Delta}$::hph; mus-51$^{\Delta}$:bar a*
ISU-3036 (RTH1623.1)	*rid; fl; sad-2$^{\Delta}$::hph A*
ISU-3037 (RTH1623.2)	*rid; fl; sad-2$^{\Delta}$::hph a*
ISU-3211 (RTH1158.8)	*rid; Sk-2 rsk$^{\Delta}$::hph rfk-1^{3211}; mus-51$^{\Delta}$::bar a*
ISU-3223 (RTH1294.17)	*Sk-2 leu-1; mus-51$^{\Delta}$::bar A*
ISU-3243 (HAH16.1.1)	*rid his-3^{+}::AH14^{Sk-2}::hph A*
ISU-3311 (RDS1.1)	*Sk-2 leu-1 v31$^{\Delta}$::hph; mus-51$^{\Delta}$::bar A*
ISU-3313 (RDS2.3)	*Sk-2 leu-1 v32$^{\Delta}$::hph; mus-51$^{\Delta}$::bar A*

(Table continues)

Table 1 continues. Strains used in this study.

Name (alias)	Genotype
ISU-3315 (RDS3.9)	*Sk-2 leu-1 v33$^{\Delta}$::hph a*
ISU-3318 (RDS4.8)	*Sk-2 leu-1 v34$^{\Delta}$::hph A*
ISU-3321 (RDS5.9)	*rid; Sk-2 leu-1 v35$^{\Delta}$::hph; mus-51$^{\Delta}$::bar a*
ISU-3478 (RDS13.9.1)	*rid; Sk-2 v37$^{\Delta}$::hph; mus-51$^{\Delta}$::bar A*
ISU-3482 (RDS14.4.2)	*rid; Sk-2 v38$^{\Delta}$::hph A*
ISU-3483 (RDS15.1.1)	*rid; Sk-2 v39$^{\Delta}$::hph A*
ISU-3485 (RDS16.4.1)	*rid; Sk-2 v40$^{\Delta}$::hph A*
ISU-3656 (HAH42.1)	*rid his-3^{+}::AH30^{Sk-2}::hph A*
ISU-3658 (HAH43.1)	*rid his-3^{+}::AH31^{Sk-2}::hph A*
ISU-3660 (HAH44.1)	*rid his-3^{+}::AH32^{Sk-2}::hph A*
ISU-4269 (RAH64.1.1)	*rid his-3^{+}::AH37^{Sk-2}::hph; mus-52$^{\Delta}$::bar a*
ISU-4271 (RAH63.1.2)	*rid his-3^{+}::AH36^{Sk-2}::hph; mus-52$^{\Delta}$::bar A*
ISU-4273 (HNR12.6.1)	*rid his-3^{+}::AH36^{Sk-2}::hph; A*
ISU-4275 (HNR10.4.2)	*rid his-3^{+}::AH36^{3211}::hph; A*
P8-42	*rid; mus-51$^{\Delta}$::bar a*
P8-43	*rid; mus-52$^{\Delta}$::bar A*
P15-53 (RTH1122.22)	*rid; Sk-2; mus-51$^{\Delta}$::bar A*

Table 2. Interval positions.

name	start	end
Deleted intervals		
v3	15640	15664
v4	36166	36426
v5	18042	28759
v31	18042	21464
v32	18042	25268
v33	18042	26951
v34	18042	27667
v35	25837	28759
v37	27242	28759
v38	27602	28759
v39	28126	28759
v40	27602	28198
Transgene intervals		
AH4	16579	22209
AH6	19408	25648
AH14	25632	28324

(Table continues)

Table 2 continues. Interval positions.

name	start	end
AH30	27528	29702
AH31	27900	29702
AH32	28304	29702
AH36	27900	29380
AH37	27900	29512

The coordinates of each interval are based on the *rfk-1* region as defined by sequence KJ908288.1 (GenBank).

Table 3. PCR primers used in this study.

Primer Number	Sequence (5'-> 3')
hph^+	
12	AACTGATATTGAAGGAGCATTTTTTGG
13	AACTGGTTCCCGGTCGGCAT
v3	
73	CAAGACCCAGAACAACGCCAACA
74	AAAAAATGCTCCTTCAATATCAGTTCCTCGCTCCTCTTCCGCAAATTA
75	GAGTAGATGCCGACCGGGAACCAGTTTGGTGGGATACTCGGTGCAGGT A
76	CGACACCTCGAATACGCCCTCTC
77	CCGGAAACGTCAGCAAACACGTA
78	GCGCCAGCTCCTCTACACTCTCC
v4	
79	CCAAGCCAAACTCAAGGGAATCG
80	AAAAAATGCTCCTTCAATATCAGTTAATGGCGGTGATCTTCGACTGCT
81	GAGTAGATGCCGACCGGGAACCAGTTGCCCAGACTCAGCTTGCATTGA C
82	TCACCTTGGCCCTGGAGTACCTG
83	CAAACGGGACGCAACCTCTATGA
84	CCAAGCGGGTTCCAGATAAGACG
v5	
85	CACCATGTAGTCGGAGCGGAAGA
86	AAAAAATGCTCCTTCAATATCAGTTTCATCTTGACGGGCAGAACTGAA
87	GAGTAGATGCCGACCGGGAACCAGTTGCTAACCAGGAACAGGCGCTTA CC
88	CATCGAAAGGGAGAGGCACTTCG
89	GCCTTCCTTCTTCACACGGAGGT
90	ACAGGATCTGGTCATCCCGCTTC
v31	
85	CACCATGTAGTCGGAGCGGAAGA
86	AAAAAATGCTCCTTCAATATCAGTTTCATCTTGACGGGCAGAACTGAA
167	GAGTAGATGCCGACCGGGAACCAGTTATTGAGGTGAGGACAAGCGAT GA
168	CATACGGCCCATGTTACCGCACT
89	GCCTTCCTTCTTCACACGGAGGT
170	CAACGAAGCAGGCTCCCATACAG

(Table continues)

Table 3 continues. PCR primers used in this study.

Primer Number	Sequence (5'-> 3')
v32	
85	CACCATGTAGTCGGAGCGGAAGA
86	AAAAAATGCTCCTTCAATATCAGTTTCATCTTGACGGGCAGAACTGAA
173	GAGTAGATGCCGACCGGGAACCAGTTGTCGTCCGTGAATCGTGATCCTT
174	AATTCGCCGTGTACTTCGCTGTG
89	GCCTTCCTTCTTCACACGGAGGT
176	CGGTTGTATCTGCCGGTTTGAAGA
v33	
85	CACCATGTAGTCGGAGCGGAAGA
86	AAAAAATGCTCCTTCAATATCAGTTTCATCTTGACGGGCAGAACTGAA
3	GAGTAGATGCCGACCGGGAACCAGTTCATGGCAGTGAAGTGGACAAGCTG
4	GTGGTAAGCGCCTGTTCCTGGTTAG
89	GCCTTCCTTCTTCACACGGAGGT
6	TGCGGCCTGTTTACGAAATCCAA
v34	
85	CACCATGTAGTCGGAGCGGAAGA
86	AAAAAATGCTCCTTCAATATCAGTTTCATCTTGACGGGCAGAACTGAA
9	GAGTAGATGCCGACCGGGAACCAGTTCTCGATTGCCCGACACCTTCTGT
4	GTGGTAAGCGCCTGTTCCTGGTTAG
89	GCCTTCCTTCTTCACACGGAGGT
11	CGAAAGACAGAGAGGACCGAGAGGA
v35	
1	TCGGAAGGATTGCTGACTTGTGTGT
2	CCAAAAAATGCTCCTTCAATATCAGTTAGTTGGTAGCTGGCGCGGAAAG
87	GAGTAGATGCCGACCGGGAACCAGTTGCTAACCAGGAACAGGCGCTTACC
88	CATCGAAAGGGAGAGGCACTTCG
5	GCGCAGACGAACATCAAGGAGAA
90	ACAGGATCTGGTCATCCCGCTTC
v37	
7	GGCAGATACAACCGACGACCAAA
8	CCAAAAAATGCTCCTTCAATATCAGTTTCCGTTTCGCTTATGATGTTAATGATG
87	GAGTAGATGCCGACCGGGAACCAGTTGCTAACCAGGAACAGGCGCTTACC
88	CATCGAAAGGGAGAGGCACTTCG
10	CACGTAGGGAAGGAGGTTGAAGGT
90	ACAGGATCTGGTCATCCCGCTTC

(Table continues)

Table 3 continues. PCR primers used in this study.

Primer Number	Sequence (5'-> 3')
v38	
309	ACGCCAAAAGGTGTAGGGGGATT
310	CCAAAAAATGCTCCTTCAATATCAGTTGACCGAACAACCGGAATGACCT
87	GAGTAGATGCCGACCGGGAACCAGTTGCTAACCAGGAACAGGCGCTTACC
88	CATCGAAAGGGAGAGGCACTTCG
311	AGGTCCGCAACTATTGTCCGTTT
90	ACAGGATCTGGTCATCCCGCTTC
v39	
309	ACGCCAAAAGGTGTAGGGGGATT
312	CCAAAAAATGCTCCTTCAATATCAGTTGCAGCTCTTGCTTTGTTTTGTCAGT
87	GAGTAGATGCCGACCGGGAACCAGTTGCTAACCAGGAACAGGCGCTTACC
88	CATCGAAAGGGAGAGGCACTTCG
311	AGGTCCGCAACTATTGTCCGTTT
90	ACAGGATCTGGTCATCCCGCTTC
v40	
309	ACGCCAAAAGGTGTAGGGGGATT
310	CCAAAAAATGCTCCTTCAATATCAGTTGACCGAACAACCGGAATGACCT
87	GAGTAGATGCCGACCGGGAACCAGTTGCTAACCAGGAACAGGCGCTTACC
88	CATCGAAAGGGAGAGGCACTTCG
311	AGGTCCGCAACTATTGTCCGTTT
90	ACAGGATCTGGTCATCCCGCTTC
AH4	
248	AAAAGCGGCCGCAGGGTGGTGTGGGTGAGGATGT
249	TTTTGCGGCCGCGAGCGGAAGTGTTTGCTTGTGTGA
AH6	
252	AAAAGCGGCCGCATCGCCAACGGGCATTCAAG
253	AAAAGCGGCCGCACCCGCCTACACATGCACCATC
AH14	
302	AAAAGCGGCCGCTGCATGTGTAGGCGGGTATTGTG
314	AAAAGCGGCCGCGGGGCAGGGCAGCAAGTAAG

(Table continues)

Table 3 continues. PCR primers used in this study.

Primer Number	Sequence (5'-> 3')
AH30	
304	AAAAGCGGCCGCGAGGACCAGCTCGACGGTAGTAGG
251	AAAAGCGGCCGCGAGGAATAGGACGTGAGGGTGTGG
AH31	
353	TTTTGCGGCCGCCATTGATACCGAGTCTTTCCGTTC
251	AAAAGCGGCCGCGAGGAATAGGACGTGAGGGTGTGG
AH32	
351	AAAAGCGGCCGCAACTCCTCACCCATCCCCATTTG
251	AAAAGCGGCCGCGAGGAATAGGACGTGAGGGTGTGG
AH36	
353	TTTTGCGGCCGCCATTGATACCGAGTCTTTCCGTTC
639	AAAAGCGGCCGCGACGGTGTAGCGGGACGTTTTCC
AH37	
353	TTTTGCGGCCGCCATTGATACCGAGTCTTTCCGTTC
640	AAAAGCGGCCGCGTTCGCTGACTTTCCCGACCA

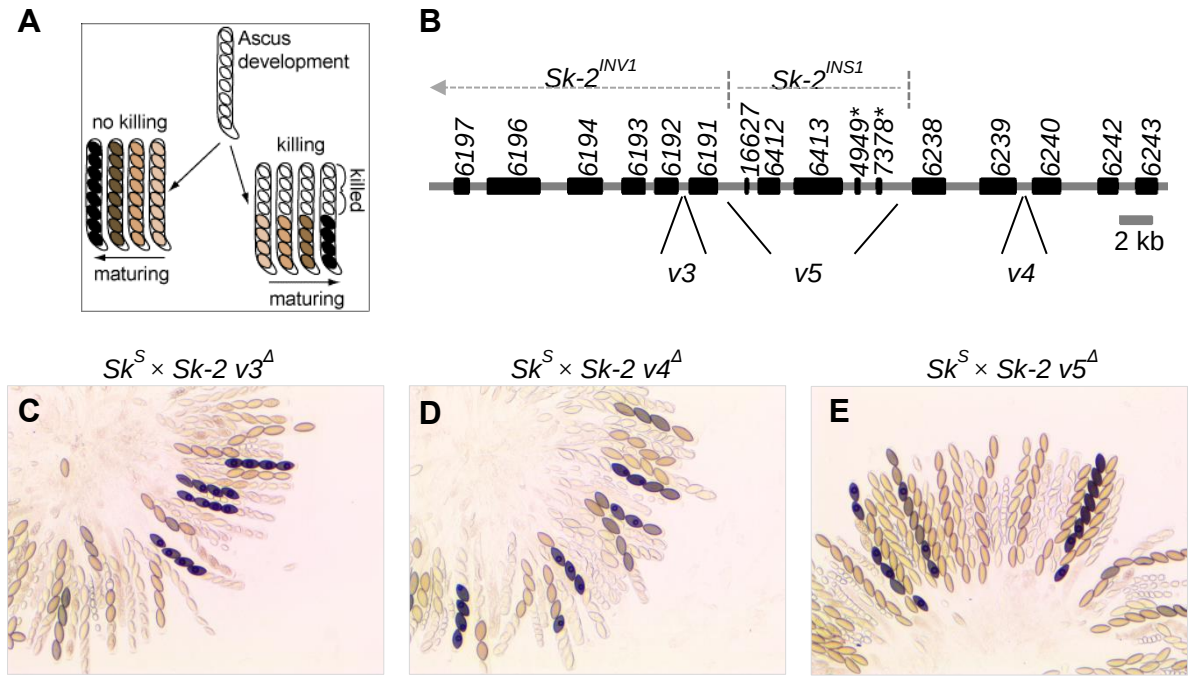

Figure 1. The *Sk-2*^{INS1} locus harbors a genetic element required for spore killing. (A) The diagram illustrates phenotypic differences between asci that develop normally and asci that experience spore killing. Asci that have undergone spore killing typically contain four viable ("black") and four inviable ("white") ascospores. Asci with eight viable ascospores have not undergone spore killing. Viable ascospores may appear brown or tan depending on their level of maturity. (B) Annotation of the *rfk-1* region as described by Harvey *et al.* (2014). Locations of 14 predicted genes and two predicted pseudogenes are depicted with black rectangles. Gene numbers are listed above the rectangles. Names of putative pseudogenes are appended with an asterisk. *Sk-2*^{INV1} is an inversion found in *Sk-2* genotypes but not *Sk*^{S} genotypes (Harvey *et al.* 2014). *Sk-2*^{INS1} is an 11 kb insertion. The *v3*, *v4*, and *v5* symbols indicate the locations of three intervals replaced with *hph* selectable markers. (C) Asci from *Sk*^{S} × *Sk-2 v3*$^{\Delta}$ crosses display a 4B:4W spore killing phenotype (F2-23 × ISU-3023). (D) Asci from *Sk*^{S} × *Sk-2 v4*$^{\Delta}$ crosses also display a 4B:4W spore killing phenotype (F2-23 × ISU-3017). (E) *Sk*^{S} × *Sk-2 v5*$^{\Delta}$ crosses produce asci with an 8B:0W phenotype (F2-23 × ISU-3029).

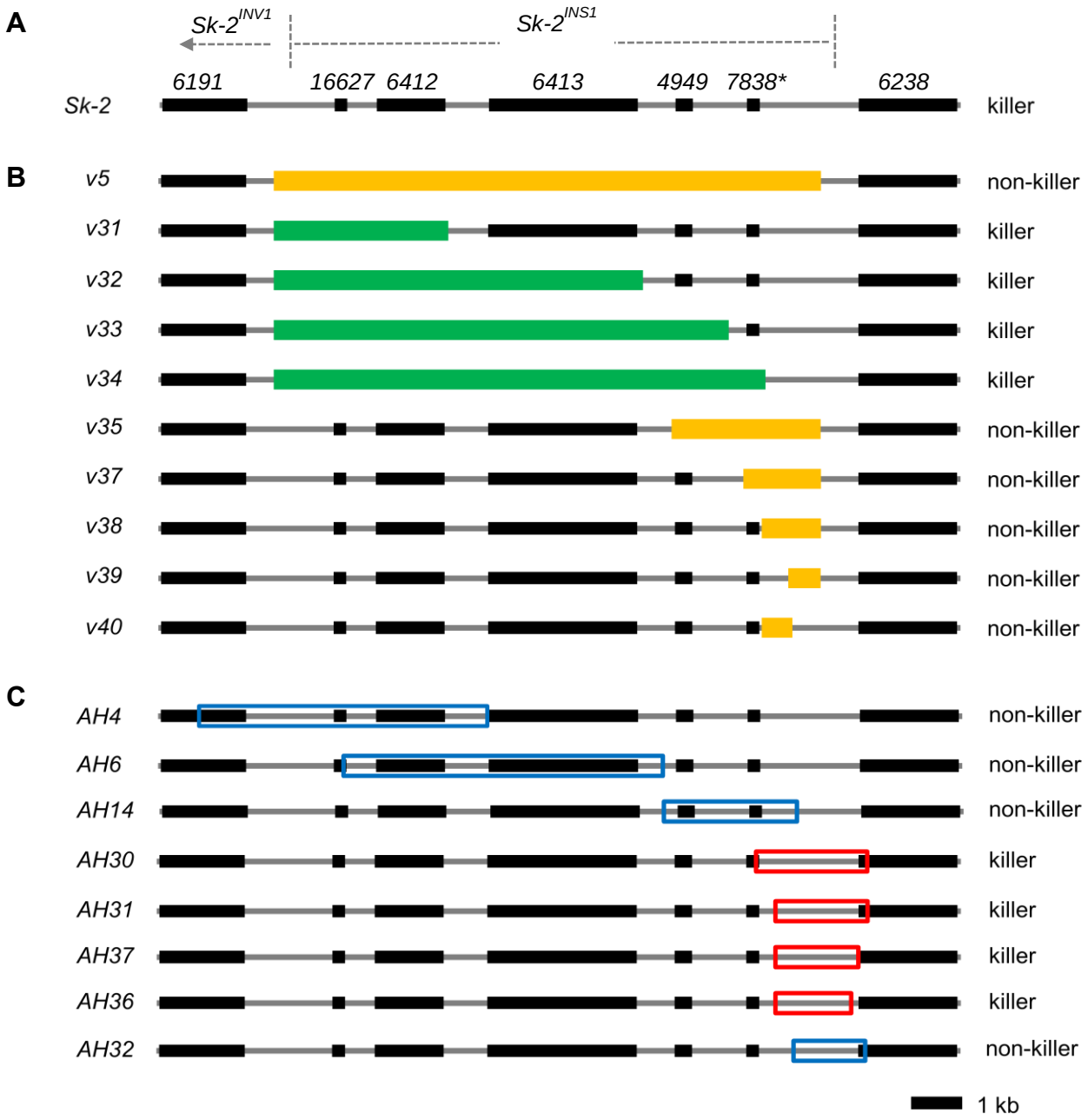

Figure 2. *Sk-2*^{INS1} interval positions. (A) A diagram of *Sk-2*^{INS1}. Predicted genes and pseudogenes are indicated by black rectangles, and putative pseudogenes are appended with an asterisk. (B) Ten intervals of *Sk-2*^{INS1} were deleted and replaced with *hph*. Intervals were named (e.g., *v5*) according to the name of the deletion vector (e.g., V0005) used to delete the interval. Orange rectangles depict intervals that disrupt spore killing when deleted. Green rectangles depict intervals that have no effect on spore killing when deleted. (C) Nine intervals were transferred from *Sk-2*^{INS1} to an *Sk*^{S} strain. Intervals (e.g., *AH4*) were named according to the name of the plasmid (e.g., pAH4) created during interval cloning. Red and blue open rectangles depict killer intervals and non-killer intervals, respectively. (B and C) See Table 2 for specific interval position information.

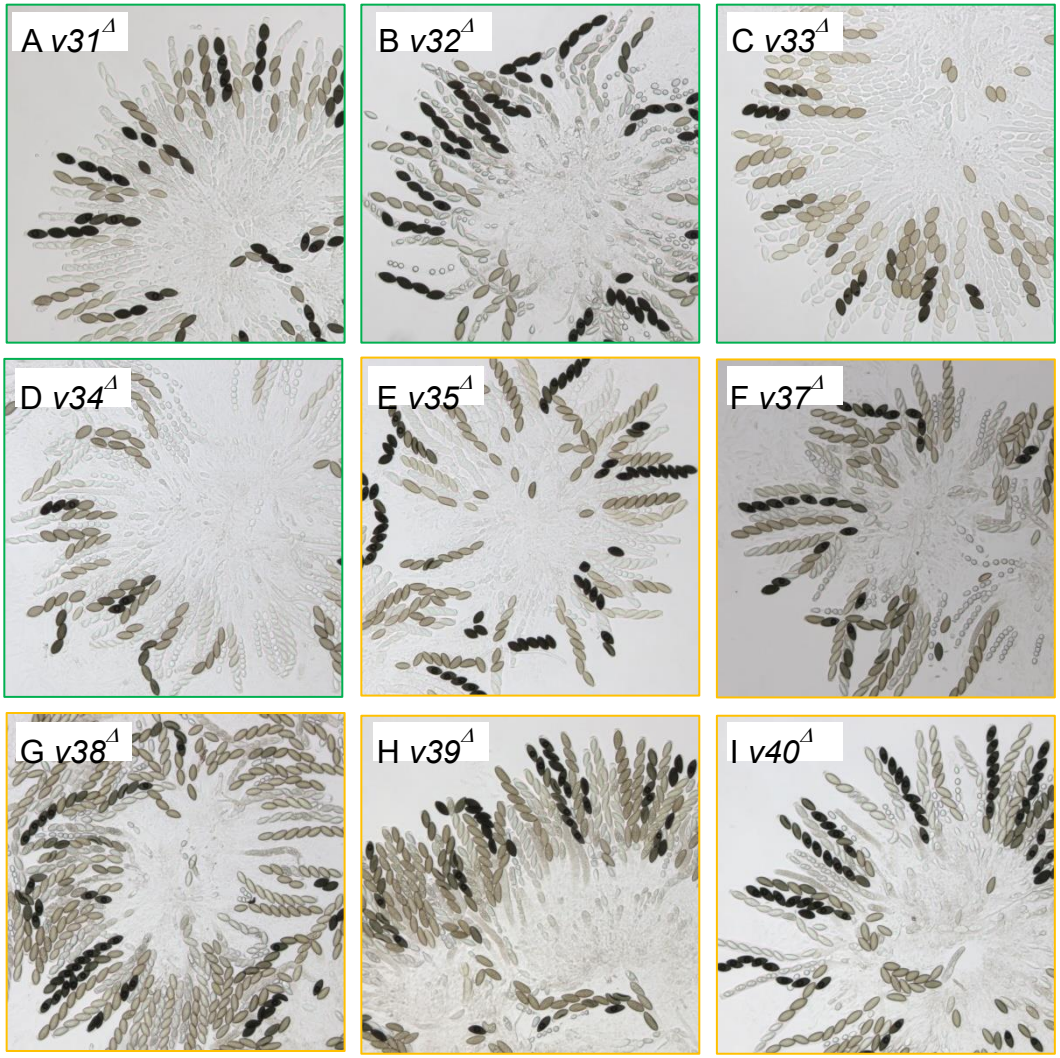

Figure 3. Deletion of a genetic element between pseudogene *7378** and the right border of *Sk-2*^{INS1} eliminates spore killing. (A–H) The images depict asci from crosses between *Sk*^{S} and *Sk-2* deletion strains. Each *Sk-2* deletion strain is missing a different interval of *Sk-2*^{INS1}. Images are outlined according to phenotype (green, non-killer; orange, killer). Crosses are as follows: (A) F2-26 × ISU-3311, (B) F2-26 × ISU-3313, (C) F2-23 × ISU-3315, (D) F2-26 × ISU-3318, (E) F2-23 × ISU-3321, (F) F2-26 × ISU-3478, (G) F2-26 × ISU-3482, (H) F2-26 × ISU-3483, and (I) F2-26 × ISU-3485.

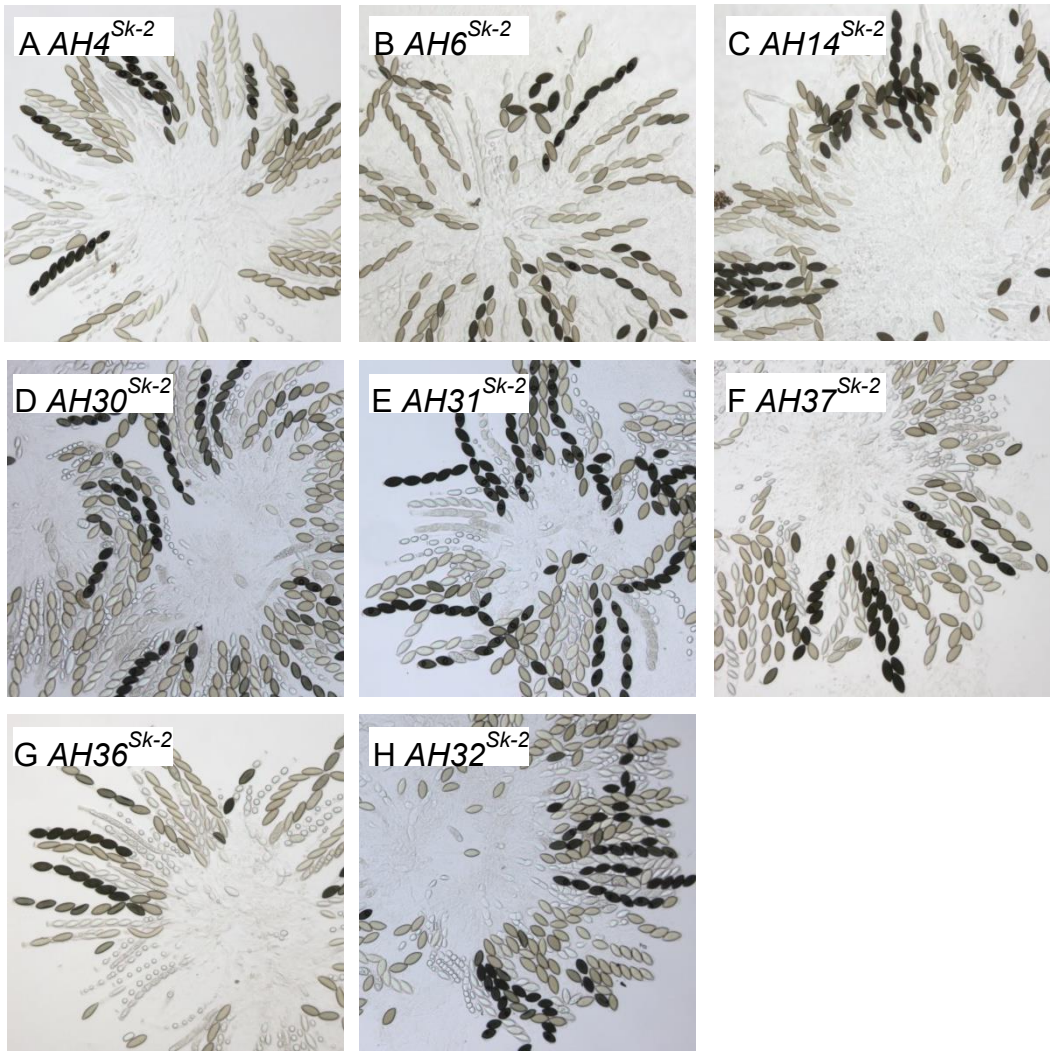

Figure 4. Unpaired *Sk-2*^{INS1}-intervals do not kill ascospores in MSUD-proficient crosses. (A–H) The images depict asci from crosses between *Sk*^{S} strains, one of which carries an interval of the *Sk-2*^{INS1} locus (e.g., *AH4*$^{Sk-2}$, *AH6*$^{Sk-2}$, *etc*.). All crosses produced asci with an 8B:0W phenotype. Crosses are as follows: (A) F2-26 × ISU-3224, (B) F2-26 × ISU-3228, (C) F2-23 × ISU-3243, (D) F2-26 × ISU-3656, (E) F2-26 × ISU-3658, (F) F2-23 × ISU-4269, (G) F2-26 × ISU-4271, and (H) F2-26 × ISU-3660.

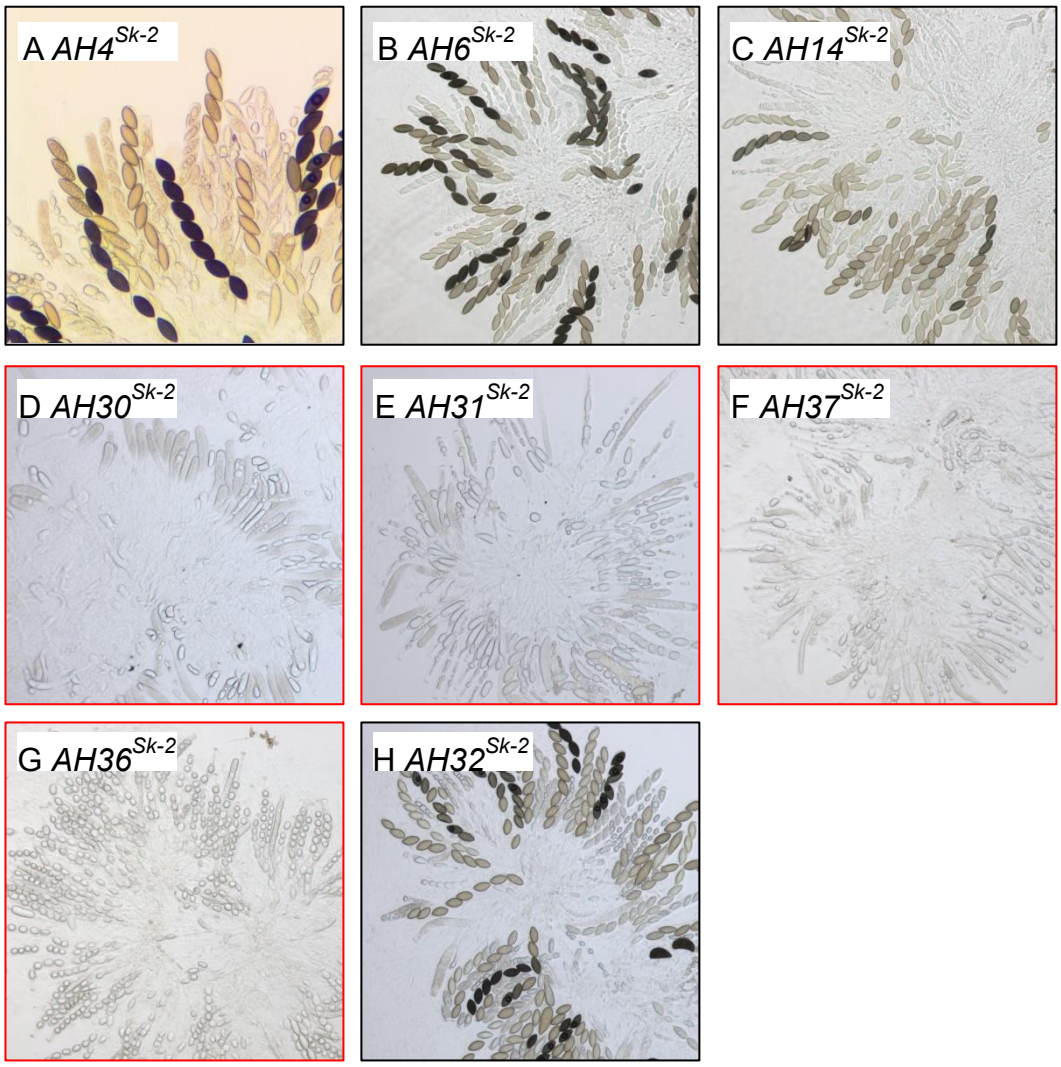

Figure 5. A genetic element found between pseudogene *7378** and the right border of *Sk-2*^{INS1} induces an ascus abortion phenotype. (A–H) The images depict asci from crosses between a *sad-2*$^{\Delta}$ strain and an *Sk*^{S} strain carrying an interval of the *Sk-2*^{INS1} locus. The *sad-2*$^{\Delta}$ allele suppresses MSUD. Two primary phenotypes are present in the images: either 1) most asci develop as normal without evidence of spore killing or 2) most asci abort meiosis, the post-meiotic mitosis, or ascosporogenesis. Images are outlined according to phenotype (blue, normal; red, aborted). Crosses are as follows: (A) ISU-3037 × ISU-3224, (B) ISU-3037 × ISU-3228, (C) ISU-3036 × ISU-3243, (D) ISU-3037 × ISU-3656, (E) ISU-3037 × ISU-3658, (F) ISU-3036 × ISU-4269, (G) ISU-3037 × ISU-4271, and (H) ISU-3037 × ISU-3660.

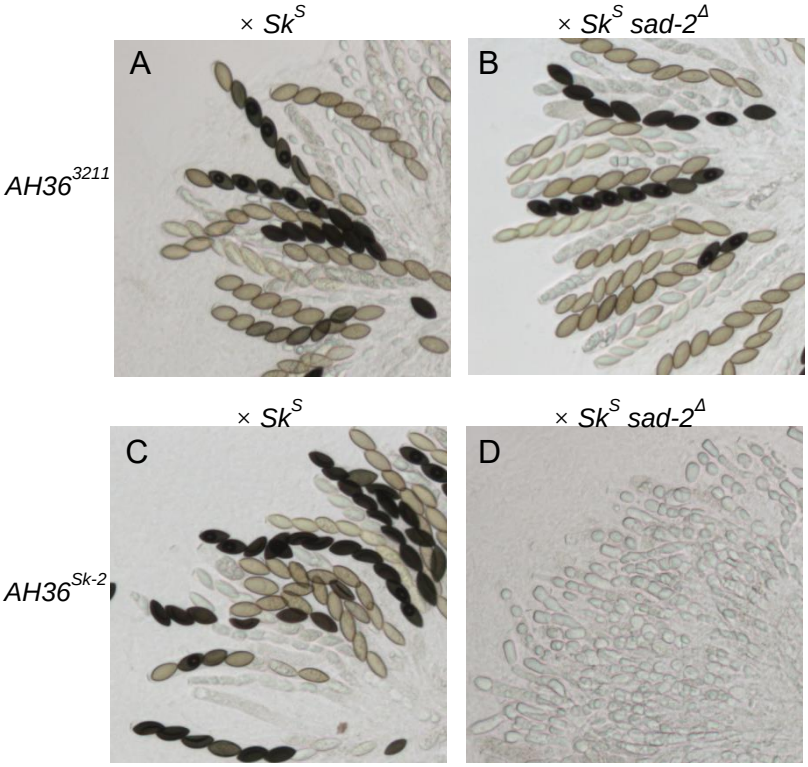

Figure 6. The *AH36* interval from an *rfk-1* mutant does not cause ascus abortion. (A and B) Two crosses were made to determine if the *AH36* interval from an *rfk-1* mutant (ISU-3211) induces an ascus abortion phenotype. (A) An $Sk^S \times AH36^{3211}$ cross produced asci with an 8B:0W phenotype (F2-26 × ISU-4275). (B) An Sk^S *sad-*$2^{\Delta} \times AH36^{3211}$ cross also produced asci with an 8B:0W phenotype (ISU-3037 × ISU-4275). These observations demonstrate that $AH36^{3211}$ does not cause ascus abortion. (C and D) As a control, the *AH36* interval from an *Sk-2* strain (F2-19) was retransformed into an Sk^S background and crosses were performed. As expected, (C) an $Sk^S \times AH36^{Sk-2}$ cross (F2-26 × ISU-4273) produced asci with an 8B:0W phenotype and (D) an Sk^S *sad-*$2^{\Delta} \times AH36^{Sk-2}$ (ISU-3037 × ISU-4273) cross produced mostly aborted/bubble asci.

A

```
CATTGATACCGAGTCTTTCCGTTCTTAAGGTTGGAGTGAGGATATGATCCGGCACGTCGAAGGAGGAACTAT
GGTAAATAAGTCAGTCATCATCAAGGAAAAGAACAGTATTAGGTGCCTTCAAGTTACCTACCTTCTCCGACG
GGGGCCCTGCCTTCCCTTAGTTCTCTCATGAAGCTGGAAGTTATATCCTAACCCACTACTGACAAAACAAAG
CAAGAGCTGCTGCCCCAACTATAGACAGCACGCTTTTCCACCTCAGTTGGGGCACCTAGAAAGCTATAAGAT
CCCTCTTCCCCCGGCCCAACCTCTCCTCAGAATTTCTTTTTTTCTCCAACATTGTTAAGAACTTTGTTTTTG
GAAAATGGCCTGCCCCACAGGGTTTTTTACCGCTCTTTTTGGCAAACTCCTCACCATCCCCATTTGGGTGTT
GGTGTTTGTATTCAATGCTCTGTTTGTCTTCCCCCGGTTTTGGGTCTGGTAAGTCTCCTTCATGTTCCAATT
CATTTTTGTTTTTTCCTTTCTCTTCTCGTCTCCTTCATGTTCCAATTCATTTTTGTTTTTTTCCTTTCTCTT
CTCGTCTCCTTCATGTTCCAGTTCATTTTTGTTTTTTCCTTTCTCTTCTCGTCTCCTTCATGTTCCAATTCA
TTTTTGTTTTTTTCCTTTCTCTTCTCGTCTCCTTCATGTTCCAGTTCATTTTTGTTTTTTCCTTTCTCTTCT
CGTCTCCTTCATGTTCCAATTCATTTTTGTTTTTTTCCTTTCTCTTCTCGTCTCCTTCATGTTCCAATTCAT
TTTTTTTTGTCCTTTCTCTTCTCGTCTCCTTACAGTTTACCTTATCCTCTCGGTCCTCTCTGTCTTTCGCTA
ACCAGGAACAGGCGCTTACCACCACGGCTGCAACACGAGCAGCAGCAGGACCGGAACGATGACGAATGG
CAGCGGCAGCAACAGGACAGGCGGGTTGTGGTTTGGCACCCACCGCCCCCTCCAGACGTGGAGATGGCCCTC
CAAGACAATCCCACTGCCGCCCCCGCAGAGCCGGCTGACCTCGACCACCCAGCGCCGTAGTGGCGGCGCTGG
GTGGCCGACGAGTAGGTCAATGCTATTCCCAGATTATGAAATGTATCGCTGACAGTTGCACACCAGTGCCTA
CCCGGCCGTCCACTTCTGCGTGACCGCAGCCAATGCGGTCACGCAGGGGTTGTAATTCCACGTGAGCATTCC
CCACCTTCTCTCGGGACCGACTTCCGTATCAACCCCAAATTTATCGGACTGACCCGTCCGAATCAAGGCGAA
CCGAGAGGACACAGACAAGGCCCACGTCCGCCATCAGCATTCCCAGCTGGCCGACCGCACCGCCGCAACTCC
CACTTTACCTCAACACCAGAATACGGAATCGGTACATCGACAGCAGCATCATCATCATCAATATCACCACCT
CCACTTGGCGCGCACTTGCGGAAAACGTCCCGCTACACCGT
```

B

```
Repeat A  GTCTCCTTCATGTTCCAATTCATTTTTG-TTTTTTCCTTTCTCTTCTC 47
Repeat B  GTCTCCTTCATGTTCCAATTCATTTTTGTTTTTTTCCTTTCTCTTCTC 48
Repeat C  GTCTCCTTCATGTTCCAGTTCATTTTTG-TTTTTTCCTTTCTCTTCTC 47
Repeat D  GTCTCCTTCATGTTCCAATTCATTTTTGTTTTTTTCCTTTCTCTTCTC 48
Repeat E  GTCTCCTTCATGTTCCAGTTCATTTTTG-TTTTTTCCTTTCTCTTCTC 47
Repeat F  GTCTCCTTCATGTTCCAATTCATTTTTGTTTTTTTCCTTTCTCTTCTC 48
Repeat G  GTCTCCTTCATGTTCCAATTCATTTTT--TTTTGTCCTTTCTCTTCTC 46
Repeat H  GTCTCCTT---------------------------------------- 8
```

Figure 7. Six point mutations exist in *AH36*^{3211}. (A) The sequence of the 1481 bp *AH36*$^{Sk-2}$ interval is shown. A region containing seven complete repeats and one partial repeat of a 46–48 bp sequence is highlighted with red and blue font. The colors alternate with each iteration of the repetitive element. The *AH36*^{3211} sequence contains six G to A transition mutations relative to *AH36*$^{Sk-2}$. The mutant bases are highlighted with white font and a black background. The non-mutated sequence is shown. (B) An alignment of the repetitive elements shown in panel A.

Literature Cited

Alexander, W. G., N. B. Raju, H. Xiao, T. M. Hammond, T. D. Perdue *et al.*, 2008 DCL-1 colocalizes with other components of the MSUD machinery and is required for silencing. Fungal Genet. Biol. 45: 719–727.

Altschul, S. F., T. L. Madden, A. A. Schäffer, J. Zhang, Z. Zhang *et al.*, 1997 Gapped BLAST and PSI-BLAST: a new generation of protein database search programs. Nucleic Acids Res. 25: 3389–3402.

Aramayo, R., and E. U. Selker, 2013 *Neurospora crassa*, a model system for epigenetics research. Cold Spring Harb. Perspect. Biol. 5: a017921.

Burt, A., and R. Trivers, 2008 *Genes in Conflict: The Biology of Selfish Genetic Elements*. Belknap Press of Harvard University Press.

Campbell, J. L., and B. C. Turner, 1987 Recombination block in the *Spore killer* region of Neurospora. Genome Natl. Res. Counc. Can. 29: 129–135.

Carroll, A. M., J. A. Sweigard, and B. Valent, 1994 Improved vectors for selecting resistance to hygromycin. Fungal Genet. Newsl. 41: 22.

Dalstra, H. J. P., K. Swart, A. J. M. Debets, S. J. Saupe, and R. F. Hoekstra, 2003 Sexual transmission of the [Het-S] prion leads to meiotic drive in *Podospora anserina*. Proc. Natl. Acad. Sci. U. S. A. 100: 6616–6621.

Davis, R. H., 2000 *Neurospora: Contributions of a Model Organism*. Oxford University Press, USA.

Ebbole, D., and M. Sachs, 1990 A rapid and simple method for isolation of *Neurospora crassa* homokaryons using microconidia. Fungal Genet. Newsl. 37: 17–18.

Hall, T. A., 1999 BioEdit: a user-friendly biological sequence alignment editor and analysis program for Windows 95/98/NT. Nucleic Acid Symp Ser 41: 95–98.

Hammond, T. M., 2016 Sixteen Years of Meiotic Silencing by Unpaired DNA. Adv Genet 97 doi. 10.1016/bs.adgen.2016.11.001. Epub 2016 Dec 29.

Hammond, T. M., D. G. Rehard, H. Xiao, and P. K. T. Shiu, 2012 Molecular dissection of Neurospora *Spore killer* meiotic drive elements. Proc. Natl. Acad. Sci. USA. 109: 12093-12098.

Hammond, T. M., W. G. Spollen, L. M. Decker, S. M. Blake, G. K. Springer *et al*., 2013a Identification of small RNAs associated with meiotic silencing by unpaired DNA. Genetics 194: 279–284.

Hammond, T. M., H. Xiao, E. C. Boone, L. M. Decker, S. A. Lee *et al.*, 2013b Novel proteins required for meiotic silencing by unpaired DNA and siRNA generation in *Neurospora crassa*. Genetics 194: 91–100.

Hammond, T. M., H. Xiao, D. G. Rehard, E. C. Boone, T. D. Perdue *et al.*, 2011 Fluorescent and bimolecular-fluorescent protein tagging of genes at their native loci in *Neurospora crassa* using specialized double-joint PCR plasmids. Fungal Genet. Biol. 48: 866–873.

Harvey, A. M., D. G. Rehard, K. M. Groskreutz, D. R. Kuntz, K. J. Sharp *et al.*, 2014 A critical component of meiotic drive in Neurospora Is located near a chromosome rearrangement. Genetics 197: 1165-1174.

Kanizay, L. B., T. Pyhäjärvi, E. G. Lowry, M. B. Hufford, D. G. Peterson *et al*., 2013 Diversity and abundance of the abnormal chromosome 10 meiotic drive complex in *Zea mays*. Heredity 110: 570–577.

Larracuente, A. M., and D. C. Presgraves, 2012 The selfish *Segregation Distorter* gene complex of *Drosophila melanogaster*. Genetics 192: 33–53.

Lee, D. W., R. J. Pratt, M. McLaughlin, and R. Aramayo, 2003 An argonaute-like protein is required for meiotic silencing. Genetics 164: 821–828.

Lee, D. W., K.-Y. Seong, R. J. Pratt, K. Baker, and R. Aramayo, 2004 Properties of unpaired DNA required for efficient silencing in *Neurospora crassa*. Genetics 167: 131–150.

Lindholm, A. K., K. A. Dyer, R. C. Firman, L. Fishman, W. Forstmeier *et al*., 2016 The ecology and evolutionary dynamics of meiotic drive. Trends Ecol. Evol. 31: 315–326.

Lyon, M. F., 2003 Transmission ratio distortion in mice. Annu. Rev. Genet. 37: 393–408.

Marchler-Bauer, A., M. K. Derbyshire, N. R. Gonzales, S. Lu, F. Chitsaz *et al.*, 2015 CDD: NCBI's conserved domain database. Nucleic Acids Res. 43: D222-226.

Margolin, B. S., M. Freitag, and E. U. Selker, 1997 Improved plasmids for gene targeting at the his-3 locus of *Neurospora crassa* by electroporation. Fungal Genet. Newsl. 44: 34–36.

McCluskey, K., A. Wiest, and M. Plamann, 2010 The Fungal Genetics Stock Center: a repository for 50 years of fungal genetics research. J. Biosci. 35: 119–126.

Morgulis, A., G. Coulouris, Y. Raytselis, T. L. Madden, R. Agarwala *et al.*, 2008 Database indexing for production MegaBLAST searches. Bioinforma. Oxf. Engl. 24: 1757–1764.

Perkins, D. D., 1974 The manifestation of chromosome rearrangements in unordered asci of *Neurospora*. Genetics 77: 459–489.

Raju, N. B., 1979 Cytogenetic behavior of *Spore killer* genes in Neurospora. Genetics 93: 607–623.

Raju, N. B., 1980 Meiosis and ascospore genesis in Neurospora. Eur. J. Cell Biol. 23: 208–223.

Raju, N. B., D. D. Perkins, and D. Newmeyer, 1987 Genetically determined nonselective abortion of asci in *Neurospora crassa*. Canadian Journal of Botany 65: 1539-1549.

Raju, N. B., 1994 Ascomycete *Spore killers*: Chromosomal elements that distort genetic ratios among the products of meiosis. Mycologia 86: 461-473.

Rhoades, M., 1952 Preferential Segregation in Maize, pp. 66–80 in Heterosis: a record of researches directed towards explaining and utilizing the vigor of hybrids, edited by J. W. Gowen. Iowa State College Press, Ames Iowa USA.

Saupe, S. J., 2011 The [Het-s] prion of *Podospora anserina* and its role in heterokaryon incompatibility. Semin. Cell Dev. Biol. 22: 460–468.

Shiu, P. K., N. B. Raju, D. Zickler, and R. L. Metzenberg, 2001 Meiotic silencing by unpaired DNA. Cell 107: 905–916.

Shiu, P. K. T., D. Zickler, N. B. Raju, G. Ruprich-Robert, and R. L. Metzenberg, 2006 SAD-2 is required for meiotic silencing by unpaired DNA and perinuclear localization of SAD-1 RNA-directed RNA polymerase. Proc. Natl. Acad. Sci. USA. 103: 2243–2248.

Smith, Z., S. Bedore, S. Spingler, and T. M. Hammond, 2016 A mus-51 RIP allele for transformation of *Neurospora crassa*. Fungal Genet. Rep. 62: 1–7.

Sugimoto, M., 2014 Developmental genetics of the mouse *t*-complex. Genes Genet. Syst. 89: 109–120.

Turner, B. C., 2001 Geographic distribution of Neurospora *Spore killer* strains and strains resistant to killing. Fungal Genet. Biol. 32: 93–104.

Turner, B. C., and D. D. Perkins, 1979 *Spore killer*, a chromosomal factor in Neurospora that kills meiotic products not containing it. Genetics 93: 587–606.

Wang, Y., K. M. Smith, J. W. Taylor, M. Freitag, and J. E. Stajich, 2015 Endogenous small RNA mediates meiotic silencing of a novel DNA transposon. G3 5: 1949–1960.

Westergaard, M., and H. K. Mitchell, 1947 Neurospora V. A synthetic medium favoring sexual reproduction. Am. J. Bot. 34: 573–577.

Yu, J.H., Z. Hamari, K.H. Han, J.A. Seo, Y. Reyes-Domínguez *et al.*, 2004 Double-joint PCR: a PCR-based molecular tool for gene manipulations in filamentous fungi. Fungal Genet. Biol. 41: 973–981.

Zhang, Z., S. Schwartz, L. Wagner, and W. Miller, 2000 A greedy algorithm for aligning DNA sequences. J. Comput. Biol. 7: 203–214.

Zimmering, S., L. Sandler, and B. Nicoletti, 1970 Mechanisms of meiotic drive. Annu. Rev. Genet. 4: 409–436.

CHAPTER V

SUMMARY

It has been nearly two decades since the discovery of MSUD in *Neurospora* as a gene silencing mechanism (Aramayo and Metzenberg 1996). It consists of two distinct steps: scanning and detection of unpaired DNA followed by silencing of unpaired DNA via an RNAi pathway. Most of the proteins involved in RNAi pathway are known to be localized into the perinuclear region forming a RNAi silencing complex. However, little is known about the proteins involved in the initiation of MSUD at a nuclear level in the presence of an unpaired DNA. Therefore, it is important to search novel proteins involved in the MSUD pathway in order to understand the unpaired DNA detection at the molecular level.

In my research findings, I was able to uncover the second MSUD protein (SAD-6) localized into the nucleus. SAD-6 is a protein with a SNF2-family helicase domain and represents the subgroup of 'Rad54-like' proteins (Flaus *et al*. 2006). Rad54 proteins are known to have function in nuclear level including homologous recombination in many eukaryotic organisms (Mazin *et al*. 2010 and Ceballos and Heyer 2011). Hence, it is possible that SAD-6 could be a protein involved in the homology search during MSUD activation. However, my MSUD suppression assays show that MSUD is partially functional in homozygous *sad-6*$^{\Delta}$ crosses suggesting that SAD-6 is not a critical MSUD protein.

Further, I was able to identify and characterize another MSUD related protein called SAD-7. It is localized into the nucleus with an interesting localization pattern. The confocal images of my study strongly suggest that SAD-7 is localized in the nucleus, concentrated around the perinuclear regions, and randomly distributed as cytoplasmic foci of meiotic cells. Among all the uncovered MSUD proteins, SAD-7 is the only protein with such a localization pattern. Even

after truncating the SAD-7 N-terminal region up to 206 amino acids, it still shows the same localization pattern suggesting that the amino acids required determining the cellular localization are located after 206 amino acids of the SAD-7. Therefore it is necessary to conduct further studies to uncover the sequence required for its localization. The fascinating localization pattern of SAD-7 could be related to its RRM domain. Perhaps SAD-7 uses its RRM to transport the aRNA produced from the unpaired DNA to the RNAi complex located in the perinuclear region of the meiotic cell.

My studies have confirmed that SAD-7 is at least involved in two vital functions in *N.crassa*. It is related to MSUD pathway and also it is a critical protein in Neurospora sexual reproduction. It is thus impossible to use $sad\text{-}7^{\Delta} \times sad\text{-}7^{\Delta}$ crosses to see if SAD-7 is a critical MSUD protein.

Additionally, I have focused on meiotic drive elements in *N. crassa*. These are selfish elements which are capable of biasing their own transmission rates in the presence of a competing locus. In general, wild type *Neurospora crassa* produces 8 black ascospores and zero white ascospores. After crossing a *Spore killer*-resistant strain to a *Spore killer*-sensitive strain, the offspring ascospore phenotype ratio is 4 black ascosporees to 4 white ascospores. This phenotype occurs due to the biased transmission of the *Spore killer*-2 element to the offspring (Turner and Perkins 1979). Recent studies have confirmed the existence of a spore killing-resistance gene called *rsk* (Hammond *et al.* 2012) and a mutant locus called *rfk-1* (Harvey *et al.* 2014). In the *N. crassa* genome, the *rfk-1* locus is located within a 45 kb region of *Sk-2* on chromosome III (Hammond *et al.* 2012). In my experiments, I was able to identify a genetic element located within 1481 bp interval (called $AH36^{Sk\text{-}2}$) of DNA from the 45 kb *rfk-1* region that is required and sufficient for spore killing. Deleting this region from *Sk-2* strains resulted in

loss of spore killing phenotype. Overall, the results of my experiments provide much needed insight to help guide future studies on the mechanisms of MSUD and Spore killing in *N. crassa*.

Literature Cited

Aramayo, R., and R. L. Metzenberg, 1996 Meiotic transvection in fungi. Cell 86: 103–113.

Ceballos, S. J., and W. D. Heyer, 2011 Functions of the Snf2/Swi2 family Rad54 motor protein in homologous recombination. Biochim. Biophys. Acta 1809: 509–523.

Flaus, A., D. M. Martin, G. J. Barton, T. Owen-Hughes, 2006 Identification of multiple distinct Snf2 subfamilies with conserved structural motifs. Nucleic Acids Res. 34: 2887–2905.

Hammond, T. M., D. G. Rehard, H. Xiao, and P. K. T. Shiu, 2012 Molecular dissection of Neurospora *Spore killer* meiotic drive elements. Proc. Natl. Acad. Sci. USA. 109: 12093-12098.

Harvey, A. M., D. G. Rehard, K. M. Groskreutz, D. R. Kuntz, K. J. Sharp *et al*., 2014 A critical component of meiotic drive in Neurospora Is located near a chromosome rearrangement. Genetics 197: 1165-1174.

Mazin, A. V., O. M. Mazina, D. V. Bugreev, and M. J. Rossi, 2010 Rad54, The motor of homologous recombination. DNA Repair 9: 286–302.

Shiu, P. K. T., D. Zickler, N. B. Raju, G. Ruprich-Robert, and R. L. Metzenberg, 2006 SAD-2 is required for meiotic silencing by unpaired DNA and perinuclear localization of SAD-1 RNA-directed RNA polymerase. Proc. Natl. Acad. Sci. USA. 103: 2243–2248.

Turner, B. C., and D. D. Perkins, 1979 *Spore killer*, a chromosomal factor in Neurospora that kills meiotic products not containing it. Genetics 93: 587–606.